Anti-inflammatory Constituents from *Croton stellatopilosus* Leaves

Charoenwong Premprasert

A Thesis Submitted in Partial Fulfillment of the Requirements for the Degree of

Master of Pharmacy in Pharmaceutical Sciences

Prince of Songkla University

2011

Anti-inflammatory Constituents from *Croton stellatopilosus* Leaves

Author Mr. Charoenwong Premprasert

Major Program Pharmaceutical Sciences

Major Advisor

……

(Assist. Prof. Dr. Juraithip Wungsintaweekul)

Co-advisor

……

(Assoc. Prof. Dr. Supinya Tewtrakul)

Examining Committee:

…..……Chairperson

(Prof. Dr. Kittisak Likhitwitayawuid)

……..……Committee

(Assist. Prof. Dr. Juraithip Wungsintaweekul)

…….Committee

(Assist. Prof. Dr. Sirima Mahattanadul)

…….Committee

(Assist. Prof. Dr. Supreeya Yuenyongsawad)

The Graduate School, Prince of Songkla University, has approved this thesis as partial fulfillment of the requirements for the Master of Pharmacy Degree in Pharmaceutical Sciences

……..……..

(Prof. Dr. Amornrat Phongdara)

Dean of Graduate School

ชื่อวิทยานิพนธ์ สารต้านอักเสบจากใบเปล้าน้อย

ผู้เขียน นาย เจริญวงค์ เปรมประเสริฐ

สาขาวิชา เภสัชศาสตร์

ปีการศึกษา 2554

บทคัดย่อ

ในการศึกษานี้เป็นการแยกองค์ประกอบทางเคมีจากใบเปล้าน้อยที่มีฤทธิ์ต้านอักเสบ โดยอาศัยหลักของการแยกโดยใช้ฤทธิ์ทางชีวภาพเป็นแนวทาง ในการศึกษาด้านพฤกษเคมี สารสกัดหยาบถูกเตรียมด้วยตัวทำละลายต่างชนิดกัน ใน 2 วิธี กล่าวคือ วิธีที่ 1 สกัดด้วยเอทานอล ที่ให้ความร้อน และสกัดแบบแยกชั้นด้วยเฮกเซน และวิธีที่ 2 สกัดด้วยการหมักด้วยตัวทำละลาย ที่มีขั้วแตกต่างกัน ได้แก่ เฮกเซน ไดคลอโรมีเทน และเอทานอล ตามลำดับ ส่วนของสารสกัดทั้งหมดถูกนำมาตรวจหาฤทธิ์ยับยั้งการสร้างไนตริกออกไซด์ ในเซลล์แมคโครฟาจ ชนิด RAW264.7 ที่กระตุ้นด้วยสารไลโปโพลีแซคคาไรด์ (LPS) ผลการทดลองพบว่าสารสกัดที่มีฤทธิ์ยับยั้งการสร้างไนตริกออกไซด์ ได้แก่ สารสกัดชั้นเอทานอล เฮกเซน (สกัดแบบวิธีที่ 1) มีค่า IC_{50} เท่ากับ 7.20 และ 49.31 ไมโครกรัมต่อมิลลิลิตร และสารสกัดชั้นเฮกเซน ไดคลอโรมีเทน เอทานอล (สกัดแบบวิธีที่ 2) มีค่า IC_{50} เท่ากับ 8.37, <3 และ 5.94 ไมโครกรัมต่อมิลลิลิตร ตามลำดับ จากผลการทดลองดังกล่าวได้นำชั้นเฮกเซน (สกัดแบบวิธีที่ 1) และชั้นไดคลอโรมีเทน (สกัดแบบวิธีที่ 2) มาแยกด้วยวิธีทางโครมาโตกราฟี ได้สารรวม 3 ชนิด คือ **CS-1** มีลักษณะเป็นของเหลวหนืด **CS-2** และ **CS-3** ที่มีลักษณะเป็นผลึกสีขาว เมื่อนำไปวิเคราะห์ด้วยเทคนิคทางสเปคโตรสโคปี ได้ผลการวิเคราะห์ว่าสาร **CS-1**, **CS-2** และ **CS-3** คือ เปลาโนทอล เปลาโนไลด์ และเปลานอล อี ตามลำดับ

เมื่อประเมินฤทธิ์ยับยั้งการสร้างไนตริกออกไซด์ ในเซลล์แมคโครฟาจของสาร acyclic diterpene (เปลาโนทอล) และสาร furanoditerpenes (เปลาโนไลด์ และเปลานอล อี) พบว่า เปลาโนทอล เปลาโนไลด์ และเปลานอล อี สามารถยับยั้งการสร้างไนตริกออกไซด์ โดยมีค่า IC_{50} เท่ากับ 3.41, 17.09 และ 2.79 ไมโครโมลาร์ ตามลำดับ ผลการทดลองนี้สามารถสรุปได้ว่าสารทั้งสามชนิดมีฤทธิ์ต้านอักเสบ

ในการศึกษากลไกการออกฤทธิ์ยับยั้งการอักเสบของสารทั้งสามชนิดต่อเซลล์แมคโครฟาจ โดยวัดระดับการแสดงออกของยีนที่เกี่ยวข้องกับกระบวนการอักเสบ ได้แก่ ไซโคลออกซิจีเนส-1 (*COX-1*), *COX-2* และอินดิวซิเบิลไนตริกออกไซด์ ซินเทส (*iNOS*) ถูกประเมินด้วยวิธี qRT-PCR โดยแสดงในรูปของค่าปริมาณสัมพัทธ์ (Relative Quantitation, RQ) ผลการทดลองพบว่าสารเปลาโนทอลกระตุ้นการแสดงออกของยีน *COX-1* และ *COX-2* แต่กดการแสดงออกของ ยีน *iNOS* ได้ ในทางตรงกันข้ามสารเปลาโนไลด์สามารถยับยั้งยีนทั้งสามชนิด ทั้งนี้ขึ้นกับความเข้มข้นที่ให้ และสารเปลานอล อี ยับยั้งได้เฉพาะ *COX-2* แต่ไม่มีผลต่อ *COX-1* และ *iNOS* ผลการทดลองนี้แสดงให้เห็นว่าเปลาโนทอล เปลาโนไลด์ และเปลานอล อี มีคุณสมบัติต้านอักเสบโดยมีกลไกการออกฤทธิ์ที่แตกต่างกัน กล่าวคือ เปลาโนทอลออกฤทธิ์ผ่านระบบอิมมูน ส่วนเปลานอล อี ออกฤทธิ์ผ่านกระบวนการสร้างพรอสตาแกลนดิน โดยยับยั้ง *COX-2* อย่างจำเพาะ และสารเปลาโนไลด์ออกฤทธิ์ต้านอักเสบผ่านทั้งกระบวนการสร้างพรอสตาแกลนดิน และระบบอิมมูน ผลจากการศึกษานี้สรุปได้ว่าสารไดเทอร์ปีนในใบเปล้าน้อยนั้นมีฤทธิ์ต้านอักเสบ ในเซลล์แมคโครฟาจชนิด RAW264.7 และมีศักยภาพในการพัฒนาให้เป็นสารต้านอักเสบต่อไปในอนาคต

Thesis Title Anti-inflammatory constituents from *Croton stellatopilosus* leaves

Author Mr. Charoenwong Premprasert

Major Program Pharmaceutical Sciences

Academic Year 2011

ABSTRACT

In this study, anti-inflammatory constituents from *Croton stellatopilosus* leaves were investigated by bioassay-guided isolation approach. In the phytochemical study, the crude extracts were prepared from 1) reflux with ethanol and partitioned with hexane and 2) maceration with hexane, dichloromethane (CH_2Cl_2) and ethanol, consecutively. All fractions were screened for an inhibitory activity against nitric oxide (NO) production in the lipopolysaccharide (LPS)-induced RAW264.7 cells by Griess reaction. The results showed that the extracts that possessed the inhibitory activity on NO production were ethanol and hexane fractions (from method 1) with IC_{50} of 7.20 and 49.31 μg/ml; hexane, CH_2CL_2 and ethanol fractions (from method 2) with IC_{50} of 8.37, <3 and 5.94 μg/ml, respectively. Based on these results, the hexane extract (from method 1) and the CH_2Cl_2 extract (from method 2) were further purified by means of column chromatography. An oily liquid substance (**CS-1**) and two amorphous powders (**CS-2** and **CS-3**) were obtained. By using spectroscopic techniques, the **CS-1**, **CS-2** and **CS-3** were elucidated to be plaunotol, plaunolide and plaunol E, respectively.

The acyclic diterpene (plaunotol) and two furanoditerpenes (plaunolide and plaunol E) were assessed for inhibitory activity on NO production. The results indicated that plaunotol, plaunolide and plaunol E exhibited an inhibitory activity on NO production with IC_{50} of 3.41, 17.09 and 2.79 μM, respectively. From these data, it can be concluded that plaunotol, plaunolide and plaunol E have anti-inflammatory activity.

In order to understand the mechanism of anti-inflammatory activity, the RAW264.7

cells were treated with plaunotol, plaunolide and plaunol E. Genes expressions of *COX-1*, *COX-2* and *iNOS* were determined using quantitative real-time (qRT)-polymerase chain reaction (PCR) technique. The level of gene expression was expressed as relative quantitation (RQ) according to the comparative C_T method. The results indicated that plaunotol has stimulated on *COX-1* and *COX-2* expressions but suppressed the *iNOS* expression significantly. On the other hand, the expressions *COX-1*, *COX-2* and *iNOS* gene were down-regulated by treating cells with plaunolide in concentration dependent manner. Nevertheless, plaunol E could only inhibited the *COX-2* expression but not *COX-1* and *iNOS*. The results suggested that all three compounds possessed the anti-inflammatory activity with different mechanisms of action. Plaunotol suppressed the *iNOS* mRNA expression in the immune system. Plaunol E acted as a *COX-2* inhibitor in prostaglandin biosynthesis. And plaunolide performed anti-inflammatory action via mixed inhibition actions against prostaglandin and NO productions. The present study revealed that the diterpenes plaunotol, plaunolide and plaunol E from *C. stellatopilosus* leaves exhibit anti-inflammatory activity in the murine macrophage RAW264.7 cells, supporting that they could be further developed to be an alternative anti-inflammatory agent.

ACKNOWLEDGEMENTS

This thesis was not completed without the assistance of a large cast of all members of the Department of Pharmacognosy and Pharmaceutical Botany, Faculty of Pharmaceutical Sciences, Prince of Songkla University.

I would like, first of all, express my sincere gratitude and thanks to Assistant Professor Dr. Juraithip Wungsintaweekul for her supervision of the research work, ideal, keen interest, kindness, continual encouragement, and understanding during the course of practical work and also presentation of the thesis. I would like to express my deepest grateful thank to my co-advisor, Associate Professor Dr. Supinya Tewtrakul for her helpful advice of the research work, ideal, keen interest, kindness, encouragement, and suggestions throughout the course of this work. I wish to express my deepest appreciation and grateful thank to Assistant Professor Dr. Anuchit Plubrukarn for his guidance, suggestion and helpful for the structure elucidation. I would also like to special thanks to Mr. Anan Chaikitwatana from Tipco Foods (Thailand) Public Co. Ltd. for support the plant material. I would like to thanks to Faculty of Pharmaceutical Sciences, PSU for the scholarship and the PSU Graduate school for partial financial support on research. I also thank the Department of Pharmacognosy and Pharmaceutical Botany, the Pharmaceutical Laboratory Service Center, Faculty of Pharmaceutical Sciences and Scientific Equipment Center (SEC), PSU for their support in the scientific equipments and instruments. Many thanks go to all staff members and my friends at the Department of Pharmacognosy and Pharmaceutical Botany, Faculty of Pharmaceutical Sciences, Prince of Songkla University, for their contribution and help throughout this thesis. Most importantly, I would like to thank my parents, brothers, lovely friends and friends for their understanding, encouragement, love and support throughout my life. Finally the study in the Master‘s Degree, I could not have done any of this without them.

Charoenwong Premprasert

CONTENTS

CONTENTS (CONTINUED)

CONTENTS (CONTINUED)

LIST OF TABLES

LIST OF FIGURES

LIST OF SCHEMES

LIST OF ABBREVIATIONS AND SYMBOLS

br	broad signals for NMR spectrum
cDNA	complementary deoxyribonucleic acid
cm	centimeter
COSY	correlation spectroscopy
C_T	threshold cycle
DEPT	distortionless enhancement by polarization transfer
EIMS	electron-impact mass spectroscopy
g, kg, mg	gram, kilogram, miligram
HMBC	heteronuclear multiple bond correlation
HMQC	heteronuclear multiple-quantum coherence
IC_{50}	50% inhibitory concentration
IR	infrared
J	coupling constant (for signal of NMR)
l, ml	liter, milliliter
M, mM	molar, milimorlar
m/z	mass-over-charge ratio
mRNA	messenger ribonucleic acid
MS	mass spectroscopy
NMR	nuclear magnetic resonance
OD	optical density
p	p-value (for statistical)
PCR	polymerase chain reaction
pH	potential of hydrogen (-log hydrogen concentration)
qRT-PCR	quantitative real-time polymerase chain reaction

LIST OF ABBREVIATIONS AND SYMBOLS (continued)

Rn	normalized reporter
RNase H	ribonuclease H
RQ	relative quantitation
rpm	round per minute
s, d, t, m	singlet, doublet, triplet, multiplet (The signal for NMR spectrum)
sec, min, h	second, minute, hour
T_m	melting temperature
TLC	thin layer chromatography
UV-VIS	ultraviolet-visible
v/v	volume by volume
w/v	weight by volume
w/w	weight by weight
WHO	world health organization
Δ	delta, in the greek alphabet also used as a mathematical symbol
δ	chemical shift in ppm
γ_{max}	maximum wavelength
ν	wave number
$^{\circ}C$	degree of celsius
μl	microliter
μM	micromolar
%	percentage
®	trade name
TM	trade mark

CHAPTER 1

INTRODUCTION

1.1 Background and rationale

Plaunoi (เปล้าน้อย) or *Croton stellatopilosus* Ohba (Euphorbiaceae) is a woody plant and indigenous to Thailand. Plaunoi was formerly well known as *C. sublyratus* (Esser and Chayamarit, 2001). For folklore medicine, Plaunoi is used commonly in combination with Plauyai (เปล้าใหญ่) (*C. poilanei* Gagnep.) for widely purposes such as anthelmintic, digestant, transquilizer and stomachic (Bunyapraphatsara**,** 1989). Plaunoi is also used as a dermatologic agent for skin diseases (Ponglux *et al*., 1987). In early 1970, drug discovery based on ethno-pharmacological knowledge led Ogiso and his co-workers (1978) to investigate the potential of Plaunoi as agent used for gastro-intestinal diseases. Plaunoi extract from stems showed significant inhibitory activities against Shay-ulcer in rat and reserpine-induced ulcer in mouse (Ogiso *et al*., 1978). Bioassay-guided isolation of the extract afforded acyclic diterpene alcohol and several furanoditerpenes, which possessed anti-reserpine activity and anti-Shay ulcer activity. The structure of bioactive acyclic diterpene was determined to be (*E*,*Z*,*E*)-7-hydroxymethyl-3,11,15-trimethyl-2,6,10,14-hexadecatetraen-1-ol (Ogiso *et al*., 1978) and named as "plaunotol". The chemistry, pharmacognosy, pharmacology, metabolism, safety evaluation and clinical aspects of plaunotol were extensively studied. In 1983, plaunotol was registered to World Health Organization (WHO) under the name of "CS-684". Since plaunotol is an oily substance, Sankyo Ltd., Tokyo, Japan manufactured CS-684 in the form of soft-gelatin capsule (combined with corn oil) under the tradename of Kelnac™ (Ogiso *et al*., 1985). Since then, plaunotol has become an anti-peptic ulcer drug and is combined with antibiotics and proton pump inhibitors for treatment of *Helicobacter pylori*-induced peptic ulcer (Koga *et al*., 2002; Sasaki *et al*., 2007).

Beside the discovery of plaunotol, furanoditerpenes were also isolated including plaunol A, plaunol B (Kitazawa *et al*., 1979), plaunol C, plaunol D, plaunol E (Kitazawa *et al*., 1980) and plaunolide or plaunol F (Takahashi *et al*., 1983) as well as other cyclic diterpene alcohol such as *ent*-3α -hydroxy-13-epimanool, *ent* –16β-,17 dihydroxykaurane (Kitazawa and Ogiso, 1981) and esters of plaunotol (Kitazawa *et al*., 1982). Evaluation of anti-Shay ulcer activity of plaunol A-E indicated that the activity was ranging from plaunol C > plaunol B > plaunol E > plaunol D, whereas plaunol A was inactive (Kitazawa *et al*., 1979, Kitazawa *et al*., 1980). Nevertheless, biological activity of plaunolide (plaunol F) has not been reported. Since plaunotol is present in Plaunoi as the main component, therefore, it can be easily isolated. Many reports on pharmacological activity of plaunotol have been published considerably during the two decades. However, there is less knowledge about the pharmacological activity of furanoditerpenes.

Regarding the pharmacological activities of plaunotol, they can be categorized into 3 groups including anti-inflammation and gastro-protection, antibacterial activity and anticancer properties. Plaunotol was shown to treat the reserpine-induced ulcer in mouse (*i.p.*) with ID_{50} of < 10 mg/kg when compared to gefarnate (ID_{50} = 300 mg/kg) (Ogiso *et al*., 1978). In 1987, Ushiyama *et al*. demonstrated that plaunotol and its metabolite (1-carboxylic plaunotol) have gastro-protective effect by increase of prostaglandin E_2 (PGE_2) and prostaglandin I_2 (PGI_2) productions in cultured cells of 3T6 fibroblasts. They suggested that plaunotol and its metabolite increased the prostaglandins level by stimulating the cellular phospholipase activity, not prostaglandin cyclooxygenase activity (Ushiyama *et al*., 1987). However, oral administration of plaunotol at dose of 300 mg/kg in rat increased the prostaglandins level in gastric mucosa. This evidence supported that plaunotol can heal the gastric lesion by this mechanism (Ushiyama *et al*., 1987). In addition, Plaunotol was also found to exert a protective effect against colonic lesion formation induced by trinitobenzene sulfonic acid, acetic acid (Makino *et al*., 1998) and C48/80-induced acute gastric mucosal lesions in rats (Ohta *et al*., 2005). These studies highlight the possibility of plaunotol in treatment of ulcer caused by gastro-intestinal tract inflammation.

Oda *et al*. (1988) reported that plaunotol could inhibit NAD^+ dependent 15-hydroxyprostaglandin dehydrogenase (15HPGDH) isolated from hog gastric mucosa, with *K*i value of 7.8 μM (Oda *et al*., 1988). Their finding supports the hypothesis that plaunotol acts on cellular phospholipase activity and increases the prostaglandin level in gastric mucosa. In conclusion, plaunotol has gastro-protective effect by stimulating secretin excretion and inhibiting phospholipase activity, not cyclooxygenases. In addition, Shiratori *et al*. (1993) reported that plaunotol released endogenous secretin, and that secretin is a potential mediator of the anti-ulcer actions of mucosal protective agents (Shiratori *et al*., 1993).

As the translocation of *Helicobacter pylori* in gastrointestinal tract causes a chronic peptic ulcer (Wallace and Ma, 2001), bactericidal effect of plaunotol on *H. pylori* and *Staphylococcus aureus* has been investigated (Koga *et al*., 1996; Matsumoto *et al*., 1998). Its hydrophobicity has been found to undertake an interaction to the bacterial cell membrane and therefore fluidizes and destroys the *H. pylori* (Koga *et al*., 1996; Koga *et al*., 1998). Since *H. pylori* infection in stomach is associated to oxidative stress (Augusto *et al*., 2007), therefore, hypothesis of plaunotol on its anti-inflammation and anti-oxidant properties has been stated. It was suggested that plaunotol exhibited not only *H. pylori* irradication but also suppressed the secretions of inflammatory mediators such as tumor necrosis factor (TNF)-α and interleukin (IL)-8. Murakami *et al*. (1999) investigation on the effect of plaunotol on the endotoxin-induced monocytes, indicated that plaunotol decreased TNF-α production in the monocyte by inhibition on the release of neutrophil elastase, the increase levels of intracellular calcium and the neutrophil activation (Murakami *et al*., 1999). Study on the effect of plaunotol on *H. pylori* induced IL-8 secretion in the human gastric cancer cell line MKN45, was also shown the suppression on the induced with *H. pylori* infection. Secretion of IL-8 by MKN45 was suppressed after co-culture with plaunotol in a dose-dependent manner (Takagi *et al*., 2000). In addition, role of plaunotol on COX expression and molecular mechanism was reported from the study in the rat gastric mucosal (RGM1) cells (Fu *et al*., 2005). In this kind of cell lines, treatment cells with plaunotol increased

PGE_2 production. Addition of 50 μM of plaunotol to the serum-starved RGM1 cells, COX-2 expression but not COX-1 was up-regulated. They suggested the mechanism appeared via the phosphorylation of the nuclear factor kappa-B (NF-κB) and activation of cyclic AMP response element (CRE) sites of *COX-2* gene promoters (Fu *et al*., 2005). It is clear that plaunotol has anti-peptic ulcer property with gastro-protective effect and healing ability to gastric lesions. *In vitro* and *in vivo* experiments supported the application of plaunotol as an anti-peptic ulcer.

Recently, potential of plaunotol for anti-angiogenic effect was reported from the study in human umbilical vein endothelial cell (HUVECs) model. Plaunotol inhibited the proliferative activity of HUVECs in a dose-dependent manner and be considered to be a candidate for anti-angiogenic drug (Kawai *et al*., 2005). Investigation the effect of plaunotol on gastric cancer cell lines including MKN-45, MKN-74 and AZ-521 demonstrated that plaunotol (10-40 μM) inhibited growth of all gastric cancer cell lines by apoptosis induction (activation of caspase-3, -8 and -9) (Yamada *et al*., 2007). Moreover, plaunotol also induced the caspase-3, -8 and -9 mediated apoptosis in colon cancer (Yoshikawa *et al*., 2009). It was suggested that plaunotol has potential for anticancer drug via induction of apoptosis but needs confirmation by clinical trial.

Considering the wide range of pharmacological activities of plaunotol, the compound is still "a molecule of interest" worth investigating for other activities such as anti-inflammatory activity. No doubt about the gastric cell lines, plaunotol is clear to protect gastrointestinal tract by healing of lesion. As demonstrated in the RGM1 cells, COX-2 expression is a crucial role in PGE_2 production (Fu *et al*., 2005). Controversial results appeared in the 3T6 fibroblast cells. It was reported that stimulation of PGE_2 and PGI_2 productions was not involved in the prostaglandin cyclooxygenase but cellular phospholipase activity (Ushiyama *et al*., 1987). It is interesting to investigate plaunotol in the alternative model for anti-inflammatory activity e.g. murine macrophage RAW264.7 cells, to see it possesses similar action or not. Diterpene alcohol and furanoditerpenes from Plaunoi also attracted us to explore in order to obtain supporting evidence for further clinical usages of these substances.

Cell-based assay technology provides a simple *in vitro* assay for discovery of biologically active compounds and can be developed for high throughput screening. For screening of anti-inflammatory agents, the murine macrophage RAW264.7 cell, in particular, is widely used. Activation of macrophage cells with interleukin-1β, TNF-α, interferon-γ, lipopolysaccharide (LPS), for instance, pro-inflammatory mediator such as nitric oxide (NO) is expressed (Hemmrich *et al*., 2005). It is well known that NO is involved in the regulation of diverse physiological and patho-physiological mechanisms in cardiovascular, nervous and immunological systems. NO acts as an important host defense effecter in the immune system. It carries free oxygen radical ($NO^{\cdot}$) and can act as cytotoxic agent in pathological processes, particularly in inflammatory disorders (Aktan, 2004). The production of NO is catalyzed by nitric oxide synthases (NOSs) including endothelial NOS (eNOS), and neuronal NOS (nNOS), which are present in the resting cells as a constitutive NOS and an inducible NOS (iNOS). The isoform of iNOS is not present in resting cells and can be induced by noxious stimuli. Inhibition of iNOS can reveal the potential on anti-inflammatory activity and, therefore, iNOS can be used as a drug target in the bioactivity screening.

Generally, macrophages recognize and are activated by conserved components of microorganisms, and respond with cascade of transcription output. Expression profiling has revealed thousands of genes that are induced or repressed in macrophages in response to the classical activating agent lipopolysacharide (LPS) (Aung *et al*., 2006). The LPS activates the transcription factors such as NO, COX-2, NF-κB site, a C/ERP site, cAMP response element-1 (CRE-1), CRE-2, and AP-1 site and an E-box (Kang *et al*., 2006). This feature matches for screening an inhibitor of corresponding genes and mechanistic study in the molecular level. Measuring the gene expression profiles by means of Northern blotting, nuclear run-on assays and RT-PCR can answer the effect of compound on the inhibition or activation in the LPS-induced cells.

Anti-inflammatory constituents of Plaunoi leaves are still interesting to us. Our study aimed to perform phytochemical study of Plaunoi leaves by bioassay-guided isolation. The inhibition of NO production in the murine macrophage RAW264.7 cells was performed in order to estimate the anti-inflammation potential of the isolated compounds. For mechanistic study on the inflammation process, genes expressions including *iNOS*, *COX-1* and *COX-2* mRNA were measured using the quantitative RT-PCR. Results from this study may provide the alternative pharmacological activities for further development of this Thai medicinal plant.

1.2 Inflammation and inflammatory mediators

The inflammatory response is a basic concept in pathology. Inflammation is a normal defense mechanism in the body and is intended to localize and remove the injurious agent (Gould, 2002). Without the inflammatory process, wounds would not heal, and minor infections would become overwhelming (Immunity and inflammation). In the context of infections, inflammatory response is a complex reaction of the innate or non-specific immune system (Rosenberg and Gallin, 1984).

1.2.1 Acute and chronic inflammation

Inflammation has traditionally been categorized into acute and chronic responses. Acute inflammation is the rapid, short lived (minute to days), relatively uniform response to acute injury and is characterized by accumulations of fluid, plasma, protein, and granulocytic leukocytes. In contrast, chronic inflammation has longer duration and includes influx of lymphocytes and macrophages and fibroblast growth.

The events characteristic of acute and chronic inflammation are as follows:-

(Rosenberg and Gallin, 1984)

- Injuring agent evades or destroys primary barriers such as epithelial cells or endothelial cells. This injurious agent initiates the acute inflammatory response.
- Tissue damage initiates a series of molecular event that results in the production of pro-inflammatory mediators. These mediators promote the hallmark physical sign of inflammation that include increase blood flow and vascular permeability, migration of leukocytes from peripheral blood into the tissue. Leukocyte responds to eliminate the foreign substance.
- When the initiating agent is eliminated, anti-inflammatory agents then take over to limit damage to the tissues. If not complete elimination of injury, inflammatory process is then developed to be chronic inflammation.

Acute inflammation

The acute inflammatory process occurs to protect the host against pathogen, especially bacteria (Huang *et al*., 2004). This response is relatively non-specific immune system, its main roles being to clear away dead tissues, protect against local infection and allow the immune system access to the damaged area (Steven and Lowe, 2000). It can be characterized as a cascade of events that result in complex, yet coordinate, interaction between blood leukocytes, blood vessels and cells of the tissue involved. These events are directed toward removal injurious agent and restoration of normal tissue structure and function.

For the initiation of the acute inflammatory response; the way, in which the inflammatory process is initiated, depends in the part of nature and portal of entry of the foreign substance. Pathogens can stimulate the inflammation by a number of distinct and idiosyncratic mechanisms, including activation of plasma protease system by interaction with degradation products of the bacterial cell walls and by secretion of toxins that can activate inflammatory response directly. The injured cells or tissue themselves can release degradation product, which stimulate cells in the immune's defense process to initiate inflammatory process. Their products initiate one or

more of plasma protease cascades and can augment expression of pro-inflammatory cytokine that promote the inflammation (Vallochi *et al*., 2008).

The cardinal signs of acute inflammation are: (Macfalane *et al*., 2000)

Redness (rubor): An acutely inflamed tissue appears red, for example skin affected by sunburn, cellulitis caused by bacterial infection or acute conjunctivitis. This is due to the dilatation of small blood vessels within the damaged area.

Heat (calor): Increase of temperature on the skin is seen only in peripheral parts of the body. It is due to increase blood flow through the region, resulting in vascular dilatation and the delivery of warm blood to the area.

Swelling (tumor): Swelling results from edema. The accumulation of fluid in the extra-vascular space as part of the fluid exudates and the physical mass of the inflammatory cells migrates into the area.

Pain (dolor): It results partly from the stretching and distortion of tissues due to inflammatory edema and, in particular, from pus under pressure in an abscess cavity. Some of the chemical mediators of acute inflammation, including bradykinin, prostaglandins and serotonin, are known to induce pain.

Loss of function: Loss of function is a well-known consequence of inflammation. Movement of an inflamed area is consciously and reflexly inhibited by pain, while severe swelling may physically immobilize the tissues.

Chronic inflammation

When the acute inflammation persists, either through incomplete clearance of initial inflammatory focus or as a result of multiple acute events occurring in the same location, it becomes chronic inflammation. In contrast to acute inflammation, which is characterized by a primarily neutrophil influx, the histological findings in chronic inflammation include accumulation of macrophages and lymphocytes and growth of fibroblast and vascular tissue.

These latter two features result in the tissue scaring that is typically seen at site of prolonged or repeated inflammatory activity (Rosenberg and Gallin, 1984). Among the most interesting sequence of chronic inflammation is the formation of tissue granulomas. A granuloma is a collection of inflammatory cells-principally macrophages and lymphocytes, which are eventually surrounded by fibrotic wall that form in the tissue. Several unusual cell types are characteristic of granulomas, including fusions of epithelioid cells and macrophage (Rosenberg and Gallin, 1984).

Among the causes of chronic inflammation are foreign bodies such as talc, silica, asbestos and surgical suture materials. Many viruses provoke chronic inflammatory responses, as do certain bacteria, fungi, and larger parasites of moderate to low virulence. Immunologic mechanisms are thought to play an important role in chronic inflammation and granulomatous inflammation (Porth, 2003).

Non-specific chronic inflammation involves a diffuse accumulation of macrophages and leukocytes at the site of injury. Macrophages accumulate at the site because of infiltration from the tissue because of chemotaxis and prolonged survival and immobilization of these cells within the inflammatory areas. These mechanisms lead to fibroblast proliferation with the subsequent scar formation that in many cases replaces the normal connective tissue or functional parenchymal tissues of the involved structures (Porth, 2003).

1.2.2 Inflammatory mediators

Although inflammation is precipitated by injury, its signs and symptoms are presented from the inflammatory mediators (Porth, 2003). Many factors which mediate the events of acute inflammation have been documented. These chemical mediators play important roles, since the process can be modified by drug therapy to minimize unwanted and potentially damaging effects. The physiological features of the inflammation are including initiation, regulation, and elimination of the pro-inflammatory mediators. Some of these mediators are kept within cells in the inactive form, which are not injury substances. When the pathogen attack the body causing

inflammatory response, the mediator are activated by products of inflammation. Moreover the inflammatory mediators are synthesized or released from cellular sources, or both also in response to the product of acute inflammation, or by other soluble inflammatory mediators (Rosenberg and Gallin, 1984)

Inflammatory mediators in the living organism may be synthesized locally from cells at the site of inflammation or the mediators are produced from the liver cells. It may be circulating in the plasma as inactive precursors and are activated at site of injury. The mediator from plasma gain entry to the damage area via the inflammatory exudates. Table 1.1 & 1.2 summarize the inflammatory mediators, which are grouped into plasma-derived and cell-derived mediators. Although the inflammation is precipitated by injury, its signs and symptoms are produced by chemical mediators (Porth, 2003), which can described as the eicosanoids (including prostaglandins, leukotriene and thomboxane) and non eicosanoids (cytokines and NO) are described.

1.2.2.1 Eicosanoids (prostaglandins, leukotrienes and thomboxane)

The eicosanoids are oxygenation products of polyunsaturated long chain fatty acids. Arachidonic acid is the most abundant and probably the most important of the precursors of the eicosaniods (scheme 1.1). Arachidonic acid is a 20-carbon (C20) fatty acid that contains four double bonds beginning at the omega-6 position to yield a 5, 8, 11, 14-ecosatetraenoic acid. For eicosaniod synthesis to occur, arachidonic acid must first be released or mobilized from membrane phospholipids by one or more lipases of the phospholipase A_2 (PLA_2). Two unique but related cyclooxygenase (COX) isozymes have been discovered that convert arachidonic acid into prostaglandin endoperoxide. Prostaglandin H (PGH) synthase-1 (COX-1) is constitutively expressed, i.e, it is always present. In contrast, PGH synthase-2 (COX-2) is inducible, i.e, its expression varies markedly depending on the stimulus. The two isozymes also differ in function

in that COX-1 is widely distributed and has housekeeping function, e.g, gastric cytoprotection. Two to fourfold increase occur following humoral stimulation. In contrast, COX-2 is an immediate early response gene product in inflammatory and immune cells and is prominently expressed (ten-fold to eighteen-fold) by growth factors, tumor promoters and cytokines (Vame *et al*., 1994; Foegh *et al*., 1998; Sugiatno *et al*., 2006).

The cyclooxygenase pathway is responsible for the productions of thromboxane A_2 (TXA_2), prostacyclin (PGI_2) and stable prostaglandins (PGE_2, $PGF_{2\alpha}$, PGD_2). These mediators are produced from different tissues and have unique pathologically responses as shown below.

TXA_2: It was predominantly from platelet, which effects to platelet aggregation and vasoconstriction.

PGI_2: It was predominantly from vascular endothelium, it effects on vasodilatation and inhibition of platelet aggregation.

PGE_2: It effects such as contraction of bronchial, relaxation of smooth muscle, inhibition of gastric secretion, increasing gastric mucus secretion.

$PGF_{2\alpha}$: It found in smooth muscle and corpus luteum, which effects to the contraction of uterus

PGD_2 : It derived predominantly from mast cells, which acts vasodilation and inhibition of platelet aggregation

In addition to cytokines, metabolites of arachidonic acid also participate in the inflammatory process. Products produced by the metabolism include both cyclooxygenase products (prostaglandins, thromboxanes) and lipoxygenase products (leukotrienes, LTB). Prostaglandins, thromboxanes and leukotrienes have implicated in diverse physiological processes, including asthma, inflammation, carcinogenesis, hemostasis, parturition, maintenance of renal function, pain and fever. The current treatment of inflammation includes aspirin, nonsteriodal anti-inflammatory medications and dexamethasone. The sites of action of these

compounds range from inhibition of enzymes responsible for production of arachidonic acid metabolites to inhibit cytokine expression (Lantz *et al*., 2007; Nakao *et al*., 2002). The anti-inflammatory mechanisms of indomethacin are thought to suppress both COX-1 and COX-2 expression (Chien *et al.*, 2008). Cyclooxygenase activation resulting from high levels of PGE_2 can react with superoxide anions to form peroxynitrite (Cruz-Vega *et al*., 2002). Increased production of prostaglandins during an inflammatory response is achieved by induction of COX-2, which is mediated by NF-κB activation (Lantz *et al*., 2005; Shishodia *et al*., 2003).

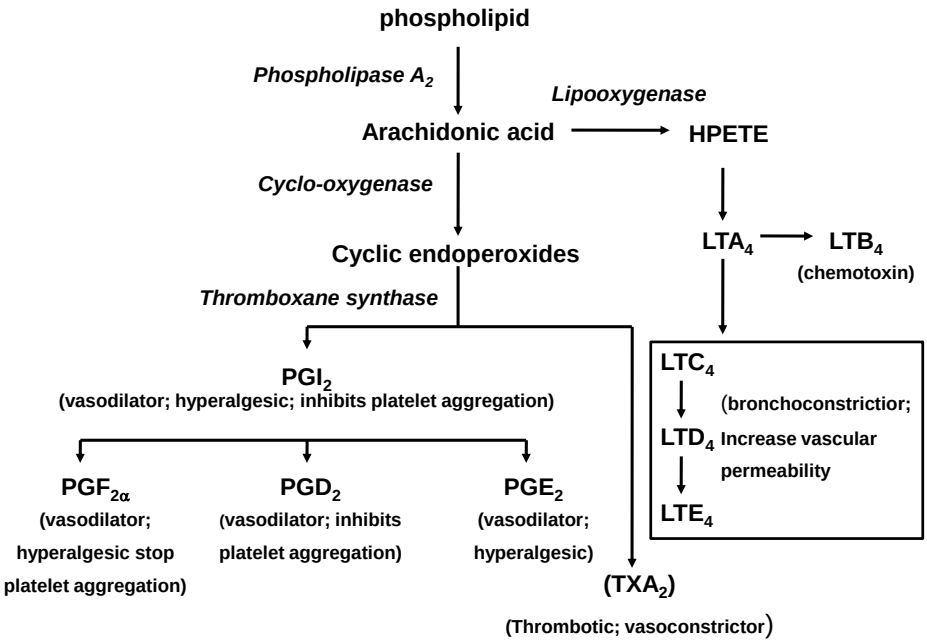

Scheme 1.1 Mediators derived from phospholipids and their actions. The eicosanoids as prostaglandin (PG), thromboxane (TX), leukotriene (LT) and prostacyclin (PGI_2) and hydroperoxyeicosatetraenoic acid (HPETE) (Source: modified from Rang *et al*., 1999).

Table 1.1 Plasma-derived inflammatory mediators.

Source: Inflammation. 2011. Wikipedia, the free encyclopedia (accessed July 7, 2008).

Name	**Produced by**	**Description**
Bradykinin	Kinin system	Induce vasodilation, increase vascular permeability, cause smooth muscle contraction, and induce pain.
C3	Complement system	Cleaves to produce C3a and C3b. C3a stimulates histamine release by mast cells, thereby producing vasodilation. C3b is able to bind to bacterial cell walls and act as an opsonin, which marks the invader as a target for phagocytosis.
C5a	Complement system	Stimulates histamine release by mast cells, thereby producing vasodilation. It is also able to act as a chemoattractant to direct cells via chemotaxis to the site of inflammation.
Membrane attack complex	Complement system	Combine and activate of this range of complement proteins forms the membrane attack complex, which is able to insert into bacterial cell walls and causes cell lysis with ensuing death.
Factor XII (Hageman Factor)	Liver	Activate three plasma systems involved in inflammation: the kinin system, fibrinolysis system, and coagulation system.
Plasmin	Fibrinolysis system	Break down fibrin clots, cleave complement protein C3, and activate Factor XII.
Thrombin	Coagulation system	Cleaves the soluble plasma protein fibrinogen to produce insoluble fibrin, which aggregates to form a blood clot. Thrombin can also bind to cells via the PAR1 receptor to trigger several other inflammatory responses, such as production of chemokines and nitric oxide.

Table 1.2 Cell-derived inflammatory mediators.

Source: Inflammation. 2011. Wikipedia, the free encyclopedia (accessed July 7, 2008).

Name	Source	Description
Enzymes		
Lysosome granules	Granulocytes	Break down a number of substances, some of which may be plasma-derived proteins which allow these enzymes to act as inflammatory mediators.
Vasoactive amine		
Histamine	Mast cells, basophils, platelets	Store in performed granules, release in response to a number of stimuli and causes arteriole dilation and increased venous permeability.
Cytokine		
IFN-γ	T-cells, NK cells	Act as antiviral, immunoregulatory, and anti-tumour. This interferon was originally called macrophage-activating factor, and is especially important in the maintenance of chronic inflammation.
IL-8	Primarily macrophages	Activate and chemo-attract of neutrophils.
TNF-α and IL-1	Primarily macrophages	Induce many similar inflammatory reactions: fever, production of cytokines, endothelial gene regulation, chemotaxis, leukocyte adherence, activation of fibroblasts.
Eicosanoid		
Leukotriene B4	Leukocytes	Mediate leukocyte adhesion and activation, allowing them to bind to the endothelium and migrate across it. In neutrophils, it is also a potent chemoattractant, and is able to induce the formation of reactive oxygen species and the release of lysosome enzymes by these cells.
Prostaglandins	Mast cells	Cause vasodilation, fever, and pain.
Soluble gas		
Nitric oxide	Macrophages, endothelial cells, neurons	Vasodilate, relaxes smooth muscle, reduces platelet aggregation, aids in leukocyte recruitment, exhibit antimicrobial activity in high concentrations.

1.2.2.2 Non- eicosanoids (cytokines and nitric oxide)

Cytokines (interleukins and tumor necrosis factors)

The interleukins (ILS) are biochemical produced by macrophages or lymphocytes in response to stimulation by an antigen or by products of inflammation. These IL are produced by a large variety of cells and have effects on many other cells, frequently independent of antigen stimulation. It is produced mostly by macrophage and antigen-presenting cells that have been stimulated by substances associated with tissue injury, including bacteria, end toxins (bacterial pyrogens), interferon and antigen. Many other IL affects the expression of adhesion molecules by neutrophil and endothelial cells and has effects on many other cells, frequently independent of antigen stimulation (Rote, 2002).

Tumor necrosis factor**: (**TNF)-α and β are cytokines that bind to common receptors on the surface of target cells and exhibit several common biological activities. Human TNF-α and TNF-β are of 17 and 25 kDa, respectively (Feghali and Wright, 1997). TNF is produced by activated macrophage, as well as mast cells, endothelial cells and some other cell types. Its secretion is stimulated by microbial products, such as bacterial end toxin and immunological complexes. The principal role of this cytokines in inflammation is in endothelial activation. TNF stimulates the expression of adhesion molecule on endothelial cells, resulting in increased leukocyte binding and recruitment, and enhances the production of additional cytokines and eicosanoids. TNF also increases the thrombogenicity of endothelium and causes aggregation and activation of neutrophils. Although TNF is secreted by macrophages and other cells at sites of inflammation, it may enter the circulation and act at distant sites to induce the systemic acute-phase reaction that is often associated with infection and inflammatory diseases. Components of this reaction include fever, lethargy and neutrophil release into the circulation (Kumar *et al*., 2007).

IL-1 and TNF-α, produced by macrophages as well as other cells, are central to development and amplification of inflammatory response. These cytokines activate endothelial cells to express adhesion molecules and release cytokines and chemokines. IL-1 and TNF-α are also among the mediators of fever, catabolism of muscle and shifts in protein synthesis (Murphy, 2008)

Nitric oxide (NO)

Nitric oxide (NO˙, formula N=O), a free radical gas, is formed in atmosphere during lightning storm. It is also formed in an enzyme-catalysed reaction between molecular oxygen and L-arginine in mammal as well as more primitive species. The convergence of several lines of research led to revelation that NO acts as a key signaling mechanism in the cardiovascular and nervous systems, and has important role in host defence (Rang *et al*., 1999).

NO has a variety of physiology function and it was independently first discovered in the endothelial cells. It is the endogenous activator of soluble guanylase catalate cycase, leading to cyclic GMP (cGMP) formation that function as a second messenger in many cells such as nerves, smooth muscle, monocyte and platelets (Rang *et al*., 1999).

Nitric oxide (NO) is also one of the inflammatory mediators causing inflammation in many organs. This inorganic free radical has been implicated in physiologic and pathologic processes, such as vasodilation, non-specific host defense and acute or chronic inflammation. NO is produced by the oxidation of L-arginine by NO synthase (NOS). There are three known isoforms of NOS; an inducible form iNOS or (miNOS or NOS-II) (that is expressed in macrophages and Kupffer cells, neutrophils, fibroblasts, vascular smooth muscle and endothelial cells in response to pathological stimuli such as invading microorganisms) and two so called; constitutive forms (cNOS) that are present under the physiological conditions in endothelium and neurons and are referred to as eNOS or (ecNOS or NOS-III) and nNOS or (ncNOS or NOS-I) respectively. The expressions of both enzymes are constitutive and nitric

oxide is produced at lower steady state levels (picomolar) (Hevel *et al*., 1991). The eNOS is not restricted to endothelium, also being present in the cardiac myocytes; renal mesangial cells; osteoblasts and osteoclasts; and in small amount in platelets. The eNOS produces NO responsible for vasodilation. The nNOS is present in central nervous system (CNS) that responsible to cell communication

In the contrast, iNOS that is approximately a thousand times greater (Rang *et al*., 1999) in macrophages and endothelial cells. It is involved in pathological aspects and is expressed in response to pro-inflammatory agents such as TNF-α, IL1-β and LPS (bacterial endotoxin) (Fang *et al*., 1997) in various cell types especially macrophages. It is responsible for production of NO in the inflammatory reaction, which has important role as a host defense following: damaging pathogenic DNA and as a regulatory molecule with homeostatic activities, regulating vascular tone and in signaling neurotransmission (Moncada *et al*., 1991) and as an important component of the antimicrobial armament of macrophages (Coleman *et al*., 2001). However, the overproduction of NO by iNOS may lead to circulatory shock, chronic inflammation and carcinogenesis (Hidaka *et al*., 1997). It can combine with other superoxide radicals and acts as a reactive radical which directly damages the function of normal cell (Tewtrakul and Itharat, 2007). NO and its functions have been shown to be more and more complex in physiological and pathological processes. For example, NO can regulate vascular tone, smooth muscle cell relaxation, neurotransmission, neuromodulation, apoptosis (Kim *et al*., 2004) and modulate mitochondrial energy generation (Moncada and Erusalimsky, 2002). NO also has been implicated in different mechanisms of diseases such as atherosclerosis (Barton and Haudenschild, 2001), asthma neurologic disorders and septic shock (Thiemermann *et al*., 1997).

Due to the role in the patho-physiological responses underlying some relevant inflammatory disorders, the possible the interaction between NO and PGs biosynthetic pathway has been described. In particular, increasing evidences suggested that there is considerable “cross talk” between NO and PG biosynthetic pathway, which involve an active back modulation

operated by reaction and end products including NO and PGs. However, the final effect of the interaction between NO and PG generating machinery occurs at multilevel. Indeed, NO may interact with directly with COX expression and PG biosynthesis (Mollace *et al*., 2005)

1.2.3 Methods for evaluating anti-inflammatory agents

As mentioned earlier, there are several processes of inflammation based on the duration of inflammation. During inflammation process, inflammatory mediators are released from the injured tissues consecutively. The methods for evaluating anti-inflammatory agents, therefore, should be aware of the stage of inflammation. Generally, anti-inflammatory agents should have effects on prime causative factors, blocking effect on initial reaction; thereby inhibit the established inflammation and effect on end results of established inflammation. There are two types of evaluating methods, including the *in vivo* and *in vitro* methods. Advantage/disadvantage must be considered in each method. The *in vivo* method requires the amount of test compound more than the *in vitro* method. On the other hand, the *in vitro* methods give many false positive results, which may lead to a wrong conclusion. However, the *in vitro* tests hint the certain clues regarding the possible site and mechanism of action, which can be used for screening a large number of compounds as a preliminary test (Naik and Sheth, 1976).

The *in vitro* method is quite simple and rapid, which affords as screening procedure for many compounds. It can perform via the chemical reactions of the expected biosynthesis and cell line-based assay. Most of the screenings of anti-inflammatory agents are focused on the enzymes involved in the prostaglandin biosynthesis especially cyclooxygenases, in which utilize arachidonic acid as precursor. Arachidonic acid is released from a phospholipid molecule by the enzyme phospholipase A_2 (PLA_2) and can also be generated from diacylglycerol (DAG) by diacylglycerol lipase. Arachidonic acid is a precursor in the production of eicosanoids by 1) cyclooxygenase and peroxidase leading to prostaglandin H_2, to produce prostaglandins, prostacyclin, and thromboxanes; 2) 5-lipoxygenase leading to 5-HPETE, which in turn is used to

produce the leukotrienes and 3) by epoxygenase, converting into hydroxyeicosatetraenoic acids (HETEs) and epoxyeicosatrienoic acids (EETs). Therefore, enzymes involved in this pathway are targets for the screening of anti-inflammatory agents.

Another model currently used, is the evaluation via the animal cell lines such as mouse (*Mus musculus*) cell lines model. Because of the power and widespread availability of gene-deletion technology, there are now many strains of mice in which genes encoding one or more pro-inflammatory mediators have been eliminated (Rosenberg and Gallin, 1984). Although these strains of mice have added substantially to the understanding of the role of various pro-inflammatory mediators *in vivo*, it is important to keep in mind that no one rodent model is absolutely perfect at all times and for all questions.

Microsomal sheep vesicles are rich source of COX-1 and can be used to explore whether the exogenous application of NO can augment further COX-1 activity (Salvemini *et al*., 1993). NO gas directly increases COX-1 activity of microsomal sheep seminal vesicles as well as murine recombinant COX-1; this leads to a remarkable 7-fold increase in PGE_2 formation (Salvemini *et al*., 1993). COX-2 is also activated by NO. Indeed, evidence exists that COX-2, but not inducible NO synthase, is induced in human fetal fibroblast by IL-1β. Therefore, IL-1β-stimulated fibroblasts can be used as a cellular model to investigate the effects of exogenous NO on COX-2 activity (Salvemini *et al*., 1993). Exposure of IL-1β-stimulated fibroblasts increased COX-2 activity by at least 4-fold. More recently, NO was shown to enhance the release of PGI_2 from endothelial cells, and by this mechanism, NO and NO-stimulated PGI_2 contributed to the marked antiplatelet effects associated with the administration of nitrovasodilators (Salvemini *et al*., 1996). This observation is also in keeping with earlier work illustrating synergies between the vascular action of NO and PGI_2. The ability of NO to directly activate COX-2 was supported by the evidence that NO increases the activity of purified recombinant COX-2 enzymes.

In 1978, Raschke *et al*. introduced the functional macrophage cell lines transformed by Abelson leukemia virus, namely the macrophage murine-like RAW264.7 cells

(ATCC TIB-71™) (Raschke *et al*., 1978). The RAW264.7 cell line is a mouse leukemic monocyte macrophage cell line. The whole cell lysate, which was established from tumor ascites induced in male mouse (*Mus musculus)* by intraperitoneal (*i.p*) injection of Abelson leukemia virus (A-MuLV). This cell line is currently widely used in the screening of anti-inflammatory agents. The RAW264.7 cells are negative for surface immunoglobulin, Ia and Thy-1.2. This line does not secrete detectable virus particles and is negative in the XC plaque formation assay. The cells will pinocytose neutral red and will phagocytose latex beads and zymosan. It can be induced with interleukin-1β, TNF-α, interferon-γ, lipopolysaccharide (LPS), for instance (Hemmrich *et al*., 2005). Then, macrophages are activated and respond with cascade of transcription output. Expression profiling has revealed thousands of genes that are induced or represses in macrophages in response to the classical activating agent LPS (Aung *et al*., 2006). The LPS activates the transcription factors such as NO, COX-2, NF-κB site, a C/ERP site, cAMP response element-1 (CRE-1), CRE-2, and AP-1 site and an E-box (Kang *et al*., 2006). This feature matches for screening inhibitors of corresponding genes and mechanistic study in the molecular level.

With regard to the RAW264.7 cell line, these cells have monocyte/macrophage characters. Generally, the macrophages are the main cells responsible for the innate immunity, and their activation by LPS and IFN-γ from host immune cell is important for controlling infections. However, the overwhelming activation of macrophages can cause a severe inflammatory state (Cho *et al*., 2008). Inappropriate or prolonged macrophage activation is largely responsible for the pathology of acute (e.g. septic shock) and chronic (e.g. rheumatoid arthritis, inflammatory bowel disease and chronic obstructive pulmonary disease) inflammatory conditions (Schroder *et al*., 2006). LPS is one of the major constituents of the outer membrane of gram-negative bacteria, and the immune system is constantly exposed to low levels of LPS through infections. LPS recognition and signal transmission are the key events aimed at elimination an invading pathogen. LPS induces an acute phase stress response characterized by

translocation of NF-κB into the nucleus of cells, subsequently inducing the expression of a variety of proteins, including inflammatory mediators (Cobb *et al*., 2000).

1.3 Literatures Review

1.3.1 Chemotaxonomy of *Croton* species

The genus *Croton* belongs to the Subfamily Crotonoideae, tribe Crotoneae of the Euphobiaceae family. This genus is comprised of around 1300 species, which are widely distributed in tropical regions of the old and new worlds. Several species have a long role in the traditional use of medicinal plants in Africa, Asia and South America (Salatino *et al*., 2007). There are 800 or more species, pantropical with the center of diversity (species and sections) in America. In Asia there are slightly less than 100 species, and 30 species have been reported in Thailand (Welzen, editor, 2010).

In Thailand, *Croton* species are available including: (Welzen, editor, 2010).

1. *C. acutifolius* Esser
2. *C. argyratus* Blume.
3. *C. bonplandianus* Baill.
4. *C. cascarilloides* Raeusch
5. *C. caudatus* Geiseler
6. *C. columnaris* Airy Shaw
7. *C. crassifolius* Geiseler
8. *C. decalvatus* Esser
9. *C. delpyi* Gagnep.
10. *C. griffithii* Hook. f.
11. *C. hirtus* L'Hérit
12. *C. hutchinsonianus* Hosseus
13. *C. kerrii* Airy Shaw
14. *C. kongensis* Gagnep.
15. *C. kongkandanus* Esser
16. *C. krabas* Gagnep.
17. *C. lachnocarpus* Benth.
18. *C. longissimus* Airy Shaw
19. *C. mekongensis* Gagnep.
20. *C. phuquocensis* Croizat
21. *C. poilanei* Gagnep.
22. *C. poomae* Esser
23. *C. robustus* Kurz
24. *C. roxburghii* N.P.Balakr
25. *C. sepalinus* Airy Shaw
26. *C. stellatopilosus* Ohba
27. *C. thorelii* Gagnep.
28. *C. tiglium* L.
29. *C. wallichii* Müll.Arg.
30. *C. santisukii* Airy Shaw

From the review of *Croton* species found in America, Africa and Asia, the chemical structures reported include as diterpenoids, volatile oil, pentacyclic triterpenoids, steroids, alkaloids, proanthocyanidins and other compounds. However, the chemical distribution these *Croton* species are summarized and shown in Fig. 1.1. It can be seen that the *Croton* genus produce various classes of compounds such as diterpenoids, taspine, benzylisoquinoline-like alkaloids and volatile oils. Interestingly, the most common class of compounds of *Croton* species in Asia is diterpenoids including labdanes, kauranes and trachylobane structures.

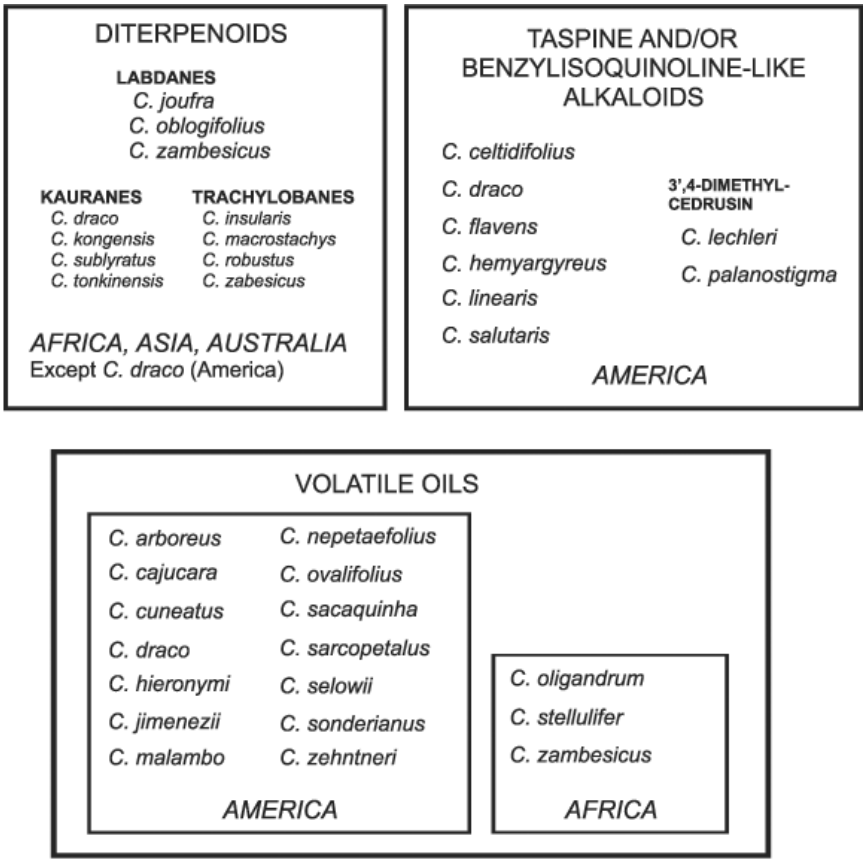

Figure 1.1 The chemical distribution in *Croton* species (Salatino *et al*., 2007).

1.3.2 Chemical structure of diterpenes: labdanes, clerodanes and kauranes

The diterpenes could be identified simply as naturally occurring compounds with 20 carbon atoms and it arises from geranylgeranyl diphosphate, (GGPP) which is formed by addition of a further IPP molecule to farnesyl diphosphate in the same as the lower terpenoids (Scheme 1.2). Diterpenes can be classified as acyclic diterpenes and cyclic diterpenes. Their structures are from different conformation and can be rationalized by considering the different type of cyclization of GGPP. The biosynthesis of diterpenes through GGPP has been revealed by the studies on the enzymes. This section focuses on the chemical structures arising from the cyclization of GGPP to cyclic diterpenes including labdanes and *ent*-labdane, clerodanes and *ent*-kauranes types (MacMillan and Beale, 1999).

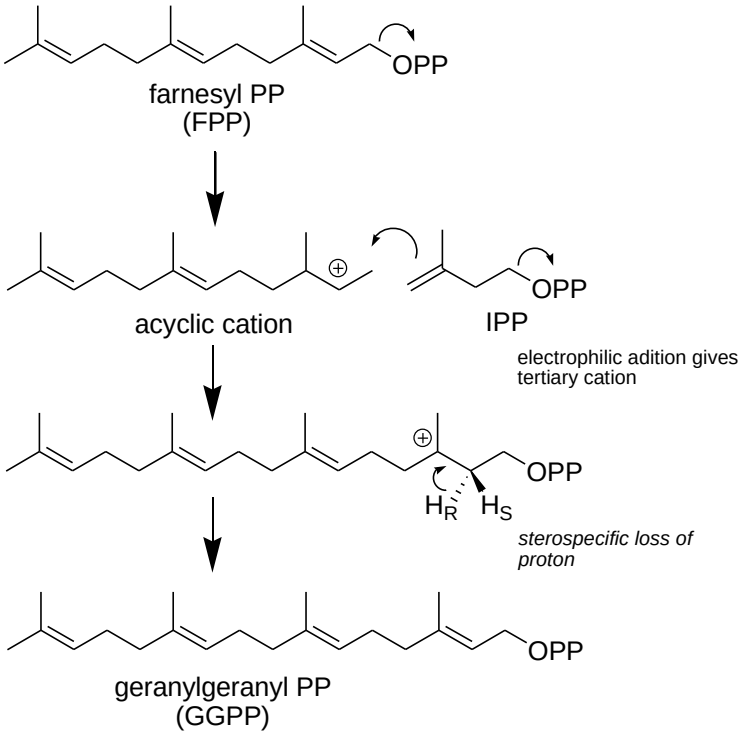

Scheme 1.2 The geranylgeranyl PP (GGPP) formation (Dewick, 2002).

The cyclization reactions of GGPP mediated by carbocation formation, plus the potential for Wagner–Meerwein rearrangements, allow many structural variants of diterpenoids to be produced. The cyclic diterpenes are from the cyclization of GGPP based on the chemical conformation. The protonation of the 14, 15-double bond of *E*,*E*,*E*-GGPP, followed by the attack of C-10 on C-15, then C-7 on C-11, give the four possible factions that are shown in the scheme 1.5. The chair-chair conformation (1) gives the 8-carbonium ion (2) of copalyl diphosphate (CPP, (3)) with the "normal" *anti,anti* absolute stereochemistry (Type B-1). The antipodal chair-chair conformation (4) of GGPP gives the 8-carbonium ion (5) of *ent*-copalyl diphosphate (*ent*-CPP, (6)) with the enantiomeric *anti,anti* absolute stereochemistry (Type B-2). The chair-boat conformation (7) of GGPP gives the 8-carbonium ion (8) of the "normal" *syn*-CPP (9) (Type B-3). The chair-boat conformation (10) of GGPP gives the 8-carbonium ion (11) of the *syn*-*ent*-CPP (12) (Type B-4).

Labdanes, derived via (2), and *ent*-kauranes, derived via (5), have wide spread occurrence but few definitive biosynthetic studies have been reported. It has been suggested that they may be derived from GGPP by a two-step process via monocyclic intermediates. The co-occurrence of enantiomeric labdanes is suggested but no enzymological studies on this point have been reported.

Clerodanes comprise a large family, considered to be derived from rearrangement of the 8-carbonium ions (2) and (5). As shown in Scheme 1.6. Trans-clerodanes can, in principle, be the products of concerted 1, 2-shifts including C-19 to C-5 (sequences a). In the case of the cis-clerodanes, a similar series of shifts cannot be concerted. For a stereoelectronic shift of C-18 to C-5, sequences b would require a conformational change in ring A, A consequence would be the prediction that the 3β-H of the bicyclic intermediates is lost in the formation of the 3, 4-dehydro-trans-clerodanes and that the 3α-H is lost in the formation of the 3, 4-dehydro-cis-clerodanes.

Kaurane and ent-kaurane are derived from *ent*-CPP (6) to *ent*-kaur-16-ene (13), this reaction is shown in the Scheme 1.7. This *ent*-kaur-16-ene gives rise to the other compound of naturally occurring *ent*-kauranoid diterpenes.

For the cyclic diterpene, the formation can be rationalized by considering the different types of GGPP cyclization. There are four kinds of cyclases (synthases) that have been reported, which are described below (MacMillan and Beale, 1999).

1. Casbene synthase catalyzes the formation of (1*S*,3*R*)-casbebe by ionization of the diphosphate of GGPP and attack on the allylic 1-carbonium by the terminal double bond.

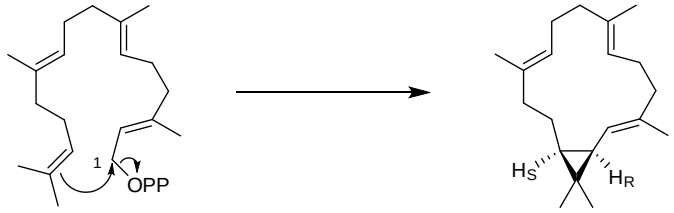

GGPP Casbene Equation **(1)**

2. *ent*-Copalyl diphosphate synthase catalyzes the formation of *ent*-copalyl diphopshate (ent-CPP) by proton-induced cyclization.

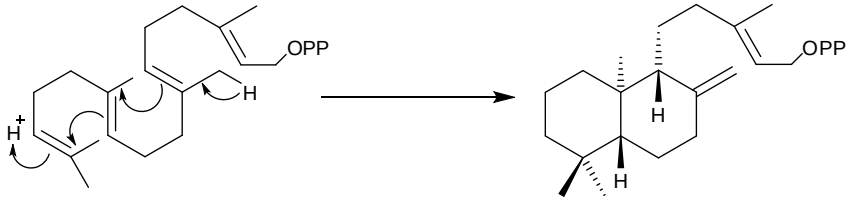

GGPP *ent*-copalyl diphosphate (*ent*-CPP) Equation **(2)**

3. Taxadiene synthase catalyzes the formation of taxa-4,11-diene by a series of cyclization steps initiated by ionization of the diphosphate and continued by proton-induced cyclization.

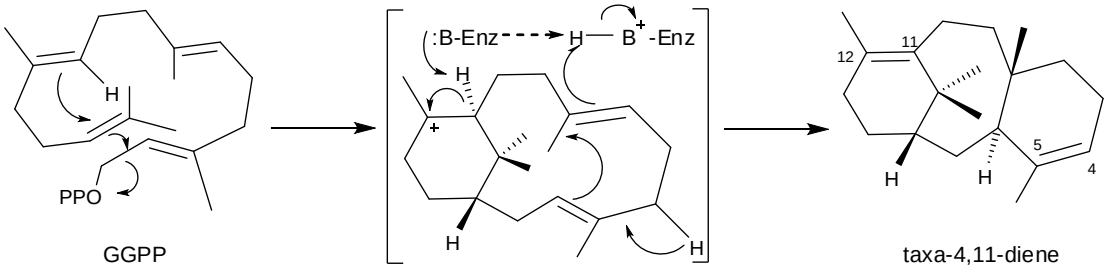

GGPP taxa-4,11-diene

Equation **(3)**

4. Abietadiene synthase catalyzes the formation of abieta-7,13-diene by a series of cyclization steps, initiated by proton-induced cyclization and continued by ionization of the diphosphate.

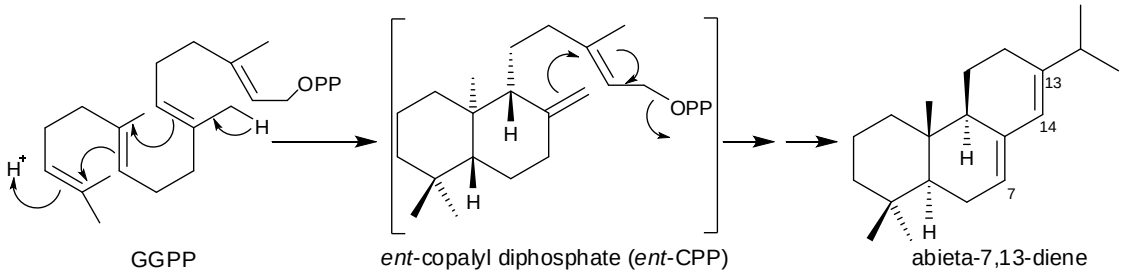

Scheme 1.3 The formation of abieta-7,13-diene.

5. *ent*-Kaurene synthase is not a GGPP cyclase, but catalyzes the formation of *ent*-kaur-16-ene from *ent*-CPP by diphosphate-induced cyclization. Thus, in contrast to abietadiene, *ent*-kaur-16-ene is formed from GGPP in two distinct steps catalyzed by two enzymes: *ent*-CPP synthase and *ent*-kaurane synthase.

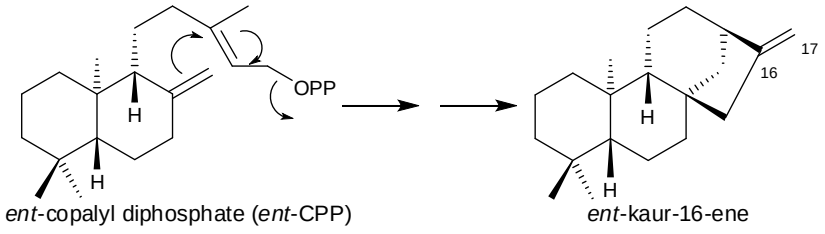

Scheme 1.4 The formation *ent*-kaur-16-ene.

Type B-1: chair-chair-"normal"

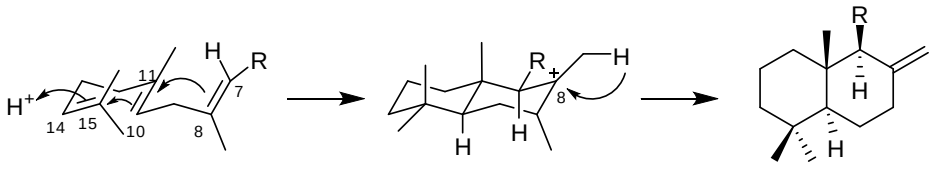

(1) (2) (3) CPP

Type B-2: chair-chair-"antipodal"

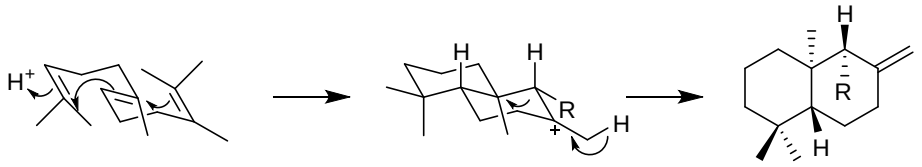

(4) (5) (6) *ent*-CPP

Type B-3: chair-boat-"normal"

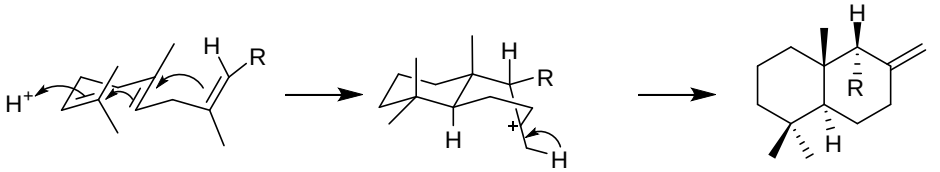

(7) (8) (9) *syn*-CPP

Type B-4: chair-boat-"antipodal"

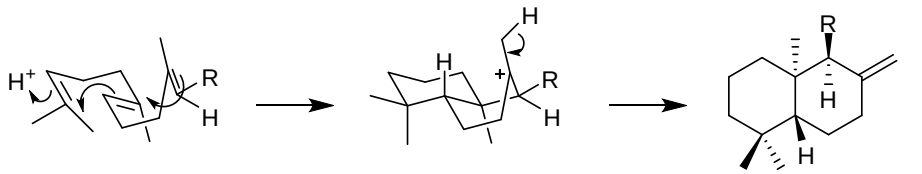

(10) (11) (12) *syn-ent*-CPP

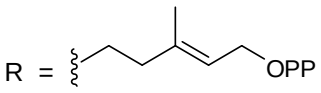

Scheme 1.5 The cyclization of GGPP.

Source: MacMillan and Beale, Comprehensive of Natural Product Chemistry, 1999.

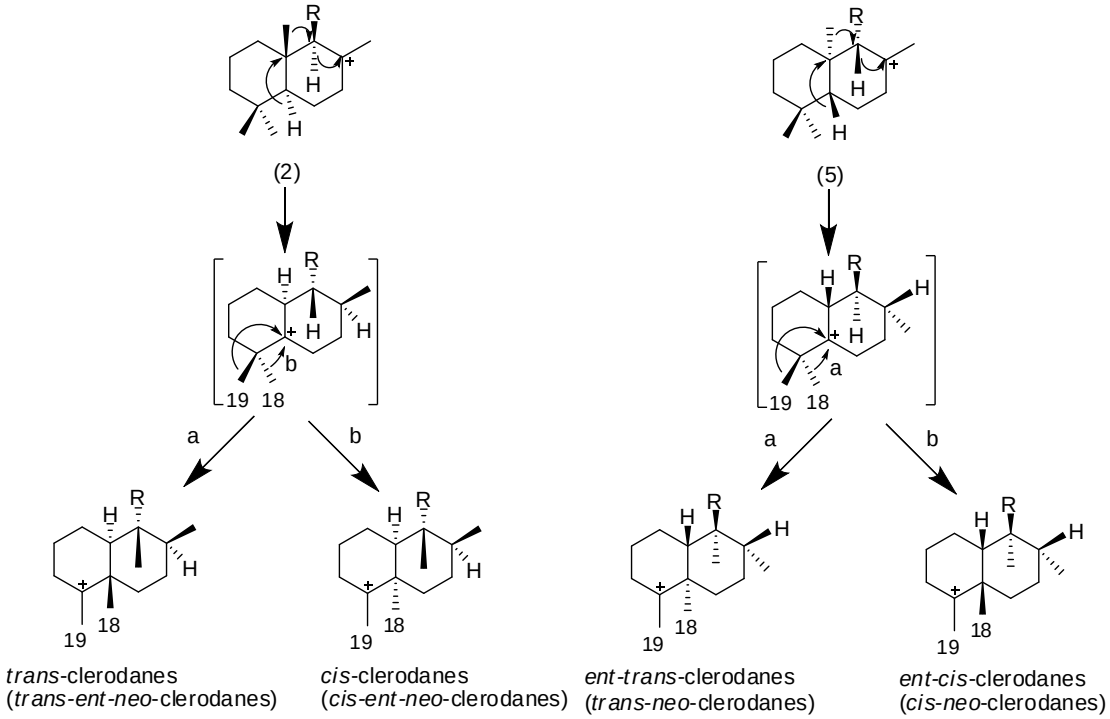

Scheme 1.6 The clerodanes conformation.

Source: MacMillan and Beale, Comprehensive of Natural Product Chemistry, 1999.

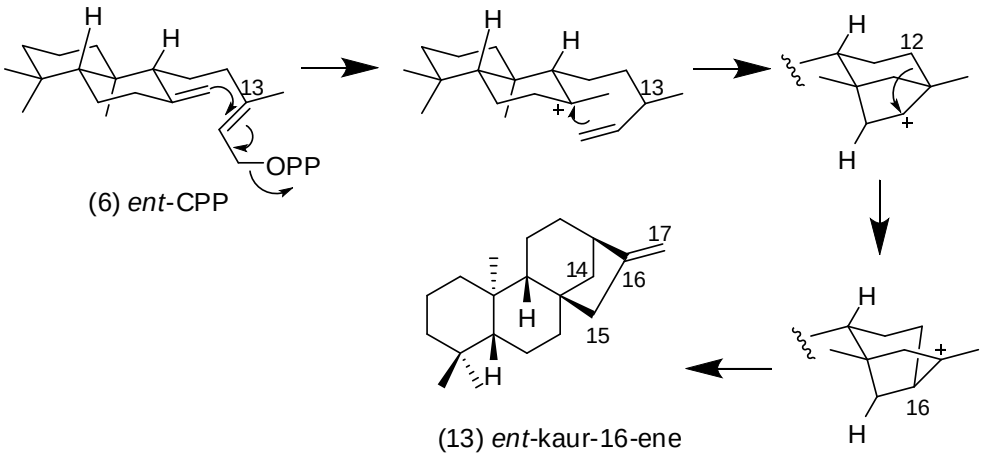

Scheme 1.7 The *ent*-kaur-16-ene formation.

Source: MacMillan and Beale, Comprehensive of Natural Product Chemistry, 1999.

1.3.3 Plaunoi (*Croton stellatopilosus* Ohba)

Plaunoi or *Croton stellatopilosus* Ohba is formerly known as *Croton sublyratus* Kurz. This plant is a tropical plant, belonging to the Euphorbiaceae family (Fig 1.2). Plaunoi is distributed in Thailand from Lop Buri (Khao Thungna), Sa Kaeo, Prachin Buri (Kabinburi), Chachoengsao, and Chon Buri (Khao Khieo). The botanical description of *C. stellatopilosus* is shrub to 6 m tall**,** branching from base. This species belongs to a complex of several similar Southeast Asian species. The characteristics of Plaunoi are stellate-dendritic hair (Esser and Chayamarit, 2001); the leaves often obovate to sometimes sub-panduriform (constricted near their base), the leaves, including the petiole, usually neither completely pubescent nor completely glabrous but with scattered hair; their basal gland more on the blade surface than the midrib; and a tendency toward strongly proterogynous flowering and fruiting, the fruit often even developing when the staminate flowers are still in bud (This information was cited in the web site of Flora of Thailand (http://www.nationaalherbarium.nl/).

Plaunoi was under the name of *C. sublyratus* Kurz until 2001. The botanical name was changed based on its taxonomic characteristics by Esser and Chayamarit (2001). The evidence for changing the name from *C. sublyratus* to *C. stellatopilosus* was described. The *C. sublyratus* as the plant of Thailand was originally identified from the Airy Show (1972) and compared with the plants from the Andaman Island of India. It appeared that *C. sublyratus* agreed with the Thai plant in the distinctly obovate-panduriform leaf shape (usually less distinctly so in *C. wallichii*, a species from south-western and peninsular Thailand). However, the Thai plant collections differ in at least character from the Andaman plants. First, the basal leaf glands are sessile and flat (distinctly protruding to nearly stipitate in *C. sublyratus*), and many plants collected with peculiarly cone-like, dense, pyramidal inflorescence buds. Their characteristics are not found in the Andaman species. Second, the leaves of Thai collection are generally slightly smaller. Therefore, both of the characteristics of plant should be sufficient to separate plants from

the two countries. *C. stellatopilosus* was described from south-eastern Thailand and is the correct name for the source plant of plaunotol in the strictest sense (Esser and Chayamarit, 2001).

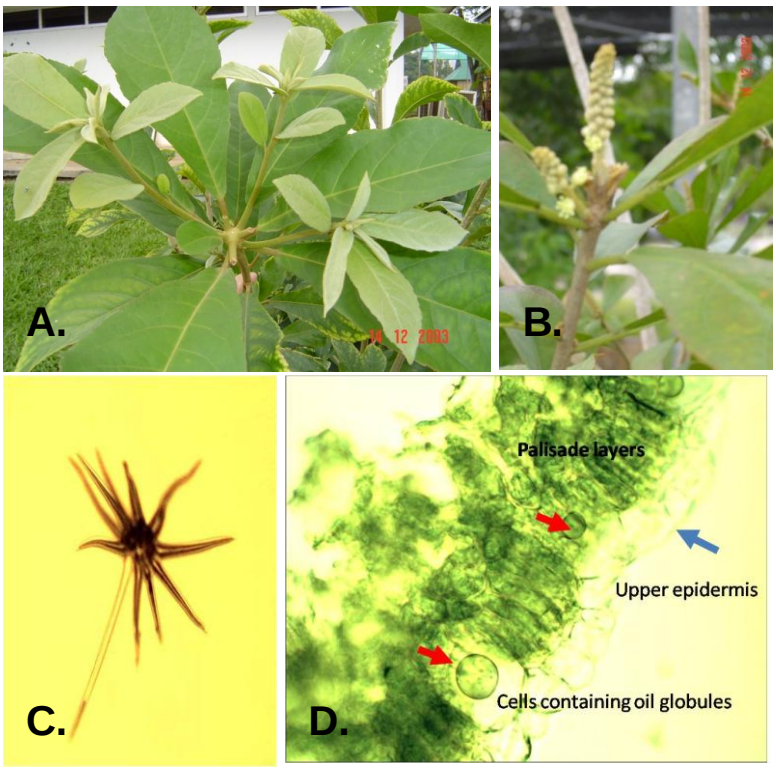

Figure 1.2 Botanical aspects of *C. stellatopilosus* Ohba (Euphorbiaceae). A, pubescent leaves in young plant; B, inflorescences; C, stellate dendritic hair, a major characteristic of plaunoi; D, transverse section of mature leaf (x400): red arrows indicate oil cells containing plaunotol in palisade layer.

1.3.4 Chemical constituents of *C. stellatopilosus*

The investigation of chemical constituent began in 1978 by Ogiso and co-workers. They isolated and identified plaunotol as an anti-peptic ulcer substance from the acetone extract of stem of *C. stellatopilosus* (Ogiso *et al*., 1978). Later Kitazawa and his co-workers in 1980 had found and isolated other compounds with antiulcer activity. There are several diterpenes including diterpene lactones, namely, plaunol A, plaunol B, plaunol C, plaunol D and plaunol E.

Additionally, furanoditerpene of clerodane type; namely plaunolide (Takahashi *et al*., 1983), labdane diterpene; ent-13α-hydroxy-13-epimanool and kaurane diterpene; ent-16β, 17-dihydroxykaurane (Kitazawa and Ogiso, 1981), esters of 18-hydroxygeranylgeraniol (Kitazawa *et al*., 1982) were reported. The chemical structures of compounds, isolated from *C. stellatopilosus*, are listed in Table 1.3.

Table 1.3 The chemical structures of compounds isolated from *C. stellatopilosus* Ohba.

Plant part/Group	Chemical structure/Name
Stem **Acyclic diterpene**	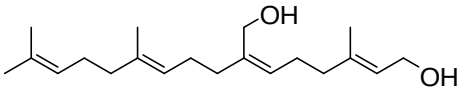 Plaunotol (18-hydroxy geranylgeraniol) (Ogiso *et al*., 1978)
Clerodane diterpene	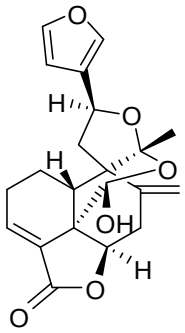 Plaunol A (Kitazawa *et al*., 1979)
	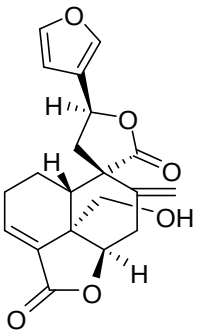 Plaunol B (Kitazawa *et al*., 1979; Kitazawa *et al*., 1980)

Table 1.3 continued

Plant part/Group	Chemical structure/Name
	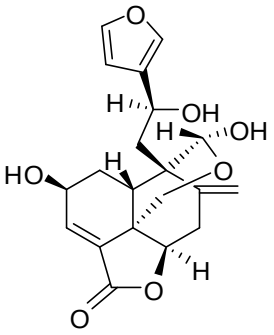 Plaunol D (Kitazawa *et al*., 1980) 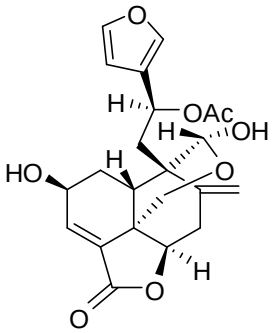 Plaunol E (Kitazawa *et al*., 1980) 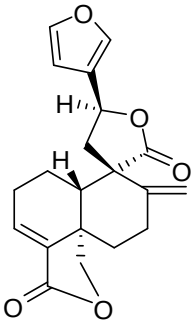 Plaunol F (Plaunolide) (Takahashi *et al*., 1983)

Table 1.3 continued

Plant part/Group	Chemical structure/Name
Labdane diterpene	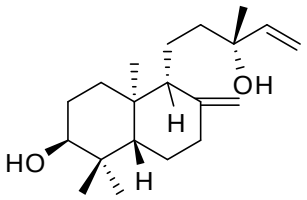 ent-13α-hydroxy-13-epimanool (Kitazawa and Ogiso, 1981)
Kaurane diterpene	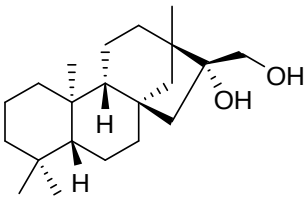 ent-16β, 17-dihydroxykaurane (Kitazawa and Ogiso, 1981)
Ester of 18-hydroxy geranylgeraniol	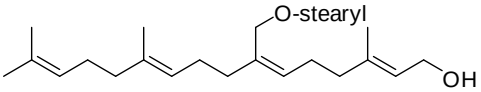 Geranylgeraniol ester A (Kitazawa *et al*., 1982) 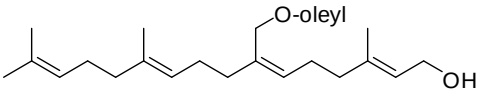 Geranylgeraniol ester B (Kitazawa *et al*., 1982) 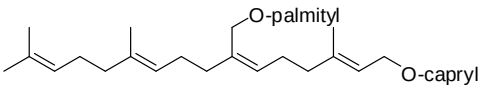 Geranylgeraniol ester C (Kitazawa *et al*., 1982) 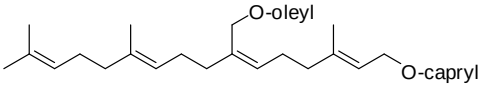 Geranylgeraniol ester D (Kitazawa *et al*., 1982) 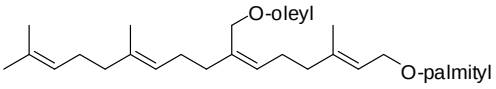 Geranylgeraniol ester E (Kitazawa *et al*., 1982) 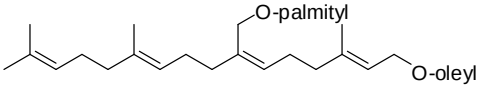 Geranylgeraniol ester F (Kitazawa *et al*., 1982)

1.3.5 Isolation of plaunotol and other diterpenes from *C. stellatopilosus*

The investigation of plaunotol, which is a major compound of *C. stellatopilosus,* was performed in acetone extract from Plaunoi stems in 1978. Chromatographic separation led to the isolation of plaunotol (Ogiso *et al*., 1978). Ogiso and his co-workers reported a method for the isolation plaunotol from a crude drug of *C. stellatopilosus*. The crude drug (81.5 kg) as starting material was first extracted three times with acetone under reflux. After evaporation of the solvent, the residue was dissolved in 10 L of 80% (v/v) aqueous methanol and washed with *n*-hexane. The concentrated methanol layer was poured into 40 L of benzene and washed with aqueous sodium hydrogen carbonate solution. After washing, the benzene solution was evaporated and the residue was extracted with ether. The ether soluble fraction was isolated by column chromatography over a silica gel (3 kg) column, eluted with benzene and ethyl acetate. This method yielded plaunotol (53 g). In addition this method afforded the furanoditerpenes from the ether residue fraction after separation by silica gel column chromatography using chloroform and methanol as eluent. The procedure for obtaining plaunotol and furanoditerpenes is shown in Scheme 1.8.

The process of plaunotol isolation was reported and registered to the World Health Organization or WHO under code CS-684. However, the modified methods for plaunotol isolation were reported in 1992 by Nilubol *et al*. and was patented a technique for extraction and purification of plaunotol. This protocol was patented in the USA (patented No. 5264638). The three processes for extraction and purification of plaunotol are described below.

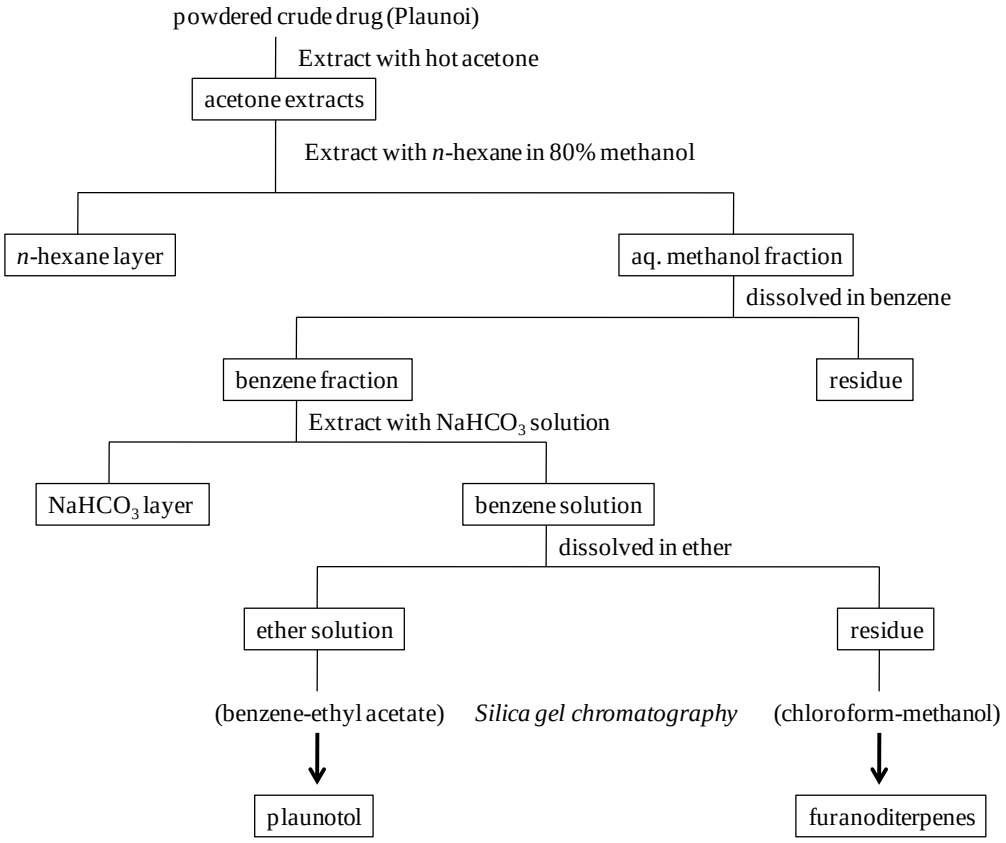

Scheme 1.8 The procedure to obtain plaunotol and furanoditerpene.

Method 1

This method started from 6 kg of dried leaves of *C. stellatopilosus*. The dried leaves were extracted with 60 l of methanol at 60°C for 120 min in an agitated extracting vessel with a working volume of 60 l. The methanol extract was evaporated to dryness and the residue was extracted with 6 l of chloroform. Then the chloroform soluble fraction was treated with by 400 g of activated charcoal under stirring for 60 min. The activated charcoal was removed by filtration and the filtrate was evaporated to dryness to yield 250 g of a semisolid residue. The residue was dissolved in 3 l of 80% v/v ethanol in water mixture and filtered. The filtrate was partitioned with 6 l of *n*-hexane and the ethanol layer was separated and evaporated to 1.5 l and 0.5 l of 10% aqueous sodium hydroxide solution was added. The mixture was heated at 110° C.

for 15 minutes. After the mixture had been cooled to room temperature, 0.5 l of water was added and the mixture was extracted with 1.5 l of *n*-hexane. The hexane phase was separated, dried over anhydrous sodium sulfate, filtered through a layer of 200 g of fullers' earth and the solvent was distilled off giving 10.5 g of plaunotol. These processes of isolation plaunotol are shown in Scheme 1.9.

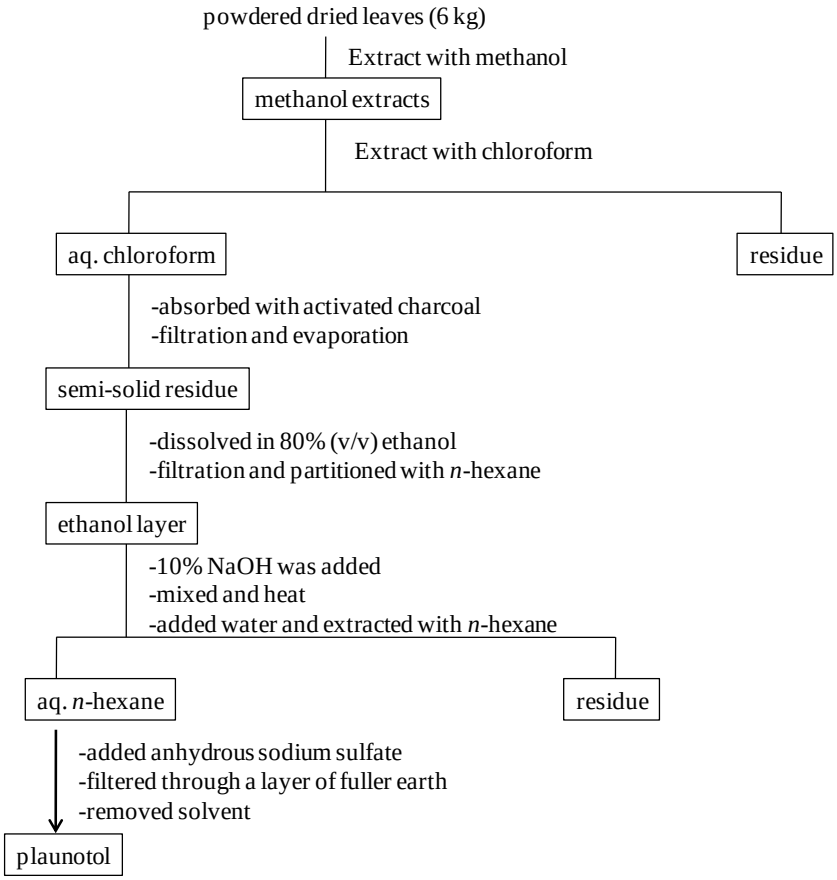

Scheme 1.9 Plaunotol isolation: method 1.

Method 2

In this method, the step of isolation was similar the first method (Scheme 1.9). This method was repeated, except that the decolorization step with activated carbon was omitted

and the solution in 80% ethanol was centrifuged before filtration, giving the diterpene alcohol, plaunotol with similar yields.

Method 3

The third method disclosed in the first method, it was repeated as follows. The dried leaves 6 kg were refluxed with 40 l of methanol. The methanol extract was evaporated leaving a crude extract which was dissolved in 1.0 l of 90% methanol and washed with *n*-hexane. The methanol layer was evaporated and the residue was suspended in 0.5 l of water and extracted with diethyl ether. The ether layer was washed with a 5% solution of aqueous sodium carbonate and dried with anhydrous sodium sulfate. The solvent was evaporated to obtain an oily residue, which was purified by column chromatography over silica gel, eluting with ethyl acetate/benzene (10% by volume) and later with ethyl acetate/benzene (30% by volume). Fractions containing the active compound were combined and the solvent was distilled off leaving 3.4 g of the pure diterpene alcohol plaunotol. These processes of isolation plaunotol are shown in scheme 1.10.

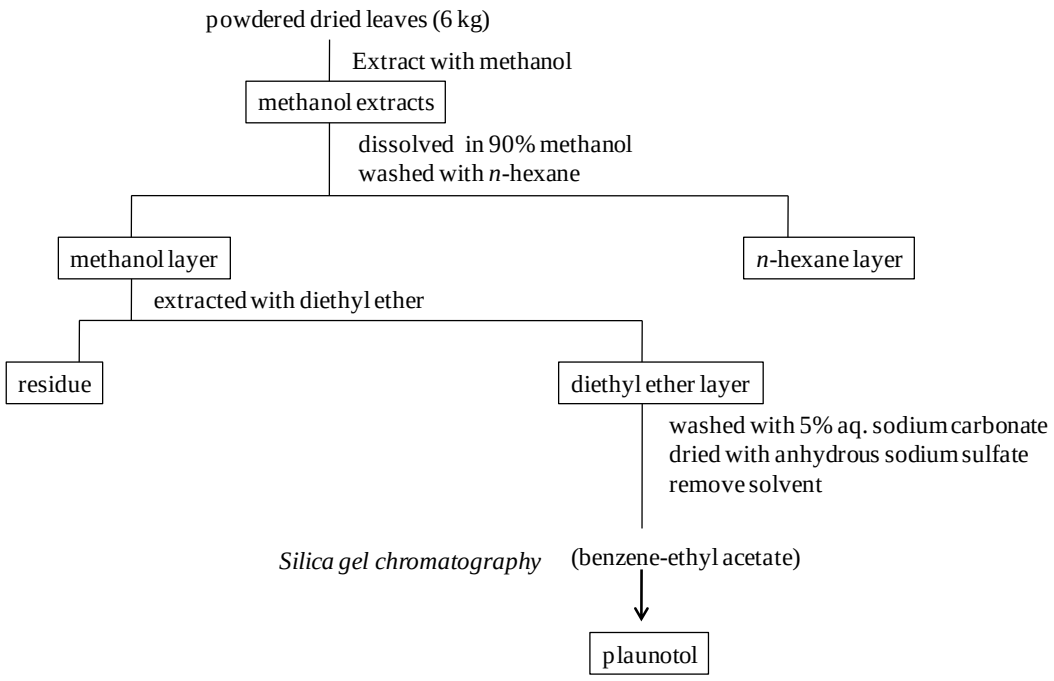

Scheme 1.10 Plaunotol isolation: method 3.

However, both of isolation procedures by Ogiso *et al*., 1978 and Nilubol, 1992 relied on the several steps of chemical solvent for extractions and separations over silica gel column chromatographic technique. For that reason, the present yield of plaunotol may be low. The many steps of isolation and purification affected the yielding of this compound. Furthermore, the many steps lead to high cost for isolation of plaunotol. Therefore, the development of plaunotol extraction and purification are still challenges.

1.3.6 Pharmacological activities

The pharmacological activities of plaunotol were investigated on acute gastric and duodenal ulcers and facilitation of the healing of chronic gastric ulcer in several experiments. The studies for acute gastric ulcer was performed in induced-gastric models when stimulated with reserpine, stress aspirin, indomethacin and pyrolous ligation. Plaunotol showed significant inhibitory effects at intraduodenal dose of 300 mg/kg. However, plaunotol exhibited a broader spectrum than over investigated anti-ulcer drugs such as cetraxate, gefarnate and sucralfate, which have been used for mucosal protective agents (Ogiso *et al*., 1985). The effect of plaunotol on chronic ulcer was studied in acetic-induced gastric ulcer in dog and clamp-induced gastric ulcer in rat as models. The results of their study revealed that plaunotol facilitated the healing of chronic ulcer significantly in rats and dogs (Ogiso *et al*., 1985).

Thus, plaunotol prevents gastric mucosal injury and has gastro-protective actions through various mucosal defensive factors. In 2002, Koga and co-workers investigated the effect of plaunotol when combined with clarithromycin or amoxicillin against *H. pylori in vitro* and *in vivo* studies. For *in vitro* studies, when combined with clarithromycin, plaunotol was shown to have synergistic activity. When combined with amoxicillin, plaunotol showed additive activity against 10 out of 14 strains of *H. pylori*. In a C57BL/6 mouse gastritis model infected with *H. pylori* SS1, the plaunotol-clarithromycin and plaunotol-amoxicillin combinations both also exhibited the synergistic effects, which allowed the effective dose of clarithromycin to be reduced

when co-administered with plaunotol. These results suggest that plaunotol may have a useful role in combination with anti *H. pylori* drugs in the treatment of *H. pylori*-associated diseases (Koga *et al*., 2002).

Moreover, plaunotol exhibited anti-bacterial activity against *Staphylococcus aureus*, which isolated from the patients with atopic dermatitis (Matsumoto *et al*., 1998). It acted on bacterial cell membrane (Inoue *et al*., 2004). Plaunotol also has been tested in cancer cell line including MKN-45, MKN-74 and AZ-521. The results showed that plaunotol inhibited growth of three types of cancer cells by mechanism of apoptosis (Yamada *et al*., 2007). Investigation of plaunotol in human colon cancer cell line (DLD1) indicated that it showed the strong inhibition of cell proliferation by inducing apoptosis (Yashikawa *et al*., 2009).

Effects of plaunotol on inhibition of inflammatory mediators' productions have been reported from *in vitro* and *in vivo* studies. Plaunotol exhibited gastro-protective activity in gastric lesion. Plaunotol was proposed to have mechanisms via increase the production of PGE_2 (Ushiyama *et al*., 1987) and endogenous secretin releasing (Shiratori *et al*., 1993). In animal experiments, plaunotol inhibited an enzyme neutrophil elastase and TNF-α production (Murakami *et al*., 1999). Pre-treatment with plaunotol in serum-starved rat gastric epithelial (RGM1) cells model revealed the mechanism of gastro-protective effect of plaunotol. Plaunotol induced COX-2 expression and increased PGE_2 production via activation of the nuclear factor kappa-B (NF-κB) and cyclic AMP response element (CRE) sites of *COX-2* gene promoters (Fu *et al*., 2005).

Plaunotol has a therapeutic effect on gastritis induced by *H. pylori* as demonstrated in the human gastric cancer cell lines, MKN45 cells. Plaunotol inhibited growth of *H. pylori* at high dose (24-48 μg/ml) when induced the IL-8 secretion with *H. pylori* infection. Co-culture MKN45 cells with plaunotol, IL-8 secretion were inhibited in a dose-dependent manner (Takagi *et al*., 2000). From these studies, it can be concluded that plaunotol prevents gastric mucosal injury through various mucosal defensive factors.

Applications of plaunotol in clinical trial have been reported. Side effect of peptic-ulcer patients, who administered long-term omeprazole, and proton pump inhibitor, is hypergastrinemia. Randomized clinical trial of administration plaunotol with omeprazole indicated that plaunotol significantly inhibited hypergastrinemia (Kaneko *et al*., 1995). They proposed that the mechanism may go through a brain-gut hormone affecting gastrin release. Hepatitis C patients, who were treated with interferon, generally suffered from stomatitis. Experiment in randomized open-label trial revealed that oral administration of plaunotol at 240 mg/day before interferon treatment and continued throughout the 24-week interferon therapy period significantly decrease the symptoms of stomatitis (Nomura *et al*., 1997).

CHAPTER 2

RESEARCH METHODOLOGY

Study on the anti-inflammatory constituents from *Croton stellatopilosus* leaves has been extracted stepwise from extraction, isolation of the compounds and structure elucidation, by means of spectrometry. Cell-based assay for anti-inflammatory activity was used to guide the active fractions throughout the isolation process. To study the inflammatory mechanism, inhibition of mRNA expressions of *iNOS*, *COX-1* and *COX-2* were investigated using quantitative real-time polymerase chain reaction (qRT-PCR).

2.1 Plant materials

Mature leaves of *C. stellatopilosus* Ohba were supplied from Tipco Foods (Thailand) Public Co. Ltd., Klong Whale, Prachupkhirikhan, Thailand. A voucher specimen was deposited at Department of Pharmacognosy and Pharmaceutical Botany, Faculty of Pharmaceutical Sciences, Prince of Songkla University, Thailand. After cleaning, leaves were dried at 50 °C for 24 h in hot air oven, ground to powder and passed through a sieve No. 120.

2.2 Chemicals

Authentic plaunotol was isolated from Kelnac® (Sankyo Co. Ltd Tokyo, Japan), a soft gelatin capsule containing 80 mg plaunotol in 240 mg corn oil by silica gel chromatography. Plaunotol was eluted with hexane: *n*-propanol; 24:1. Fractions containing plaunotol were collected. Its structure was confirmed by ^{1}H-NMR and its purity, determined by gas chromatography, was about 95%.

Chemicals used in this study were of analytical grade. Solvents were of analytical and commercial grades. Commercial grade solvents were distilled prior to use. Glacial acetic acid, chloroform, dichloromethane, ethanol (95%, absolute), ethyl acetate, hexane, *n*-propanol, isopropanol, dimethylsulfoxide, hydrochloric acid (37% w/w) were purchased from Lab-scan Asia Co., Ltd., Bangkok, Thailand. Anisaldehyde was from Fluka, Buchs, Switzerland. Anhydrous sodium sulfate was from Fisher scientific, Leicestershire, England. Sulfuric acid was obtained from J.T. Baker, New Jersey, USA. TLC plate (Silica gel GF_{254}) and silica gel 60 (SiO_2 60, 230-400 mesh) were from Merck, Darmstadt, Germany.

For cell-based assays, all reagents were of biotechnological grade. Caffeic acid phenethylester (CAPE), indomethacin, phosphate-buffered saline (PBS) were obtained from Sigma, Missouri, USA. 3-(4, 5-dimethyl-2-thiazolyl)-2, 5-diphenyl-2H-tetrazolium bromide (MTT), fetal calf serum, lipopolysaccharide (LPS; *Escherichia coli*) oss: B5 L 4005 (purified by trichloroacetic acid extraction), L-nitroarginine, Roswell Park Memorial Institute 1640 medium (RPMI 1640 medium), trypan blue and trypsin-EDTA were purchased from Gibco BRL, California, USA. The murine macrophage-like RAW264.7 cells was obtained from Cell Lines Service, Heidelberg, Germany. Penicillin G (100 U/ml) plus streptomycin (100 μg/ml) was supplied by Invitrogen®, California, USA.

For gene expression profile, agarose D-1 Low EEO was from the Research Organics, Ohio, USA. DNA ladder (0.1-10.0 kb) was purchased from Sib-enzyme, Novosibirsk, Russia. Ethidium bromide was obtained from Bio Basic INC, Ontario, Canada. β-Mercaptoethanol was from Sigma, Missouri, USA. RNeasy mini kit, used for total RNA isolation, was purchased from Qiagen, Hilden, Germany. SuperScript™ III reverse transcriptase used for cDNA synthesis was obtained from Invitrogen®, California**,** USA. Oligo dT primers were synthesized from Operon, Germany. RNase H and ribonuclease inhibitor were obtained from Takara, Shiga, Japan. Brilliant SYBR® green master mix was purchased from Agilent, California**,** USA**.**

2.3 Equipments

Autoclave	Model HA-3D (Hirayama, Japan)
Balance	Ohaus (New Jersey, USA); Avery Berkel (Ohio, USA); Sartorius TE 3102S (Goettingen, Germany); Precisa (Dietikon (Switzerland)
Centrifuge	microcentrifuge: Denver instrument company (New York, USA); high speed centrifuge: Kubota 5922 (Tokyo, Japan)
CO_2 chamber	Shel lab (Oregon, USA)
Electrophoresis	Mupid α Mini Electrophoresis System (Tokyo, Japan)
Gene amplification	TaKaRa PCR Thermal Cycler Dice Version III Model TP600 (Shiga, Japan)
Hot air oven	Memmert (Schwabach, Germany)
Incubator	Thermomixer comfort (Eppendorf, Germany)
IR spectrophotometer	JASCO IR-810, Japan Spectroscopic (Tokyo, Japan)
Laminar air flow cabinet	Ultrasafe 48, Faster (Milan, Italy)
Micropipettes	Socorex: 0.1-2.0 µl, 2-20 µl, 20-200 µl, 100-1000 µl (Ecublens, Switzerland)
Microplate reader	Biotek Power, BioTek Instruments, Inc (Vermont, USA)
Microplate	96-well, Nunc (Roskilde, Denmark)
Microscope	Olympus, CK2 model, Olympus optical Co. Ltd. (Tokyo, Japan)
Microwave oven	LG (Bangkok, Thailand)
pH meter	Eutech instruments, Cyber Scan 510 (Nijkerk, Natherland)
Real-time PCR	ABI7300 Real-time PCR system (California, USA) and used Sequence Detection Software version 1.4 (SDS V. 1.4)

Refrigerator	Sanden Intercool (4°C), (Singburi, Thailand); Whirlpool (-20°C), (Bangkok, Thailand); Deep freezer (-80°C), Forma Scientific (Ohio, USA)
UV-cabinet II	for 254, 366 nm, CAMAG (North Carolina, USA)
UV-VIS spectrophotometer	Genesis-6, Thermo scientific (Massachusetts, USA)
Vortex	MS 1 mini shaker, IKA Co., Ltd. (Petaling Jaya, Malaysia)
Water bath	Memmert (Schwabach, Germany)

2.4 General technique

2.4.1 Thin-layer chromatography (TLC)

Adsorbents:	The TLC plate for routine work was pre-coated TLC plate of silica gel 60 F-254 from Merck, Darmstadt, Germany.
Layer thickness:	250 μm
Technique:	one way, ascending, 5.0-6.5 cm or as appropriate
Temperature:	laboratory temperature (30°-35° C)
Detection:	(1) ultraviolet light at wavelength 254, 366 nm (2) anisaldehyde/H_2SO_4 spray reagent Mixed anisaldehyde (5 ml) with glacial acetic acid (10 ml) and HCl (37% w/w; 5 ml), adjusted the volume to 100 ml with distilled water.

2.4.2 Column chromatography

Adsorbents:	Silica gel (SiO_2 60, 230-400 mesh) from Merck, Darmstadt, Germany.
Packing:	(1) adsorbent poured as a suspension into the column (2) vacuum chromatography

Addition of crude extract:

Crude extract was dissolved in the small volume of solvent and gently placed on top of the column.

Technique: open column chromatography

Solvent: hexane, chloroform, dichloromethane, ethyl acetate and methanol

Examination of elute: the fractions were examined by TLC using UV light at wavelength 254, 366 nm and detected with anisaldehyde/H_2SO_4 spray reagent.

2.4.3 Spectroscopy

2.4.3.1 Ultraviolet (UV) absorption spectra were obtained with a Genesys™ 6 spectrophotometer. (Sample concentration were prepared about 0.1-0.6 mM)

2.4.3.2 Infrared (IR) spectra were recorded on IR spectrometer at wavenumber (ν) 400-4000 cm^{-1}. The materials were prepared in CH_2Cl_2 using neat technique.

2.4.3.3 Nuclear magnetic resonance (NMR) spectra were recorded on Fourier transform NMR, Varian® Unity Inova 500 spectrometer. The sample about 2-10 mg was dissolved in the solvents (NMR grade) as appropriate. The chemical shifts were reported in ppm scale, using tetramethylsilane as internal standard, and the chloroform-*d*; δ_H 7.25 ppm for residual $CHCl_3$ and δ_C 77.0 ppm; and acetone-*d6*; δ_H 2.05 ppm for residual C_3H_6O and δ_C 206.7 and 29.9 ppm) as operating solvents.

2.4.3. Mass spectrometry (MS), the spectra was recorded on Thermo Finnigan MAT 95 XT for electron-impact-mass spectrometry (EI-MS).

2.5 Extraction and isolation of compounds from *C. stellatopilosus* leaves

2.5.1 The extraction procedure

Two procedures were performed, including the reflux method and the maceration method.

2.5.1.1 Using reflux method

Dried powder (0.6 kg) of *C. stellatopilosus* leaves was refluxed at 80º C for 1 h with ethanol (2 l, 3 times). The filtrates were pooled and concentrated under reduced pressure to volume about 1 l. The latter solution was refluxed with 1 N NaOH (1 % v/v) at 80º C for 30 min. Volume of solution was reduced to 200 ml and transferred to a separator. The solution was partitioned with hexane (200 ml x 3 times). The hexane fractions were pooled and evaporated to dryness under reduced pressure to afford the hexane extract (33 g, 5.69 %w/w). The hexane extract was further purified with vacuum and column chromatography.

2.5.1.2 Using maceration method

Dried powder (0.8 kg) of *C. stellatopilosus* leaves was macerated at room temperature for three days with hexane, dichloromethane and ethanol consecutively (3 l, 3 times). The filtrates obtained from each step were concentrated under reduced pressure to give the hexane (45.11 g, 5.68 %w/w), dichloromethane (21 g, 2.65 %w/w) and ethanol extracts (63 g, 8.93 %w/w) respectively.

2.5.2 The isolation procedure

2.5.2.1 Vacuum chromatography

Crude hexane extract form 2.5.1.1 (33 g) was dissolved in chloroform and blended with silica gel and gently placed on the top of silica gel column (13 x 4 cm). The column was eluted with CH_2Cl_2 (300 ml, 2 times). Fractions were pooled as guided with TLC and evaporated to dryness under reduced pressure to give the following fraction:

(1) Fractions 1-2 were combined and assigned as fraction H-1 (5.1 g)

(2) Fractions 3-16 containing amorphous solid crystal (20 mg). The fractions were combined and assigned as fraction H-2. Fraction H-2 was re-crystallization with chloroform: methanol in a ratio 7:3 to yield 2.1 mg, 0.06% of hexane fractions.

(3) Fractions 17-34 were combined and assigned as fraction H-3 (10.1g)

(4) Fractions 35-38 were combined and assigned as fraction H-4 (6.6 g)

The isolation of fraction H-4

Part of fraction H-4 (1.6 g) was dissolved in chloroform and gently placed on the top of silica gel column (5 x 30 cm). The column was eluted with a mixture of $CHCl_3$: *n*-propanol; 24: 0.5. Fractions (15 ml) were collected and pooled as guided with TLC. Fractions with similar TLC pattern were combined to give the following portions. The fractions were pooled and evaporated to dryness under reduced pressure.

H-4a	fractions 1-34 (trace of diterpenoids compounds)
H-4b	fractions 35-38 (315.8 mg)
H-4c	fractions 39-50, it was assigned as **CS-1** (971.1 mg), yielding 2.94% of hexane fraction.
H-4d	fractions 51-65 (295.7 mg)

2.5.2.2 Column chromatography

Isolation of dichloromethane extract (2.5.1.2)

Crude dichloromethane extract (13 g) was dissolved in minimum volume of chloroform and gently loaded on the top of silica gel column (7 x 31 cm). Then the column was eluted with CH_2Cl_2: EtOAc gradient from 9:1 to 2:8 and followed with EtOAc: MeOH gradient

from 7:3 to 5:5. Fractions (100 ml) were collected and pooled as guided with TLC. Fractions with similar TLC pattern were combined to give the following portions. The fractions were pooled and evaporated to dryness under reduced pressure.

(1) Fractions 1-9 were combined and assigned as fraction D-1 (710.1 mg)

(2) Fractions 10-24 contained amorphous solid. The fractions were combined and assigned as fractions D-2 (1.0 g). Fraction D-2 was re-crystallized with dichloromethane and hexane to give a white amorphous solid. It was assigned as **CS-2** (970 mg), yielding 7.46 % of dichloromethane fractions.

(3) Fractions 25-42 were combined and assigned as fraction D-3 (1.6 g)

(4) Fractions 42-109 were combined and assigned as fraction D-4 (7.5 g)

(5) Fractions 110-120 contained amorphous solid. The fractions were combined and assigned as fraction D-5 (290 mg).

The isolation of fraction D-5

Fraction D-5 (290 mg) was dissolved in chloroform and a small volume of methanol and then placed on the top of silica gel column (2 x 30 cm). Column was isocratically eluted with $CHCl_3$: EtOAc; 1:1. Fractions (10 ml) were collected and pooled as guided with TLC. Fractions with similar TLC pattern were combined to give the following portions. The fractions were pooled and evaporated to dryness under reduced pressure.

D-5a fractions 1-8 (40.4 mg)

D-5b fractions 9-26 (68.3 mg)

D-5c fractions 27-57, it was assigned as **CS-3** (115 mg), yielding 0.88% of dichloromethane fractions.

2.6 Cell-based assay method and qRT-PCR

Murine macrophage RAW264.7 cells were used as model for anti-inflammatory activity evaluation. Fractions (from 2.5.1.2) and the isolated compounds, **CS1**-**CS3**, were assessed for their inhibition potential on nitric oxide (NO) production. Genes expressions including *iNOS*, *COX-1* and *COX-2* were determined using quantitative real-time (qRT)-PCR.

2.6.1 Preparation of solutions

Ethidium bromide solution	Ethidium bromide (10 µl) was mixed in 100 ml of distilled water. Handle with care.
Loading buffer	Contained SDS (1% w/v), glycerol (50% v/v) and bromophenol blue (0.05% w/v)
Tris-Acetate-EDTA (TAE) buffer, 50x	The 50x TAE buffer was composed of tris base (121 g), EDTA trisodium (19.7 g), glacial acetic acid (35 ml). All components were dissolved with distilled water; pH was adjusted with 1 N HCl to 8.0. The volume was adjusted to 500 ml with distilled water.
RPMI -1640 medium	RPMI powder (10.4 g) was dissolved with distilled water to a final volume of 1 L. $NaHCO_3$(2.0 g) was added, pH was adjusted to 7 with 1 N NaOH or 1 N HCl. RPMI medium (900 ml) was mixed with fetal calf serum (90 ml) and antibiotics (10 ml; composed of penicillin G (100 U/ml), streptomycin (100 µg/ml). The RPMI medium was sterilized through 0.22 µm filter membrane under vacuum.
Lipopolysaccharide (LPS) suspension (50 µg/ml)	The LPS (2.5 mg) was dissolved in RPMI medium to a final volume of 50 ml.

Phosphate buffer saline (PBS)	NaCl (80.0 g), NaH_2PO_4 (11.6 g), KCl (2.0 g) and KH_2PO_4 (2.0 g) were dissolved and adjusted the volume to 1 L in distilled water. The solution was sterilized by autoclave.
MTT solution (5 mg/ml)	MTT (200 mg) was dissolved with PBS to a final volume of 40 ml.
Griess reagent	Dissolved sulfanilamide (1.0 g), *N*-1-naphthalene diamine (0.1 g) and H_3PO_4 (85%) with distilled water and adjusted the final volume to 100 ml.
0.04 M HCl in isopropanol	Mixed 1N HCl (20 ml) with isopropanol (480 ml) and stirred.

2.6.2 Primers

Oligonucleotides for genes amplifications encoding inducible nitric oxide synthase (iNOS), cyclooxygenase 1 (COX-1), COX-2 and glyceraldehydes 3-phosphate dehydrogenase (GAPDH) were designed using online program from Eurofin MWG Operon (http://www.operon.com/technical/pcr_primer_design.aspx). Properties of oligonucleotides were set for 45-55% of GC content and about 58-60 °C of melting temperature (T_m). List of primers is shown in Table 2.1

Table 2.1 Primers used in this study.

Name of primer	Accession no.[a] (location)	Sequence ($5' \rightarrow 3'$)	Expected size (bp)
iNOS F	M84373.1 (3002-3581)	ACT TGG ATC AGG AAC CTG AA	580
iNOS R		CCT TTT TTG CCC CAT AGG AA	
COX-1F	AK160886.1 (679-947)	CCC ACC AGT TCT TCA AGA CC	269
COX-1R		AAG CAA CCC AAA CAC CTC C	
COX-2F	NM011198.3 (1281-1524)	TCT ACA ACA ACT CCA TCC TCC	244
COX-2R		GCA GCC ATT TCC TTC TCT C	
GAPDH F	NM008084.2 (258-559)	AAG CCC ATC ACC ATC TTC C	302
GAPDH R		TCC ACA ATG CCA AAG TTG TC	

[a]Accessed from http://www.ncbi.nlm.nih.gov/

2.6.3 Murine macrophage RAW264.7 cells

Murine macrophage RAW264.7 cells, stored at -80ºC, were inoculated in the cell culture flasks containing RPMI 10 ml. The RAW264.7 cells were routinely maintained in RPMI-1640 medium. Cells were incubated at 37ºC, 5% CO_2 in humidified atmosphere. Cell growth was determined as cell number per ml, estimated under microscope.

2.6.4 Treatment of RAW264.7 cells

The maintained RAW264.7 cells were prepared for cell-based assay of anti-inflammatory activity. The cell culture flasks, containing layers of the RAW264.7 cells, was washed with PBS after withdrawal of medium by vacuum. Cells were detached after treatment with 0.25% trypsin-EDTA. Cells were harvested and suspended in fresh medium. Cell number per ml was determined. For determination of NO inhibitory activities, cells were seeded in 96-well plate with

1×10^5 cells/well and allowed to adhere for 1 h, at 37ºC , under 5% CO_2, and then medium was removed. Fresh medium (100 µl) containing of LPS (50 µg/mL) was added following the test solution (100 µl) at various concentrations including 3, 10, 30 and 100 µg/ml for crude extract and 3, 10, 30 and 100 µM for isolated compounds. Cells then were incubated for 48 h. Supernatant was collected and applied for NO content determinations.

In addition, the treated cells were divided into five groups, including; (1) normal group (N) that contains only RPMI medium, (2) the control group (C) that contain only LPS-stimulated cells in RPMI, (3) sample and (4) positive control groups that contain LPS in a present of sample or positive control at various concentrations. The blank of sample group (5) contained only sample at various concentrations.

For screening the activity of the crude extracts, crude extracts were suspended in DMSO to give concentrations of 3, 10, 30, 100 µg/ml. For isolated substances, concentrations of 3, 10, 30 100 µM were prepared. Treated cell with L-nitroarginine (NA) and caffeic acid phenethylester (CAPE) were used as positive controls.

2.6.5 Nitrite determination

The NO production was determined by measuring the accumulation of nitrite, a stable oxidized product of NO. The presence of nitrite in the cell culture supernatant was measured using Griess reagent according to Griess reaction. The culture supernatant (100 µl) of treated cells (2.6.2) was removed, combined with Griess reagent (100 µl) in a 96-well plate and mixed. An OD at 570 nm was measured with microplate reader. The % inhibition of NO was calculated as shown in the equation. At 50 % inhibition of NO production, sample concentration was expressed as an IC_{50}, determined by using non-linear regression analysis of plot between concentrations versus % inhibition. The IC_{50} values were determined graphically (n=4).

$$\% \text{ inhibition of NO} = \frac{[(\text{control} - \text{blank of control}) - (\text{sample} - \text{blank of sample})]}{[(\text{control} - \text{blank of control})]} \times 100$$

Griess reaction is the reaction, which quantitate the major metabolites of NO. In the reaction, nitrite interacts with the amino group of sulfanilamide under acidic condition. Therefore, the sulfanilamide is changed to diazonium cation and couples to N-(1-naphthyl) ethylenediamine in the para-position. Then the azo compound is formed, which absorbed light at 570 nm. The overall of Griess reaction is described in the scheme 2.1.

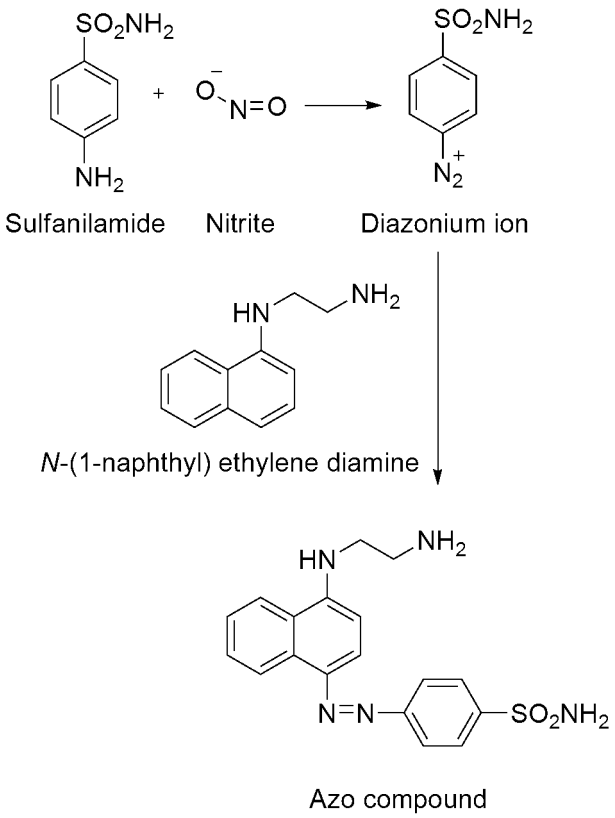

Scheme 2.1 Griess reaction, which occurred under acid condition.

2.6.6 MTT assay for cell viability

Since the observed NO inhibitory activity may be due to cell death, therefore, cell viability was determined from the treated cells in parallel. Cell viability was determined by the mitochondrial-dependent reduction of MTT reagent to formazan product. After treatment of cells with compound, supernatant was removed, the RAW264.7 cells, which attached to a well was tested for cell viability. MTT solution (10 μl) was added to a 96-well plate and incubated at 37ºC for 2 h. Then the medium was discarded and blotted with a paper towel. An isopropanol containing with 0.04 M HCl (100 μl) was added, then formazan product was generated. An OD of 570 nm was measured with microplate reader. % Cell survival was determined by comparison with control group. If the OD of sample group was less than 80 % of that in the control group, the test compound was considered to be cytotoxic.

2.6.7 Gene expression method

The expression profiles of genes involved in the inflammatory pathway e.g. *iNOS*, *COX-1* and *COX-2* were determined from the RAW264.7 cells after treatment with isolated compounds.

2.6.7.1 Treated RAW264.7 cells

The RAW264.7 cells in RPMI medium were seeded into 6-well plate with $1.5x10^6$ cells/well and incubated at 37ºC, 5% CO_2 in humidified atmosphere for 1 h. The medium was removed and the fresh RPMI medium containing 750 μl of LPS (50 μg/ml) was added. The samples (750 μl) at different concentrations (3, 10 and 30 μM in DMSO for plaunotol and plaunolide, and 0.03, 0.1, 0.3 μM for plaunol E) were added into the LPS-stimulated cells. The cells were further incubated at the same culture condition for 20 h. Cells were washed with PBS and carefully scrapped out of plate and transferred from a 6-well plate to microcentrifuge tube.

2.6.7.2 Total RNA isolation

All steps were carried out at 4ºC. To destroy an RNase, tubes and pipette tips were autoclaved and dried. The treated RAW264.7 cells were harvested by centrifugation at 1,810 rpm for 5 min at room temperature. Supernatant was carefully removed without disturbing a pellet. Tube was centrifuged again at 1,810 rpm for 1 min in order to get rid of a residual of PBS. Total RNA was isolated from the cells using RNeasy® Mini Kit. The RLT buffer (350 µl), combined with 10:1 volume of β-mercaptoethanol was added to the cells. Cells were ruptured, aided with pipetting. Chilled ethanol (70% v/v) (350 µl) was added and mixed well. The cell lysate (700 µl) was loaded onto the RNeasy mini column and centrifuged at 10,000 rpm for 30 s. Discarded flowthrough, buffer RW1 (700 µl) was added, centrifuged at 10,000 rpm for 30 s. The RNeasy mini column was transferred to a collection tube (2 ml), buffer RPE (500 µl) was added to RNeasy mini column and centrifuged at 10,000 rpm for 30 s. Discarded flowthrough, buffer RPE (500 µl) was added and centrifuged at 10,000 rpm for 2 min 30 s. Discarded flowthrough, the RNeasy mini column was centrifuged at 10,000 rpm for 1 min to dry column. The RNeasy mini column was transferred to a 1.5 ml microcentrifuge tube. To elute the total RNA from the RNeasy mini-column, RNase free water (35 µl) was added and incubated for 1 min then centrifuged at 10,000 rpm for 2 min. The amount of total RNA was estimated from an OD at 260 nm. Purity of isolated RNA was determined from a ratio of OD_{260}/OD_{280}. An rRNA was separated by 1% (w/v) agarose gel electrophoresis and stained with ethidium bromide to check an intact RNA. The isolated RNA was stored at -80ºC until used.

2.6.7.3 First strand cDNA synthesis

The first-strand cDNA was synthesized from total RNA (0.8 µg) using Superscript™ III reverse transcriptase (Invitrogen®) according to manufacture instruction. The reaction mixture (total volume 20 µl) was composed of total RNA, oligodT primer (RACE32, 5′ GACTCGAGTCGACATCGATTTTTTTTTTTTTT-3′) Froh man *et al*., 1988 and dNTP mix

(Table 2.2). The reaction was incubated at 65ºC for 5 min and chilled on ice for 1 min. The content was centrifuged briefly. Then 5x first strand buffer, 0.1 M dithiothreitol and Superscript™ III RT were added. The reaction was incubated at 50º C for 1 h. The enzyme was inactivated at 70 ºC for 15 min. RNase H (2 unit) was added and incubated at 37ºC for 20 min to get rid of the residual RNA. The resulting cDNA were obtained and used as a template for qRT-PCR.

Table 2.2 Composition of reaction for first-strand cDNA synthesis.

Components	Volume (μl)	Final amount/reaction	
Total RNA	varied	0.8	μg
Oligo dT (RACE 32) (50 mM)	1	2.5	mM
dNTP (10 mM)	1	0.5	mM
5x first strand buffer	4	1 x	
Dithiothreitol (0.1 M)	1	5	mM
Superscript™ III RT (250unit/μl)	1	250	unit
RNase out (40 unit/μl)	1	40	unit

2.6.7.4 Quantitative real-time (qRT) polymerase chain reaction

The target genes including *iNOS*, *COX-1* and *COX-2* were amplified by qRT-PCR. The nucleotide sequences of primers are shown in Table 2.1. The qRT-PCR amplification was performed using Brilliant II® SYBR Green QPCR Master Mix (Agilent Technologies).

To perform the validation experiment, firstly chosen of the target gene (*iNOS*, *COX-1* and *COX-2*) and used *GAPDH* as endogenous control. Then the dilution series of difference input amount for cDNA were performed for PCR reaction as shown in Table 2.3. The PCR components performed with two-step cycling program (Table 2.4). After 40 cycles of amplification, value of ΔRn was recorded. Linear plot of ΔRn versus cycles of amplification is

shown in Fig. 2.1. Data of qRT-PCR were analyzed. The average C_T and ΔC_T were calculated and the ΔC_T was plotted in y axis versus the amount of total RNA in log scale. The efficiency of qRT-PCR was considered from the value of slope of linear regression. As a guideline, the value of slope when plot of log input amount of total RNA versus ΔC_T should be less than 0.1.

Table 2.3 Preparation of the reaction for qRT-PCR.

Components	Volume (µl) per reaction	Final concentration as appropriate
cDNA*	1	
2x Brilliant II® SYBR Green qPCR master mix	12.5	1x
Primer F (10 µM)	0.5	0.2 µM
Primer R (10 µM)	0.5	0.2 µM
ROX dye (1:50)	0.375	
d H_2O	To final volume 25 µl	

cDNA* : In validation method, the dilution series of difference input amount for target genes and endogenous were performed equivalent to 40, 4, 0.4, 0.04 and 0.004 ng/µl of total RNA.

Table 2.4 Temperature profile of the amplification procedure.

Cycles	Duration of cycles	Temperature
1	10 min	95°C
40	30 sec	95°C
	1 min	60°C

At optimum amount of cDNA, genes expressions of treated cells were measured when GAPDH was an endogenous gene. The control group was used as calibrator. Set of data was recorded and calculated for relative quantitation (RQ). RQ was calculated using a comparative C_T method according to the following equations.

$$\Delta C_T \text{ value} = [C_T \text{ of target gene} - C_T \text{ of endogenous GAPDH}] \quad (1)$$

$$\Delta\Delta C_T \text{ value} = [\Delta C_T \text{ of target gene} - \Delta C_T \text{ of calibrator}] \quad (2)$$

$$\text{Relative quantitation (RQ)} = 2^{-\Delta\Delta C_T} \quad (3)$$

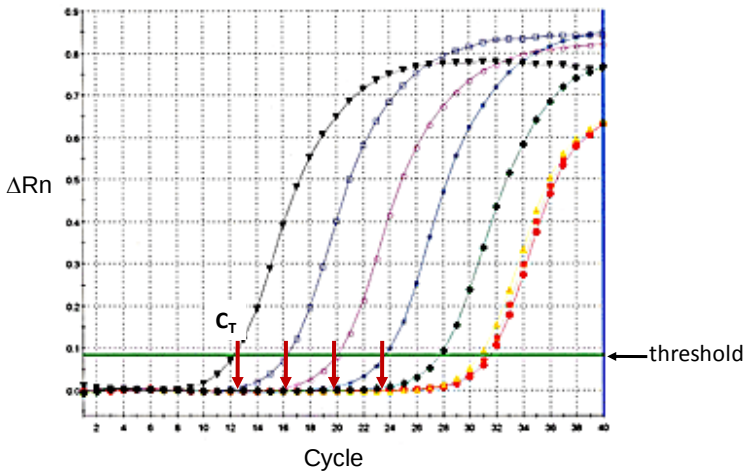

Figure 2.1 Linear plot of ΔRn versus cycles of amplification

2.7 Statistical analysis

The results of inhibitory of NO production were expressed as mean ± standard error of the mean (S.E.M.) of four determinations at each concentration for each sample. The IC_{50} value was calculated by Microsoft excel program. The significance was analyzed using one-way analysis of variance (ANOVA), followed by Dunnett's test. The critical level for significance was set at $P < 0.05$. The results of qRT-PCR analysis were expressed as average value and the significance was analyzed using one-way analysis of variance (ANOVA), followed by Dunnett's test, the critical level for significance was set at $P < 0.05$.

CHAPTER 3

RESULTS

Croton stellatopilosus leaves are an important source of plaunotol, a major ingredient in the commercial Kelnac™ drug. Plaunotol claims to be a gastro-protective agent and is recommended for peptic ulcer. In addition, plaunotol has anti-inflammatory and antibacterial activities as shown in the gastric cell lines models (Murakami *et al*., 1999). In this study, we aimed to use the murine macrophage RAW264.7 cells as *in vitro* model for anti-inflammatory activity evaluation. Information of plaunotol isolation, which established earlier, provided us to consider the process of crude extract preparation. We used a conventional method for at least plaunotol isolation and perhaps together with others hydrophobic molecules. Alternatively, maceration with organic solvents (different polarity) tracked to other diterpenes. In addition, we used murine macrophage RAW264.7 cells for screening the inhibitory activity on NO production in the fractions, so called bioassay-guided isolation. The structures of compounds were elucidated by means of spectroscopy. Pure compounds were later examined for their potential on anti-inflammatory activity. Potency of each compound was expressed as concentration of at 50% NO inhibition (IC_{50}). To determine the mechanism of inhibition, transcription profiles of genes, involved in inflammatory pathway including *iNOS*, *COX-1* and *COX-2*, were determined using technique of qRT-PCR.

3.1 Phytochemical study

Crude extracts were obtained from (1) refluxing with ethanol and partitioning with hexane and (2) maceration with dichloromethane. Using gravity silica gel chromatography, three compounds were isolated and designated as **CS-1**, **CS-2** and **CS-3**. Their structures were

elucidated by means of UV, IR, MS and NMR spectrometry. Isolation procedure is summarized in Fig. 3.1.

The yielding of isolated compounds including: plaunotol (**CS-1**) was 2.94% of hexane faction, plaunolide (**CS-2**) was 7.46 % of dichloromethane fractions and plaunol E (**CS-3**) was 0.88% of dichloromethane fractions.

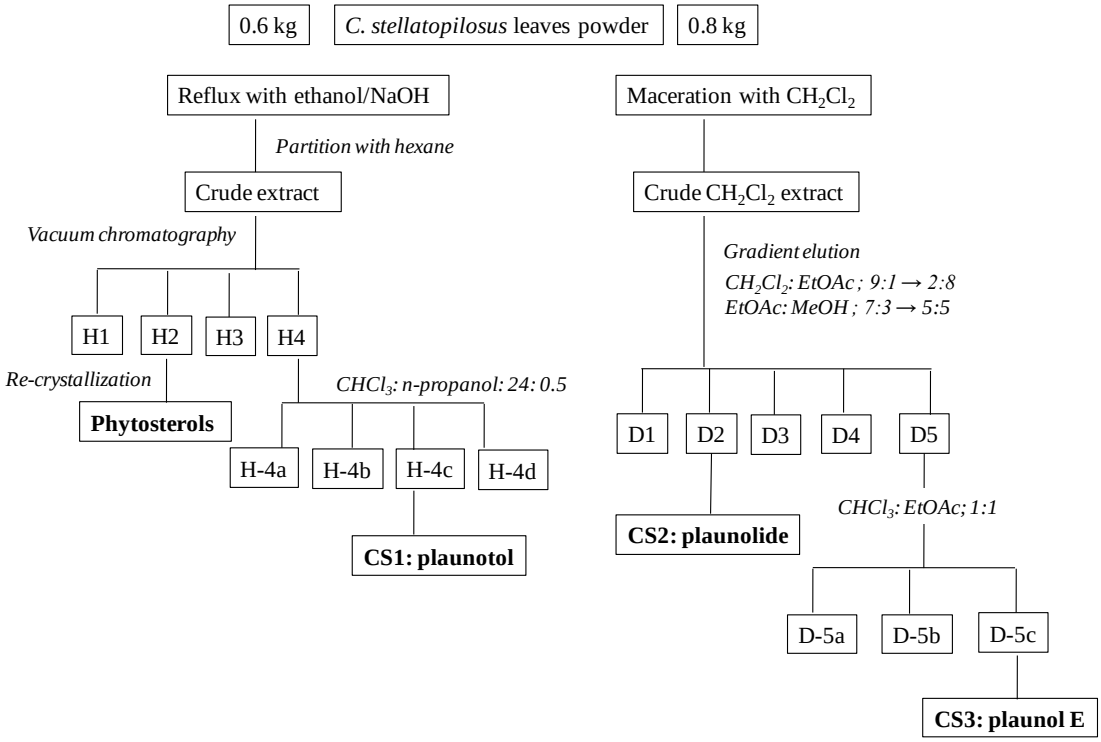

Figure 3.1 Isolation schemes of **CS-1**, **CS-2** and **CS-3** from *C. stellatopilosus* leaves.

3.1.1 Identification of CS-1 as plaunotol

Characteristic : pale yellow oil, soluble in hexane, dichloromethane, chloroform and methanol

Molecular weight : 306.255

UV λ_{max} (nm) : 290

IR absorption (ν_{max} cm^{-1}) : 3300, 1665, 1440, 1380 and 1000

^{1}H- and ^{13}C-NMR : in $CDCl_3$, 500 MHz, 125 MHz

(See all spectra of **CS-1** in the Appendix)

The molecular formula of **CS-1** was established as $C_{20}H_{34}O_2$ and required the unsaturation degree of four. The infrared spectrum of **CS-1** exhibits absorption bands at IR absorptions at 3300 cm^{-1} (O – H (stretching)), 1665 cm^{-1} (C = C (stretching)), 1440 cm^{-1} (C – H (bending)) and 1380 cm^{-1} (C – H (bending)). The MS and IR data suggested that **CS-1** had an olefins property and carried a hydroxyl group.

The ^{1}H-NMR spectrum showed singlet signals due to four vinyl methyl groups (δ 1.60, H-19; 1.60, H-20; 1.64, H-16 and 1.64, H-17), two hydroxymethyl groups (δ 4.05, s , H-18 and 4.07, d, H-1), four olefinic protons (δ 5.06, m, H-10; 5.09, m, H-14; 5.22, m, H-6 and 5.35, m, H-2), along with multiplet signal of six allyl methylene groups (δ 1.90 – 2.20), integrated for 12 protons. The ^{13}C-NMR spectrum exhibited signals of 20 carbons, including two hydroxyl groups (δ 59.8, C-1 and 58.9, C-18), four methyls, six methylenes, four methines and four quaternary carbons, accounted for 32 hydrogen atoms. Two exchangeable protons were proposed as hydroxyl groups. Therefore the molecular formula for $C_{20}H_{34}O_2$ was confirmed.

The ^{1}H-^{1}H COSY showed correlation of their proton cross-peaks for the following four partial structures. These included fragment **A** at [δ 4.07 (d; J = 7.1 Hz, H-1), 5.35 (m, H-2) and 1.64 (s, H-17)]; fragment B at [δ 5.22 (m, H-6) and 4.05 (s, H-18)]; fragment C at [δ 5.06 (m,

H-10) and 1.60 (s, H-19)]; fragment D at [δ 5.09 (m, H-14), 1.64 (s, H-16) and 1.60 (s, H-20)] as shown below.

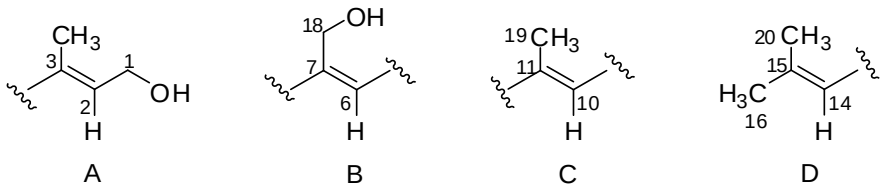

The crucial HMBC correlation included those from C-2 to H-1 and H-4; from C-6 to H-4, H-8 and H-18; from C-10 to H-8 and H-19; from C-14 to H-16 and H-20. Thus, the four olefin moieties (fragments A-D) were connected and suggesting to be acyclic diterpene structure.

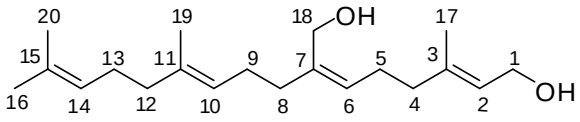

Comparison of **CS-1** with plaunotol showed similar characteristics on TLC and positive to anisaldehyde/H_2SO_4 spraying reagent. The IR, ^{1}H- and ^{13}C-NMR data suggested that **CS-1** was plaunotol, an acyclic diterpene. All data of spectroscopy are in agreement with the published data from Ogiso *et al*. (1978). The ^{1}H- and ^{13}C- NMR assignments and the HMBC correlation are summarized in Table 3.1

Table 3.1 ^{1}H- and ^{13}C- NMR spectral data of **CS-1** (500 MHz for ^{1}H; $CDCl_3$).

Carbon position	**^{1}H-**	**^{13}C-**	**HMBC**
1	4.07 (d; 7.1)	59.8 (CH_2)	H-2, H-3
2	5.35 (m)	124.2 (CH)	H-1, H-4
3		138.9 (C)	H-1, H-4
4	2.02 (m)	39.2 (CH_2)	H-2, H-3, H-5, H-6
5	2.16 (m)	25.8 (CH_2)	H-4
6	5.22 (m)	127.4 (CH)	H-4, H-8, H-18
7		138.8 (C)	H-8
8	2.10 (m)	34.8 (CH_2)	H-6, H-7, H-9, H-10
9	1.9-2.2(m)	26.7 (CH_2)	H-8
10	5.06 (m)	123.9 (CH)	H-8, H-19
11		131.3 (C)	H-19
12	2.02 (m)	39.6 (CH_2)	H-11, H-13, H-15, H-20
13	1.95 (m)	26.6 (CH_2)	H-12
14	5.09 (m)	124.0 (CH)	H-16, H-20
15		135.3 (C)	H-12, H-14, H-20
16	1.64 (s)	25.6 (CH_3)	H-14, H-15
17	1.64 (s)	16.4 (CH_3)	H-2, H-3
18	4.05 (s)	58.9 (CH_2)	H-6, H-8
19	1.60 (s)	17.6 (CH_3)	H-10, H-11, H-12
20	1.60 (s)	15.9 (CH_3)	H-14, H-15

3.1.2 Identification of CS-2 as plaunolide

Characteristic	: colorless amorphous solid, soluble in acetone, dichloromethane, chloroform, ethyl acetate and methanol
Melting point	: 170°-172° C
Molecular weight	: EI-MS; *m/z* 340 (M^+), 310 (base peak), 292, 229 and 91
UV λ_{max} (nm)	: 295
IR absorption (ν_{max} cm^{-1})	: 3140, 1760, 1640, 1500, 900 and 880
^1H and ^{13}C-NMR	: in $CDCl_3$, 500 MHz, 125 MHz

(See all spectra of **CS-2** in the Appendix)

The molecular formula was established as $C_{20}H_{20}O_5$ from the molecular ion peak [M^+] in the EI spectrum at *m/z* 340. The proposed molecular formula required the unsaturation degree of eleven. This compound was assigned of two carbonyls, three olefins, one exocyclic double bond and five rings system. The IR spectrum showed the absorption bands at 1760 cm^{-1} (C = O (stretching)) for two- γ lactone ring systems, at 3140 cm^{-1} (C - H (stretching)), 1500 cm^{-1} (C = C (stretching)) and 900 cm^{-1} for β-mono substitute furan moiety and at 1640 (C = C (stretching)) and 880 cm^{-1} for methylene function.

The ^1H-NMR spectrum of **CS-2** displayed signals for 20 protons and showed the signals due to four olifinic protons (δ 7.40, 2H, H-15, H-16; δ 6.70, H-3 and δ 6.35, H-14), one exocyclic double bond (δ 5.02, H-17 and δ 4.80, H-17). In addition the aliphatic methine protons were observed at δ 5.52, H-12 and δ 2.19, H-10. The ^{13}C NMR spectrum exhibited signals of 20 carbons, including two carbonyls (δ 176.7, C-20 and 169.5, C-18) and olefin (composed of eight carbons) (δ 147.4, C-8; 144.1, C-15; 140.0, C-16; 137.2, C-4; 133.7, C-3; 124.8, C-13; 113.4, C-17 and 108.5, C-14).

Interpretation of ^{1}H-^{1}H COSY cross peaks in the aliphatic methylene region led to four partial structures, including fragment A [δ 1.80 (m, H-1), 1.40 (m, H-1), 2.48 (m, H-2), 2.21 (m, H-2), 6.70 (dd, *J* = 7.6, 2.2 Hz, H-3), 4.30 (d, *J* = 9.3 Hz, H-19), 4.23 (dd, *J* = 9.0, 2.2 Hz, H-19)]; B [δ 2.13 (ddd, *J* = 13.2, 9.3, 6.8 Hz, H-6), 1.53 (dddd, *J* = 13.2, 10.5, 2.7, 2.7 Hz, H-6), 2.58 (m, H-7), 2.44 (m, H-7), 5.02 (d, *J* = 1.5 Hz, H-17), 4.80 (d, *J* = 0.5 Hz, H-17)]; C [δ 2.75 (dd, *J* = 13.7, 8.7 Hz, H-11), 2.60 (dd, *J* = 13.7, 6.6 Hz, H-11)]; D [δ 6.35 (d, *J* =0.98 Hz, H-14), 7.4 (d, *J* = 1.95 Hz, 2H, H-15 and H-16)] as shown below.

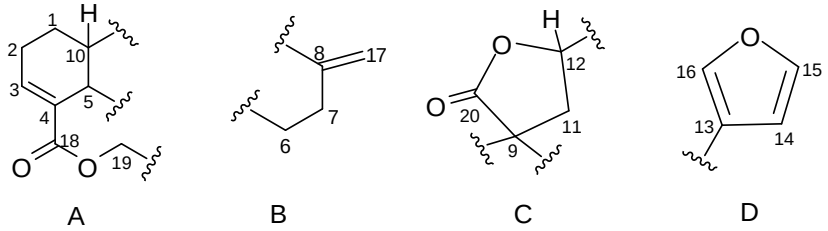

All the proposed structural fragments were interconnected with five quaternary carbons δ 137.2 (C-4), 44.1 (C-5), 147.4 (C-8), 53.5 (C-9) and 124.8 (C-13) on the basis of HMBC data (Table 3.2). The partial structures of C-6, C-19 to C-5, C-8, and C-10 to C-9 and C-12 to C-13 were found to be connected through quaternary carbons based on HMBC data. Thus, fragments A, B, C and D connected and composed of pentacyclic rings were demonstrated. The **CS-2** was elucidated to be plaunolide or plaunol F. ^{1}H-and ^{13}C- NMR assignments and HMBC correlation are summarized in Table 3.2. The ^{1}H spectral data of **CS-2** was in agreement with data from Takahashi *et al*. (1983).

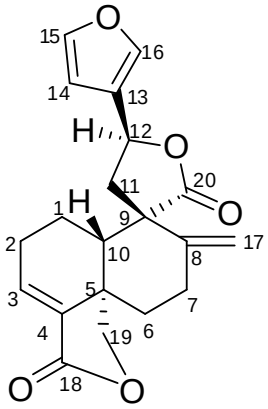

Table 3.2 ^{1}H- and ^{13}C- NMR spectral data of **CS-2** (500 MHz for ^{1}H; $CDCl_3$).

Carbon position	**^{1}H-**	**^{13}C-**	**HMBC**
1	1.40 (m)	21.5 (CH_2)	H-2, H-3
	1.80 (m)		
2	2.21 (m)	26.5 (CH_2)	H-3
	2.48 (m)		
3	6.70 (dd, 7.6 , 2.2)	133.7 (CH)	H-2,H-3
4		137.2 (C)	H-19
5		44.1 (C)	H-3, H-19
6	1.53 (dddd, 13.2, 10.5, 2.7,2.7)	32.6 (CH_2)	H-7, H-6
	2.13 (ddd, 13.2, 9.3, 6.8)		
7	2.44 (m)	27.9 (CH_2)	H-6, H-7
	2.58 (m)		
8		147.4 (C)	H-6, H-7, H-11
9		53.5 (C)	H-2, H-11
10	2.19 (m)	48.9 (CH)	H-2, H-6, H-11
11	2.60 (dd, 13.7,6.6)	43.7 (CH_2)	H-12
	2.75 (dd, 13.7, 8.5)		
12	5.52 (dd, 8.5, 6.6)	71.6 (CH)	H-11, H-12
13		124.8 (C)	H-11, H-12, H-14
14	6.35 (d, 0.98)	108.5 (CH)	H-12, H-14
15	7.40 (d, 1.95)	144.1 (CH)	H-14, H-16
16	7.40 (d, 1.95)	140.0 (CH)	H-12, H-14, H-16
17	4.80 (d, 0.5)	113.4 (CH_2)	H-11, H-17
	5.02 (d, 1.5)		
18		169.5 (CO)	H-3, H-19

Carbon position	^{1}H-	^{13}C-	HMBC
19	4.23 (dd, 9.0, 2.2) 4.30 (d, 9.0)	73.5 (CH_2)	H-6, H-19
20		176.7 (CO)	H-11

3.1.3 Identification of CS-3 as plaunol E

Characteristic : colorless amorphous solid, soluble in acetone, ethyl acetate and methanol

Melting point : 180°-182° C

Molecular weight : EIMS *m/z* 416 (M^+), 374, 356, 338, 279, 278, 97(base peak) and 81

UV λ_{max} (nm) : 295

IR absorption (ν_{max} cm^{-1}) : 3420, 3140, 1750, 1720, 1640, 1500, 900 and 880 cm^{-1}

^{1}H and ^{13}C-NMR : in acetone-*d6* (C_3D_6O), 500 MHz, 125 MHz

(See all spectra of **CS-3** in the Appendix)

The molecular formula was established as $C_{22}H_{24}O_8$ for the molecular ion peak [M^+] at *m/z* 416 in the EI spectrum. The proposed molecular formula required the unsaturation degree of ten. This compound was assigned of two carbonyls, two olefins, one exocyclic double bond and five rings system. The IR spectrum showed the absorption bands at 3420 cm^{-1} (O – H (stretching)) was suggesting a hydroxyl group, at 1750 and 1720 cm^{-1} (C = O (stretching)) for two- γ lactone ring systems, at 3140 (C - H (stretching)), 1500 (C = C (stretching)) and 880 cm^{-1} for β-mono substitute furan moiety and at 1640 (C = C (stretching)) and 900 cm^{-1} for methylene function.

The ^{1}H-NMR spectrum displayed one singlet methyl signal at δ 2.01 (3H, H-22) representing indicated an acetyl group, and olefinic protons at δ 7.48 (m, 2H, H-15 and H-16), 6.42 (m, H-14), 6.68 (d, *J* = 2.3 Hz, H-3). In addition the signal of proton at δ 5.40 (d, *J* = 2.3 Hz, H-17) and 5.06 (d, J = 2.3 Hz, H-17) indicated an exocyclic double bond. For ^{13}C-NMR spectrum, 22 carbon-signals were observed. **CS-3** carried two carbonyls, two olefins, one methylene as exocyclic double bond and aliphatic carbons (Table 3.3). The connection of all protons was assigned based on COSY and HMBC spectra. The structure of **CS-3** was proposed to be plaunol E. The ^{1}H spectral data of **CS-3** was in agreement with data from Kitazawa *et al*. (1980).

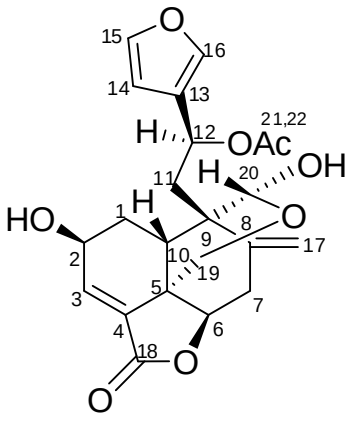

Table 3.3 ^{1}H- and ^{13}C- NMR spectral data of **CS-3** (500 MHz for ^{1}H; acetone-*d6*; C_3D_6O).

Carbon position	**^{1}H-**	**^{13}C-**	**HMBC**
1	2.25 (m)	30.0 (CH_2)	H-2, H-3, H-5, H-6
	3.20 (m)		
2	4.67 (m)	64.7 (CH)	H-1
3	6.68 (d, 2.3)	141.9 (CH)	H-1, H-18
4		132.9 (C)	H-1, H-2
5		40.9 (C)	H-1, H-2, H-3
6	4.68 (dd, 11.9, 6.2)	81.3 (CH)	H-7
7	2.45 (dd,13.5, 6.2)	38.3 (CH_2)	H-8, H-6, H-17
	2.83 (dd,13.3, 6.2)		
8		148.2 (C)	H-17, H-20
9		46.4 (C)	H-12, H-17
10	2.03 (m)	32.6 (CH)	H-4, H-5, H-8, H-9, H-10,
			H-12, H-20
11	1.97 (dd, 15.8, 1.8)	39.3 (CH_2)	H-8, H-9, H-12, H-17,
	2.72 (dd, 15.8, 10.0)		H-20
12	5.95 (dd, 10.0, 1.8)	66.3 (CH)	H-9, H-12, H-13, H-14,
			H-16, H-20, H-21
13		128.0 (C)	H-12, H-14, H-15, H-16
14	6.42 (m)	109.5 (CH)	H-15, H-16
15	7.48 (m)	144.2 (CH)	H-12, H-13, H-14,
			H-15, H-16
16	7.48 (m)	140.3 (CH)	H-12, H-13, H-14,
			H-15, H-16

Carbon position	**^{1}H-**	**^{13}C-**	**HMBC**
17	5.06 (d, 2.3)	115.5 (CH_2)	H-7, H-8, H-9, H-20
	5.40 (d, 2.3)		
18		169.1 (C)	H-3
19	3.31 (dd, 11.0, 1.4)	62.6 (CH_2)	H-1, H-6
	4.01 (d, 11.0)		
20	4.76 (d, 3.6)	101.3 (CH)	H-9, H-10
21		170.8 (C)	H-12, H-22
22	2.01 (3H, s)	21.3 (CH_3)	H-12
OH-2	4.50 (OH, d, 5.0)		
OH-20	5.57 (OH, d, 3.9)		

3.2 Inhibitory activity on nitric oxide (NO) production in RAW264.7 cells

The inhibitory activity on NO production was determined from the nitrite analysis using Griess reaction with the cultured medium. Cells treated with LPS (50 μg/ml) could significantly increase the nitrite production in cultured medium higher than untreated cells. The accumulation of nitrite was measured in the presence or absence of samples after 48 h treatment in RAW264.7 cells. Therefore, the percentage of inhibitory activity on NO production can be calculated from the level of nitrite production in control group (LPS-stimulated cells) and in sample group (LPS-stimulated cells plus sample). For each group, the basal level of cells was normalized with untreated cells.

By this assay, we assessed the potential of the extracts on the inhibitory activity of NO production in the murine macrophage RAW264.7 cells. In overview, samples as indicated in Fig. 3.2, were tested for inhibitory activity on NO production. We initially examined the inhibitory activity on NO production of the crude extracts. Then, active fractions were isolated based on the results of NO inhibition. Three compounds including plaunotol, plaunolide and plaunol E were obtained, and were further determined for their strength on the inhibition of NO production. The mRNAs expressions including *iNOS*, *COX-1* and *COX-2* were determined after treatment the RAW264.7 cells. Fig 3.2 summarizes the NO assay-guided isolation and determination of genes expression.

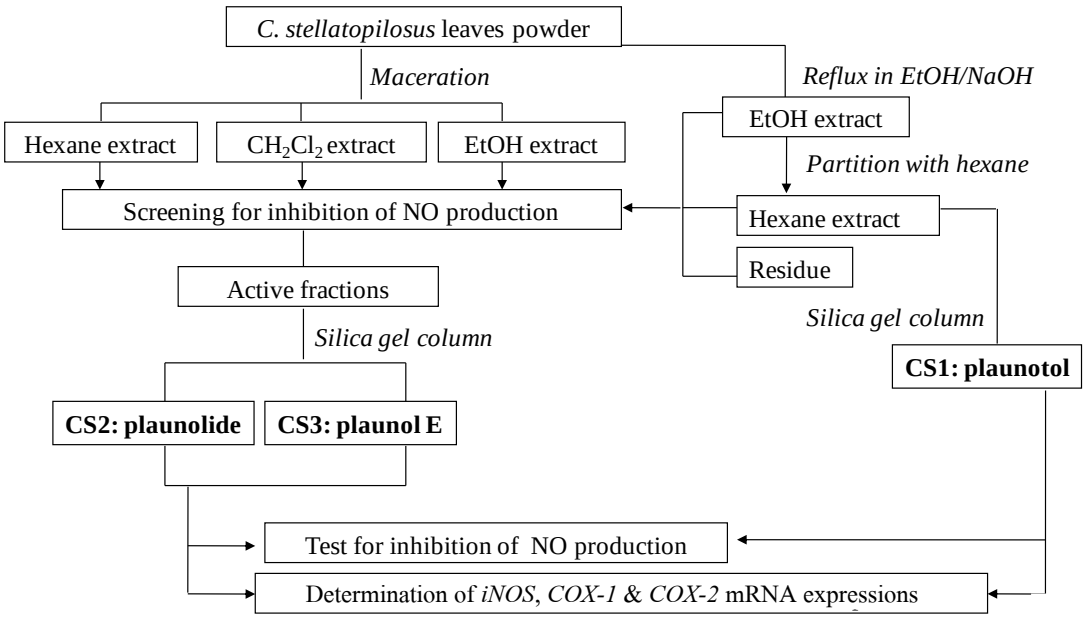

Figure 3.2 Bioassay schemes of *C. stellatopilosus* extract and pure compound.

We initially prepared the crude extract using reflux method as described in Ogiso *et al*., (1978). The ethanol fraction was partitioned with hexane, affording the hexane and the residue fractions. Preliminary screenings of the ethanol extract, hexane extract and the residue fraction on the inhibition of NO production were performed. The ethanol extract, hexane extract and residue fraction showed IC_{50} of 7.20, 49.31 and >100 µg/ml, respectively (Table 3.4). This result suggested that the ethanol extract possessed the strongest activity, followed by the hexane extract. It can be noted that the ethanol fraction may contain other compounds in addition to plaunotol, which could inhibit NO production. These compounds could not be partitioned into the hexane fraction and the concentration effect caused the less activity in the residue fraction.

To follow other compounds, the maceration method was performed. By gradually change the polarity of the solvents, *C. stellatopilosus* leaves powder was macerated with hexane, dichloromethane and ethanol, consecutively. The hexane, CH_2Cl_2 and ethanol extracts exhibited the inhibitory activity on NO production with the IC_{50} of 8.37, <3 and 5.94 µg/ml, respectively (Table 3.4). Potency of the extracts can be ranked from CH_2Cl_2 extract followed by ethanol and

hexane extracts. This evidence supported the hypothesis that there are other compounds that could inhibit the NO production. The MTT assay indicated that the crude extracts from hexane and CH_2Cl_2 at concentration of 100 μg/ml exhibited cytotoxicity activity. From these results, the hexane extract from reflux method and the CH_2Cl_2 extract from maceration method were further separated. **CS-1**, **CS-2** and **CS-3** were obtained and their structures were determined to be plaunotol, plaunolide and plaunol E, respectively (as shown in 3.1).

Various concentrations (3, 10, 30 and 100 μM) of plaunotol, plaunolide and plaunol E were prepared and tested for the inhibition of NO production in the RAW264.7 cells. CAPE, indomethacin and L-nitroarginine were used as positive controls. CAPE has an IC_{50} of 3.68 μM, more potent than indomethacin (IC_{50} 24.55 μM) and L-nitroarginine (IC_{50} 30.83 μM) (Table 3.5). CAPE has potent anti-inflammatory activity via the inhibition of the activation of the transcription of NF-κB. CAPE has stronger effect on NO production than L-nitroarginine (an NO synthase inhibitor) and indomethacin (COXs inhibitor). Plaunotol, plaunolide and plaunol E inhibited NO production with the IC_{50} of 3.41, 17.09 and 2.79 μM, respectively (Table 3.5, Fig. 3.4). Three compounds were found to significantly inhibit LPS-induced NO production in a dose-dependent manner (Fig. 3.3). Plaunotol and plaunol E have ability to inhibit NO production in the same range as CAPE. Less activity was found in plaunolide. However, its potency was closed to indomethacin and L-nitroarginine. Fig. 3.4 illustrates the IC_{50} values of the tested compounds.

Additionally, the cells, after treated for the inhibitory activity on NO production in RAW264.7 cell, were parallel examined for the cytotoxicity using the MTT assay. . After 48 h for incubation of RAW264.7 together with LPS and each sample, treated cells were investigated for cell viability by adding the MTT solution and incubated for 2 h. Then the formazan product was formed and the optical density was read at OD of 570 nm. On the cytotoxicity test, the critical value was considered to be toxic when the optical density of the sample was less than 80%, which compared in control group.

The cytotoxic effects of plaunotol, plaunolide and plaunol E were evaluated using MTT assay. Only plaunolide did not affect the cell viability of RAW264.7 cells at least up to 100 μM. But plaunotol at 100 μM and plaunol E at >10 μM affected cells viability, observed to be cytotoxic agent. It has been reported that the mechanism of plaunotol on apoptosis effect was an induction of caspases in the growth cycle of colon cancer (Yoshikawa *et al*., 2009). Interestingly, cytotoxicity of plaunol E has never been reported so far. Therefore, plaunotol E may have potential as anticancer drug.

Table 3.4 The inhibition of NO production from *C. stellatopilosus* Ohba leaves extracts.

Extract	[a]Inhibitory activity (%) at various concentrations (μg/ml)				
	3	**10**	**30**	**100**	**IC_{50}**
Reflux method					
EtOH extract	38.66±1.79**	53.83±4.05**	68.03±2.95**	93.47±4.30**	7.20
Hexane fraction	9.43±2.47	13.36±3.75	32.22±2.86**	97.05±1.41**	49.31
Residual fraction	9.82±1.65**	9.82±2.21**	19.84±1.32**	33.99±0.32**	>100
Maceration method					
Hexane extract	39.75±2.74*	48.45±2.95**	69.49±4.13**	70.47±2.12**[b]	8.37
CH_2Cl_2 extract	68.35±2.21**	102.28±2.90**	103.26±3.60**	93.96±4.18**[b]	<3
EtOH extract	24.58±3.36*	76.67±1.52**	91.25±2.19**	96.25±1.97**	5.94
CAPE	38.42±2.93**	90.52±2.85**	103.79±0.51**[b]	102.53±0.73**[b]	3.68 μM

[a]Each value represents mean ± S.E.M. of four determinations.

* Statistical significance $P < 0.05$ and ** Statistical significance $P < 0.01$.

[b] Cytotoxicity was observed.

Table 3.5 The inhibition of NO production from plaunotol, plaunolide and plaunol E.

Compound	[a]Inhibitory activity (%) at various concentration (μM)					IC_{50}
	1	3	10	30	100	
plaunotol		39.58±1.42**	103.33±2.04**	128.75±3.93**	141.67±2.04**[b]	3.41
plaunolide		20.73±1.19**	32.10±1.40**	60.21±1.59**	88.00±0.36**	17.09
Plaunol E	14.46±2.60*	53.29±2.38**	103.55±2.43**[b]	105.33±1.27**[b]	103.30±1.05**[b]	2.79
CAPE		38.42±2.93**	90.52±2.85**	103.79±0.51**[b]	102.53±0.73**[b]	3.68
indomethacin		37.05±9.06*	48.00±5.22**	53.58±5.47**	94.95±0.89**[b]	24.55
L-nitroarginine		20.74±1.49**	21.68±3.93**	45.68±2.96**	83.26±0.79**	30.83

[a] Each value represents mean ± S.E.M. of four determinations.

* Statistical significance $P < 0.05$ and ** Statistical significance $P < 0.01$.

[b] Cytotoxicity was observed.

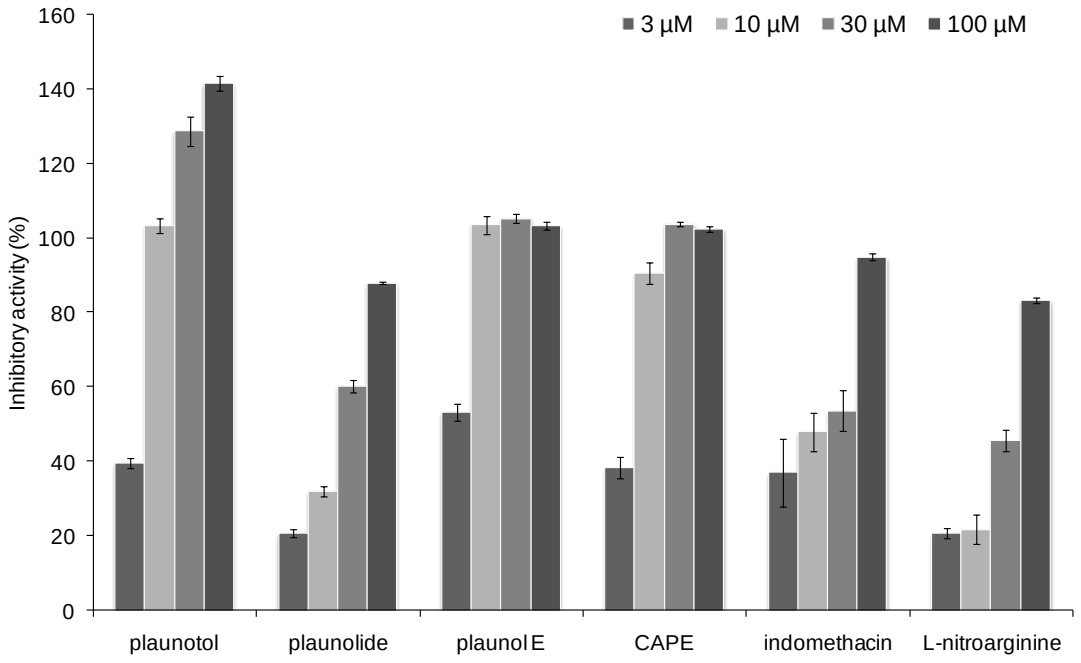

Figure 3.3 Inhibitory activity of plaunotol, plaunolide, plaunol E, CAPE, indomethacin and L-nitroarginine on NO production by LPS induced in RAW264.7 cells.

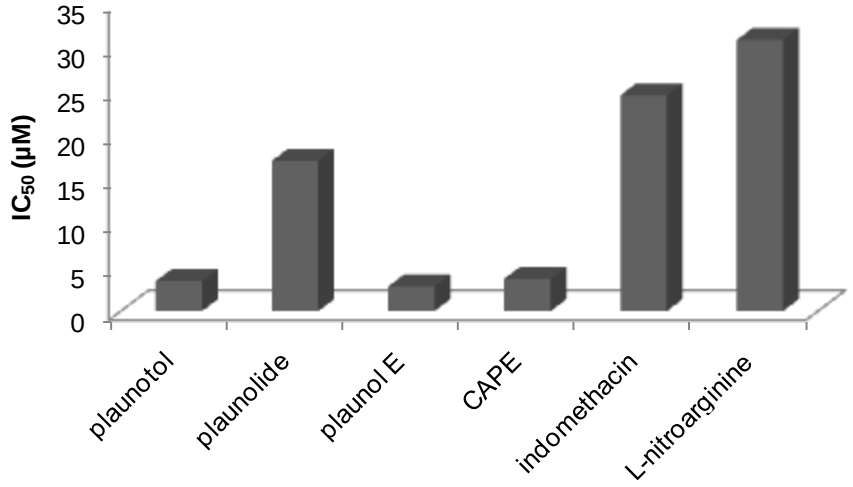

Figure 3.4 Values of IC_{50} of the tested compounds.

3.3 Effects of plaunotol, plaunolide and plaunol E on mRNAs expressions

As shown in 3.2, plaunotol, plaunolide and plaunol E have inhibitory activity on NO production with significant values in comparison to positive controls. NO is an important signaling molecule, which is involved in the regulation of diverse physiological and patho-physiological mechanisms. NO acts as a biological mediator and is an important host defense effector in the immune system. The production of NO in the body is catalyzed by nitric oxide synthases (NOSs) including endothelial NOS (eNOS), neuronal NOS (nNOS) and inducible NOS (iNOS). For the treatment of inflammatory disease, compound that acts on the inhibition of iNOS is target for inflammatory drug discovery. Generally, activity of iNOS can be induced by exogenous compounds in the cells such as macrophage cells and not present in the resting stage. On the other hand, inflammatory mediators, belonging to eicosanoids group such as prostaglandins, are considered to be target for anti-inflammatory drug design. Prostaglandins are produced from arachidonic acid via the enzyme cyclooxygenase (COX). Non-steroidal anti-inflammatory drugs act by inhibition of COX-1 and COX-2 proteins (Aktan 2004).

Thus, effects of plaunotol, plaunolide and plaunol E on the mRNAs expressions of *COX-1*, *COX-2* and *iNOS* genes were studied in the RAW264.7 cells. This result may suggest the mechanism of NO inhibition of plaunotol, plaunolide and plaunol E in this cell line. Nucleotide sequences of *GAPDH, COX-1*, *COX-2* and *iNOS* of *Mus musculus* in the database provided us to design the specific primers with aid of online primer design software from MWG operon. Quantitative RT-PCR (qRT-PCR) was used as technique for determination of gene expression. The house-keeping gene of *GAPDH* was used as the endogenous gene during running the PCR reaction.

After the PCR (2.6.7.4) was performed, the dissociation curve of the PCR product was achieved. These curves suggested the primer specificity to cDNA template and the genuine melting temperature of the PCR product. In this study, dissociation curves of *GAPDH*, *COX-1*, *COX-2* and *iNOS* are shown in Fig. 3.6. The results indicated that primers (Table 2.1) were

corresponded to the following genes. Only one derivative was observed in each PCR reaction and has the unique melting profile (temperature more than 80°C), indicating that the primer-dimer did not occurred. The sizes of the PCR products, as expected, were confirmed by agarose gel electrophoresis as shown in Fig. 3.5.

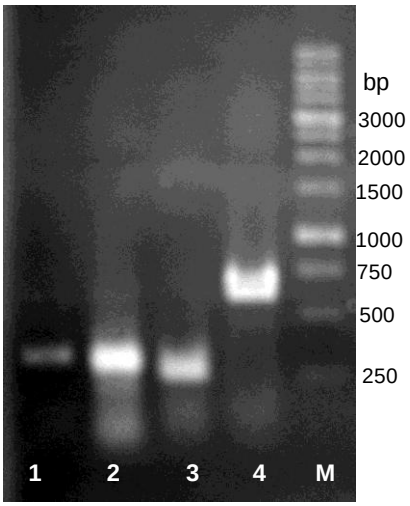

Figure 3.5 1%(w/v) agarose gel electrophoresis of the PCR products: lane 1 *GAPDH*, lane 2 *COX-1*, lane 3 *COX-2*, lane 4 *iNOS* and lane M DNA ladder (Sib-Enzyme).

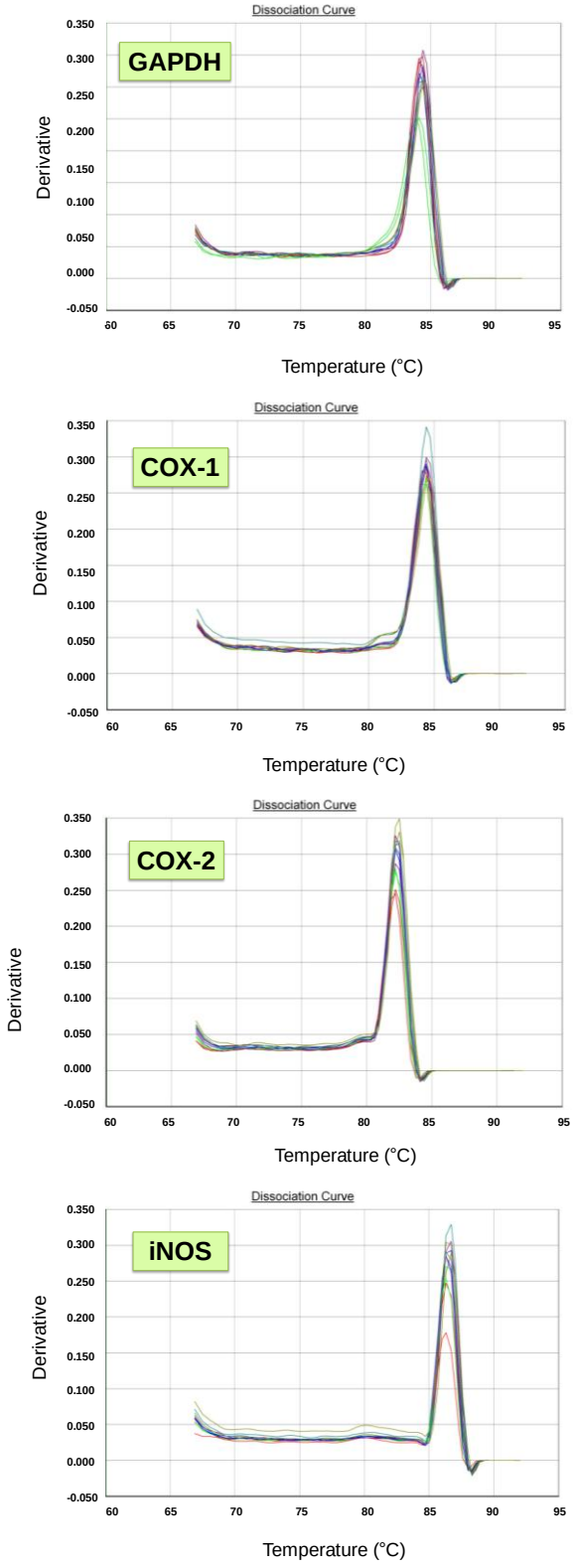

Figure 3.6 Dissociation curves of the PCR products of *GAPDH*, *COX-1*, *COX-2* and *iNOS*.

Profile of gene expression can be expressed as relative quantitation (RQ). This value was obtained either from the standard curve method or the comparative method. In this study, we used the comparative method when the endogenous gene was glyceraldehydes 3-phosphate dehydrogenase (*GAPDH*) and the control group (LPS-treated) was used as a calibrator. Unlike the standard curve method where the calculation is based on the actual amount of DNA or RNA, the comparative method estimated based on the arithmetic formula (2.6.7.4). Therefore, the amount of target was normalized to an endogenous reference (*GAPDH*) and relative to a calibrator.

Before using the comparative method for DNA quantitation, a validation experiment is required (2.6.7.4) to verify the efficiencies of target (tested genes) and reference (*GAPDH*). Moreover, an appropriate amount of total RNA in the reaction was suggested by a validation experiment as indicated in the dissociation curve. During the course of performing the PCR at various concentrations of total RNA, the ΔRn was recorded and C_T value was extrapolated from the cycles at threshold of 0.2. From a linear plot (Fig. 3.7) indicated that the C_T value was dependent upon the amount of total RNA in the reaction. The suitable amount of total RNA, in the reaction, is more than 0.4 ng as shown in Fig. 3.7.

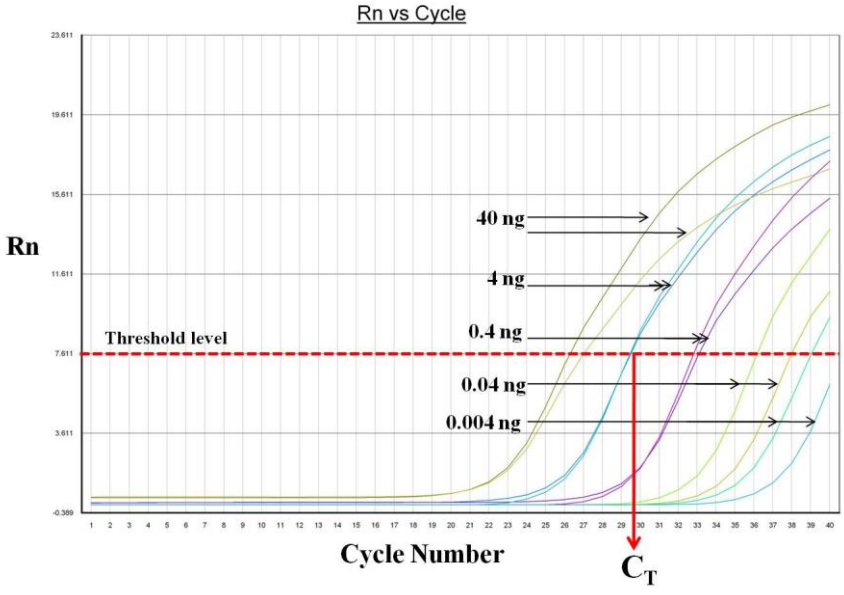

Figure 3.7 Linear plot of validation experiment at various concentration of total RNA.

From the qRT-PCR data, the ΔC_T was calculated from the normalization of the C_T value of target genes by endogenous gene of *GAPDH*. Considering the efficiency of qRT-PCR, the semi-logarithm for relative efficiency was plotted from ΔC_T against amount of total RNA. The absolute value of the slope of log input amount versus ΔC_T should be less than 0.1. The slopes of the relative efficiency plots of *COX-1*, *COX-2* and *iNOS* are -0.491, -0.614 and -0.173, respectively (Fig. 3.8). This means the PCR experiment passed on a validation test. Therefore, protocol of PCR and qRT-PCR data can be used for calculation of relative quantification by the comparative C_T method without running standard curves on the sample plate.

From the validation method, the primer specificity, the efficiency of qRT-PCR and the optimal amount of cDNA with related to input amount of total RNA at 4 ng/reaction were proved. Therefore the condition in the validation experiment was used to study the target genes including *iNOS*, *COX-1* and *COX-2* while *GAPDH* was used as endogenous gene. The PCR reaction was performed in separate tube and calculated in relation to the endogenous gene. Pair of primers was added as appropriate. After performing qRT-PCR, set of data was obtained. Relative quantitation was calculated using the comparative C_T method.

As shown as equation in 2.6.7.4, the average ΔC_T of each target genes was calculated by subtracting the average C_T value of *GAPDH* with the average C_T value of each target gene. Then the $\Delta\Delta C_T$ of each target gene was calculated following by subtracting each ΔC_T value of target gene with the ΔC_T value of calibrator (control group or LPS-treated cells). Finally, the relative quantitation (RQ) was calculated according to the following formula; $2^{-\Delta\Delta C_T}$. Results of *COX-1*, *COX-2* and *iNOS* mRNA expression are shown in Table 3.6-3.8 and Fig 3.9-3.11. Briefly, the RQ of cells treated with plaunotol suggested that plaunotol stimulated the *COX-1* and *COX-2* expressions but suppressed the *iNOS* expression significantly. On the other hand, cells treated with plaunolide, the expressions *COX-1*, *COX-2* and *iNOS* genes were down-regulated. However, the RQ of cells treated with plaunol E, which tested at 100-fold dilute concentration, suggests that plaunol E could inhibit the *COX-2*, increase *COX-1* and no effect on *iNOS* expression.

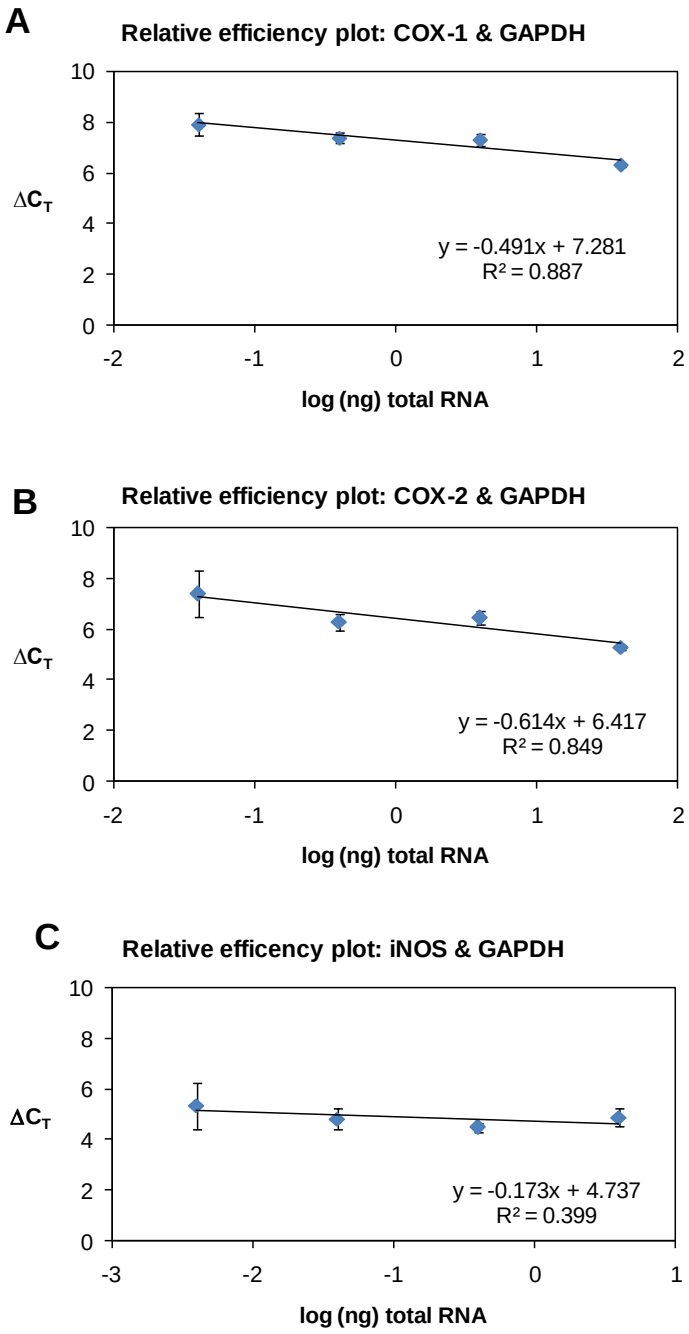

Figure 3.8 Relative efficiency plots of target genes normalized with *GAPDH*. A. *COX-1*; B. *COX-2*; C. *iNOS*.

Table 3.6 Relative quantitation (RQ) of plaunotol on *COX-1*, *COX-2* and *iNOS* mRNA expressions normalized with *GAPDH* (n = 4).

Treatment	Average C_T		ΔC_T	$\Delta\Delta C_T$	RQ
	Target gene	GAPDH			
For COX-1					
Normal	18.279±0.026	15.267±1.053	3.012±1.053	-3.338±1.053	10.112±0.087#
LPS-treated	22.141±0.491	15.818±0.028	6.323±0.492	-0.027±0.492	1.019±0.169
3 μM plaunotol	22.716±0.138	16.071±0.390	6.645±0.414	0.295±0.414	0.815±0.080
10 μM plaunotol	22.327±0.138	16.280±0.425	6.047±0.447	-0.303±0.447	1.234±0.094
30 μM plaunotol	21.393±0.124	16.115±1.127	5.278±1.134	-1.072±1.134	2.102±0.128**
30 μM indomethacin	22.832±0.495	16.450±0.874	6.382±1.004	0.032±1.004	0.978±0.192
For COX-2					
Normal	28.983±0.161	15.267±1.053	13.716±1.053	8.966±1.053	0.002±0.000#
LPS-treated	20.564±0.194	15.818±0.028	4.746±0.196	-0.004±0.196	1.003±0.064
3 μM plaunotol	20.694±0.328	16.071±0.390	4.623±0.510	-0.127±0.510	1.092±0.108
10 μM plaunotol	20.220±0.005	16.280±0.425	3.940±0.425	-0.810±0.425	1.753±0.004**
30 μM plaunotol	21.515±0.319	16.115±1.127	3.759±1.171	-0.991±1.171	1.988±0.310**
30 μM indomethacin	21.517±0.328	16.450±0.874	5.067±0.934	0.317±0.934	0.803±0.096
For iNOS					
Normal	31.495±0.057	15.267±1.053	16.228±1.055	11.279±1.055	0.000±0.000#
LPS-treated	20.741±0.474	15.818±0.028	4.923±0.475	-0.026±0.475	1.018±0.162
3 μM plaunotol	20.632±0.100	16.071±0.390	4.561±0.403	-0.388±0.403	1.309±0.064**
10 μM plaunotol	21.515±0.509	16.280±0.425	5.235±0.663	0.286±0.663	0.820±0.102
30 μM plaunotol	21.610±0.399	16.115±1.127	5.495±1.196	0.546 ±1.196	0.685±0.109**
30 μM indomethacin	23.246±1.277	16.450±0.874	6.796±1.547	1.847±1.547	0.278±0.168

[a] The average ΔC_T value was determined by subtracting the average C_T value of GAPDH with the average C_T value of target gene. The standard deviation of the difference was calculated from the standard deviations of the target gene. * $P < 0.05$ and ** $P < 0.01$ indicate significant differences from LPS-treated group and #$P < 0.01$ indicates a significant difference from LPS-treated group.

Table 3.7 Relative quantitation (RQ) of plaunolide on *COX-1*, *COX-2* and *iNOS* mRNA expressions normalized with *GAPDH* (n = 4).

Treatment	Average C_T		ΔC_T	$\Delta\Delta C_T$	RQ
	Target gene	GAPDH			
For COX-1					
Normal	20.334±0.060	15.875±0.157	4.459±0.168	-2.654±0.168	6.296±0.124#
LPS-treated	24.477±0.361	17.398±0.037	7.079±0.363	-0.034±0.363	1.024±0.208
3 μM plaunolide	24.879±0.273	17.380±0.075	7.499±0.283	0.386±0.283	0.765±0.152
10 μM plaunolide	24.715±0.039	17.344±0.314	7.371±0.316	0.258±0.316	0.836±0.016
30 μM plaunolide	24.799±0.356	16.829±0.639	7.970±0.731	0.857±0.731	0.552±0.096**
30 μM indomethacin	22.832±0.495	16.450±0.874	6.382±1.004	0.032±1.004	0.978±0.192
For COX-2					
Normal	31.115±1.200	15.875±0.157	16.240±1.210	9.966±1.210	0.001±0.000#
LPS-treated	23.602±0.521	17.398±0.037	6.204±0.522	-0.070±0.522	1.050±0.273
3 μM plaunolide	23.175±0.028	17.380±0.075	5.795±0.080	-0.479±0.080	1.394±0.022**
10 μM plaunolide	23.362±0.277	17.344±0.314	6.018±0.419	-0.256±0.419	1.194±0.188
30 μM plaunolide	23.372±0.109	16.829±0.639	6.543±0.648	0.269±0.648	0.830±0.050
30 μM indomethacin	21.517±0.328	16.450±0.874	5.067±0.934	0.317±0.934	0.803±0.096*
For iNOS					
Normal	31.132±0.842	15.875±0.157	15.257±0.857	11.279±0.857	0.000±0.000#
LPS-treated	21.360±0.261	17.398±0.037	3.962±0.264	-0.016±0.264	1.011±0.146
3 μM plaunolide	21.290±0.434	17.380±0.075	3.910±0.440	-0.068±0.440	1.048±0.278
10 μM plaunolide	22.026±0.264	17.344±0.314	4.682±0.410	0.704±0.410	0.614±0.094**
30 μM plaunolide	22.038±1.231	16.829±0.639	5.209±1.387	1.231±1.387	0.426±0.222**
30 μM indomethacin	23.246±1.277	16.450±0.874	6.796±1.547	1.847±1.547	0.278±0.168**

[a] The average ΔC_T value was determined by subtracting the average C_T value of GAPDH with the average C_T value of target gene. The standard deviation of the difference was calculated from the standard deviations of the target gene. *$P < 0.05$ and **$P < 0.01$ indicate significant differences from LPS-treated group and #$P < 0.01$ indicates a significant difference from LPS-treated group.

Table 3.8 Relative quantitation (RQ) of plaunol E on *COX-1*, *COX-2* and *iNOS* mRNA expressions normalized with *GAPDH* (n = 4).

Treatment	Average C_T		ΔC_T	$\Delta\Delta C_T$	RQ
	Target gene	GAPDH			
For COX-1					
Normal	18.889±0.016	14.336±0.329	4.553±0.329	-3.439±0.329	10.845±0.055#
LPS-treated	27.111±0.298	19.129±0.442	7.982±0.533	-0.010±0.533	1.007±0.100
0.03 μM plaunol E	23.055±0.145	15.883±0.634	7.172±0.650	-0.820±0.650	1.765±0.125**
0.1 μMplaunol E	23.335±0.087	16.009±0.585	7.326±0.591	-0.666±0.591	1.587±0.068*
0.3 μM plaunol E	23.194±0.359	16.548±0.529	7.610±0.639	-0.382±0.639	1.303±0.228
30 μM indomethacin	22.832±0.495	16.450±0.874	6.382±0.987	0.032±0.987	0.978±0.192
For COX-2					
Normal	27.245±1.169	14.336±0.329	12.909±1.214	7.158±1.214	0.007±0.004#
LPS-treated	24.859±0.426	19.129±0.442	5.730±0.614	-0.021±0.614	1.015±0.145
0.03 μM plaunol E	21.313±0.306	15.883±0.634	5.430±0.704	-0.321±0.704	1.249±0.206**
0.1 μMplaunol E	21.918±0.119	16.009±0.585	5.909±0.597	0.158±0.597	0.896±0.074
0.3 μM plaunol E	23.290±0.052	16.548±0.529	6.706±0.532	0.955±0.532	0.516±0.013**
30 μM indomethacin	21.517±0.328	16.450±0.874	5.067±0.934	0.317±0.934	0.803±0.096
For iNOS					
Normal	27.229±0.476	14.336±0.329	12.893±0.597	6.059±0.597	0.015±0.076#
LPS-treated	25.957±0.227	19.129±0.442	6.828±0.497	-0.006±0.497	1.004±0.002
0.03 μM plaunol E	21.809±0.022	15.883±0.634	5.926±0.634	-0.908±0.634	1.876±0.020**
0.1 μMplaunol E	21.829±0.608	16.009±0.585	5.820±0.844	-1.014±0.844	2.020±0.077**
0.3 μM plaunol E	22.634±1.254	16.548±0.529	6.050±1.361	-0.784±1.361	1.722±0.121**
30 μM indomethacin	23.246±1.277	16.450±0.874	6.796±1.547	1.847±1.547	0.278±0.168**

[a] The average ΔC_T value was determined by subtracting the average C_T value of GAPDH with the average C_T value of target gene. The standard deviation of the difference was calculated from the standard deviations of the target gene. *$P < 0.05$ and **$P < 0.01$ indicate significant differences from LPS-treated group and #$P < 0.01$ indicates a significant difference from LPS-treated group.

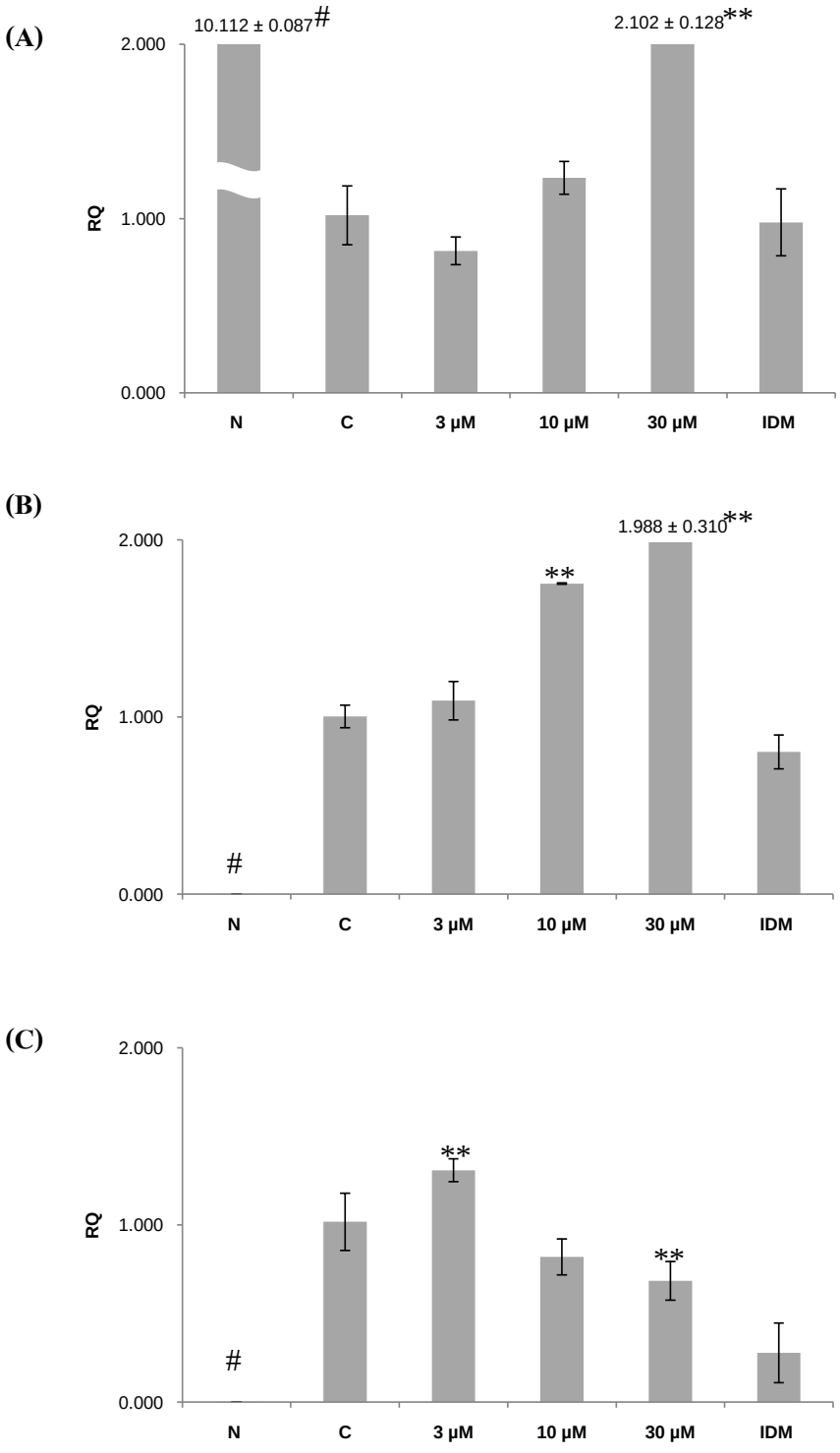

Figure 3.9 Relative quantitation of plaunotol on *COX-1* (A), *COX-2* (B) and *iNOS* (C) normalized with *GAPDH.* **P* < 0.05 and ***P* < 0.01 indicate significant differences from LPS-treated group and #*P* < 0.01 indicates a significant difference from LPS-treated group.

Abbreviation: N = normal group; C = control group (LPS-treated); IDM = indomethacin.

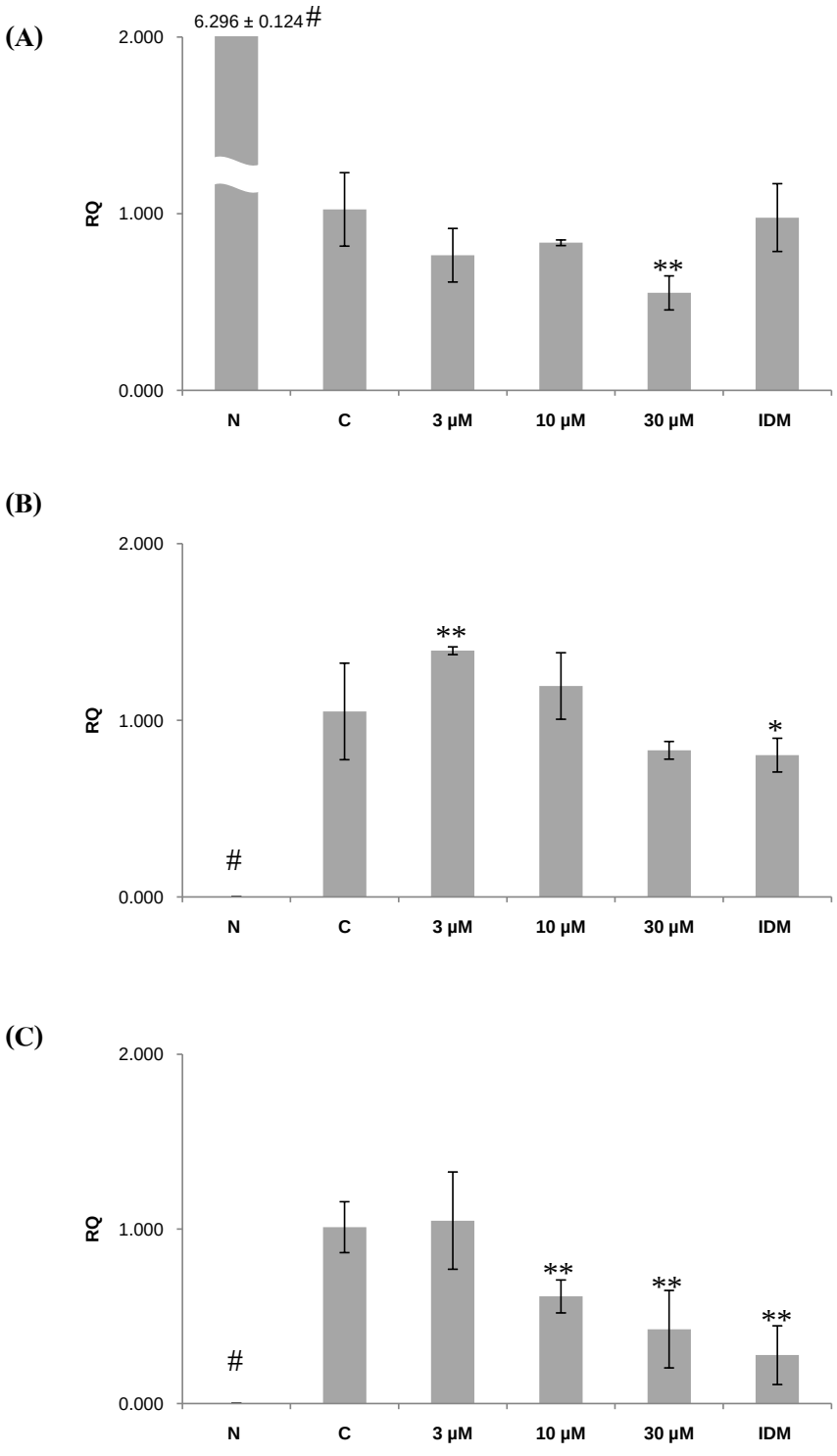

Figure 3.10 Relative quantitation of plaunolide on *COX-1* (A), *COX-2* (B) and *iNOS* (C) normalized with *GAPDH*. **P* < 0.05 and ***P* < 0.01 indicate significant differences from LPS-treated group and #*P* < 0.01 indicates a significant difference from LPS-treated group.

Abbreviation: N = normal group; C = control group (LPS-treated); IDM = indomethacin.

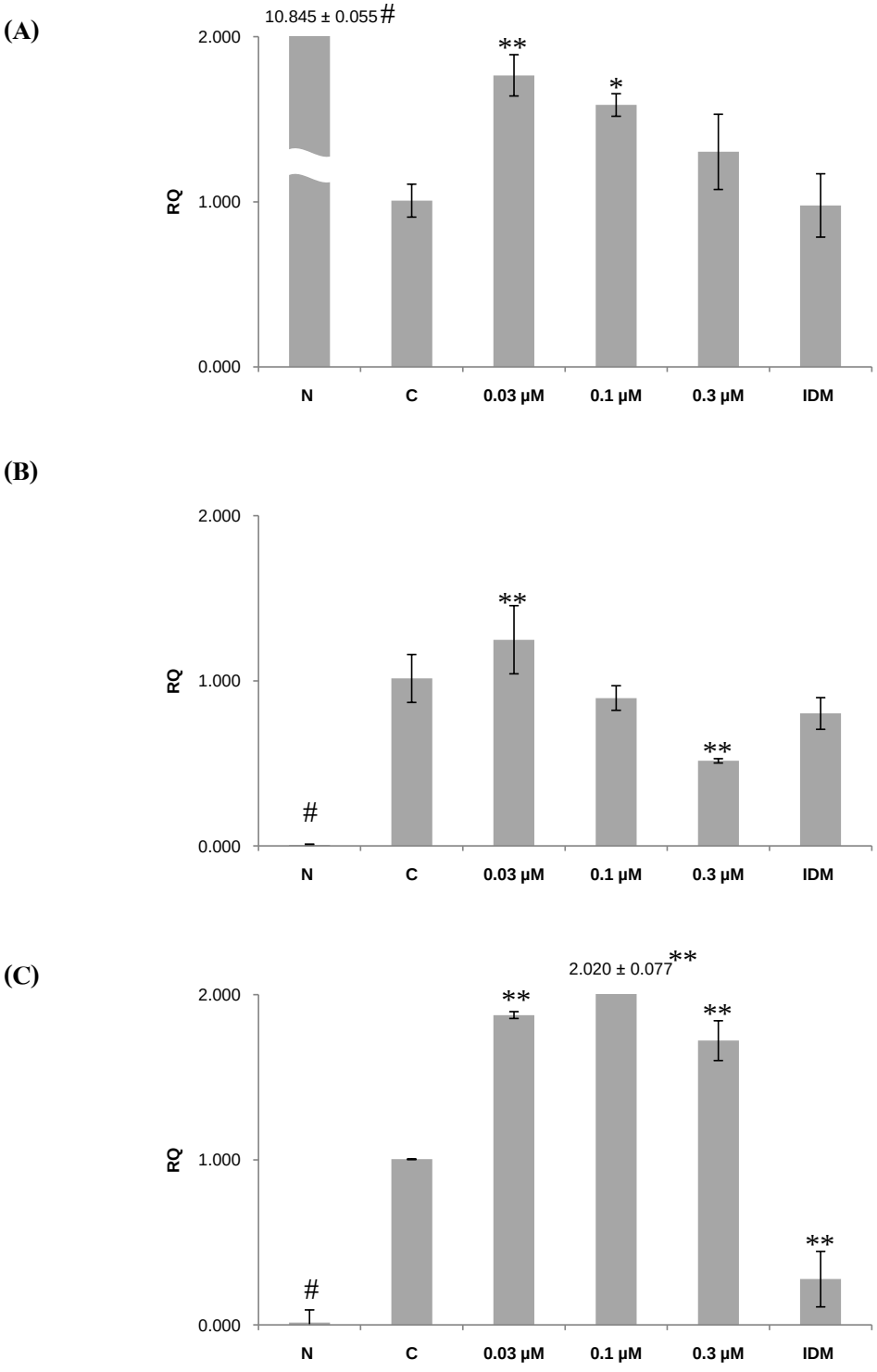

Figure 3.11 Relative quantitation of plaunol E on *COX-1* (A), *COX-2* (B) and *iNOS* (C) normalized with *GAPDH*. **P* < 0.05 and ***P* < 0.01 indicate significant differences from LPS-treated group and #*P* < 0.01 indicates a significant difference from LPS-treated group.

Abbreviation: N = normal group; C = control group (LPS-treated); IDM = indomethacin.

CHAPTER 4

DISCUSSION

Plaunoi, a Thai medicinal plant, is the only nature source of plaunotol, which is prescribed for anti-peptic ulcer. This well known plant has been thoroughly studied for chemical constituents for decades. Plenty of diterpenes have been reported and some of them e.g. derivatives of plaunol have been evaluated for the anti-peptic ulcer activity. Unlike plaunol, plaunotol has been studied in a wide array of activity including antibacterial, anticancer as well as anti-peptic ulcer activities. In light of increasing the value of Plaunoi, we continue to investigate the potential of diterpenes for anti-inflammatory activity in the murine macrophage RAW264.7 cells. Source of Plaunoi was supplied from the Plaunoi field, formerly owned by Thai Sankyo Company, where Plaunoi were cultivated for plaunotol extraction. Using phytochemical techniques, one acyclic diterpene-plaunotol and two furanoditerpenes-plaunolide and plaunol E were obtained. Evaluation of the anti-inflammatory activity was performed. The mechanism of action on the inflammatory mediators, including *COX-1*, *COX-2* and *iNOS*, was examined.

In this study, the chemical constituents from *C. stellatopilosus* were isolated. As mentioned earlier, the isolation and structure elucidation led to the identification plaunotol, acyclic diterpenes; plaunolide and plaunol E, furanoditerpenes. The spectra were examined and compared to the previously published reports (Ogiso *et al*., 1978; Takahashi *et al*., 1983; Kitazawa *et al*., 1980). Plaunotol and plaunol E have been reported for anti-shay ulcer activity in the animal model. However, plaunolide has not been reported for biological activity.

A previous study that three known compounds including plaunotol, plaunolide and plaunol E were isolated from the stem of Plaunoi with acetone and further isolation by chromatographic technique (see Chapter 1). In our study, we used the reflux method for plaunotol isolation following the previous study and used the maceration method, which was different from

the previous study, for isolated plaunolide and plaunol E. Considering these methods based on the skeleton of their structures, plaunotol is a non polar molecule, therefore, it was extracted with hexane. Traces of plaunolide and plaunol E were found in the hexane fraction. By using the maceration method, we obtained plaunolide and plaunol E since both substances have moderate polarity. Interestingly, the optimization method of extraction is important for further isolation of the compounds. In this experiment, if we had not change the reflux to the maceration method, we might have isolate only plaunotol and the not interesting molecules such as fatty acid and steroids, which were normally found in this plant. In this study, we report for the first time of ^{13}C-NMR data ($CDCl_3$) of plaunolide and plaunol E.

From the biosynthetic point of view, the structure of diterpene naturally is comprised of the 20 carbon atoms. The diterpene biosynthesis has been reported by the group of De-Eknamkul and his co-workers. Only plaunotol biosynthesis was studied in detail. Considering plaunotol structure (Scheme 4.1), plaunotol consists of four isoprene units, which are connected in head to tail fashion (Ogiso *et al*., 1985). Plaunotol is derived from the general intermediate, geranylgeranyl diphosphate (GGPP). The GGPP is formed from one molecule of dimethylallyl diphosphate (DMAPP) and three molecules of isopentenyl diphosphate (IPP), catalyzed by prenyltransferase (Spurgeon and Porter, 1981; Sitthithaworn *et al*., 2001). The GGPP is then dephosphorylated to give geranylgeraniol (GGOH) by geranylgeranyl diphosphate monophosphatase (Nualkaew *et al*., 2006). In the final step, GGOH is hydroxylated at C-18 position, affording the 18-hydroxylated-GGOH or plaunotol. The reaction is catalyzed by GGOH 18-hydroxylase (Tansakul and De-Eknamkul, 1998). Up to date, the biosynthesis of cyclic diterpene in Plaunoi is still unknown. Considering the structure of the clerodane diterpene such as plaunolide and plaunol E, it can be proposed that the furanoditerpenes are derived from the *E*,*E*,*E*-GGPP via copalyl diphosphate intermediate. However, *ent*-copalyl diphosphate synthase from this plant has not been discovered so far.

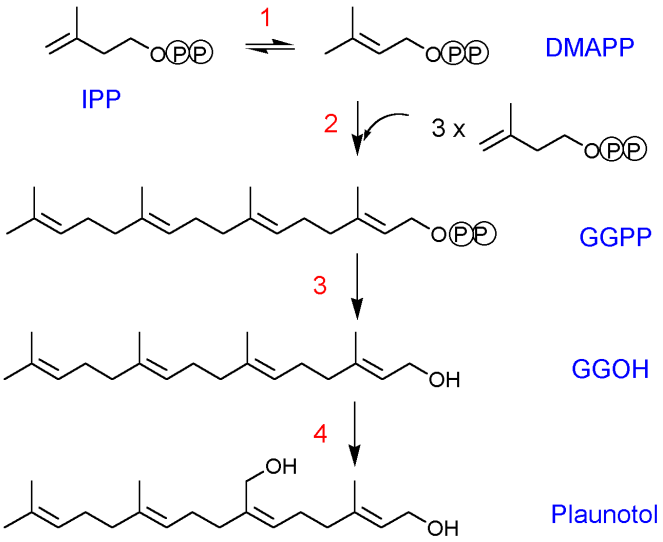

Scheme 4.1 Biosynthesis of plaunotol in *Croton stellatopilosus* Ohba. 1 = isopentenyl diphosphate isomerase; 2 = GGPP synthase ;3 = GGOH monophosphatase ; 4= GGOH-18-hydroxylase.

Since the macrophage cells such as RAW264.7 are responsible for the innate immunity, and activation by LPS from the gram-negative *E.coli* activates the macrophage to produce the reactive oxygen species and cytokines. The LPS then can activate macrophages to release the inflammatory mediators such as NO, TNF-α, PGE_2 for instance. Therefore, the inhibition of NO, PGE_2 and TNF-α productions is an important therapeutic consideration in development of anti-inflammatory agents (Cho et al., 2008).

In this study, plaunotol, plaunolide and plaunol E were tested for their potential on anti-inflammatory activity through an inhibition of NO production. As shown in the results, all three compounds significantly exhibited the inhibitory activity NO production when compared their IC_{50} with the IC_{50} of positive controls such as indomethacin, L-nitroaginine (L-NA) and caffeic acid phenethyl ester (CAPE) (Table 3.5).

The mechanism about anti-inflammatory activity of plaunotol, plaunolide and plaunol E were investigated by measuring genes expressions of *COX-1*, *COX-2* and *iNOS*, genes. The

results indicated that plaunotol stimulated on *COX-1* and *COX-2* expressions but suppressed the *iNOS* expression significantly at concentration of 30 μM. On the other hands, the expressions *COX-1*, *COX-2* and *iNOS* genes were down-regulated by treatment cells with plaunolide. Moreover, plaunol E could only inhibit the *COX-2* but increase *COX-1* expression and it has no effect on *iNOS* expression. Interestingly, plaunol E possessed the cytotoxicity at concentration more than 10 μM. The results concluded that all three compounds possessed the anti-inflammatory activity with different mechanism.

With regard to of the inflammatory mechanism, there are at least two pathways involved in the inflammation process. Firstly, pathway of NO production, NO is formed from L-arginine. Secondly, the prostaglandin (PGs) synthesis, PGs is produced from arachidonic acid, which is formed from phospholipid membrane, catalyzed by COX-1 and COX-2. Compound that has a potent anti-inflammatory activity should either inhibit of NO production or suppress COXs enzymes.

In this study, plaunotol has been shown to inhibit NO production by suppression of *iNOS* gene expression. This effect results in the anti-inflammatory activity. This is the first report about the mechanism of plaunotol on the inhibition of *iNOS* and NO production. Previously, plaunotol has been reported in the rat model to prevent gastric inflammation from irritating agents such as trinitrobenzene sulfonic acid and acetic acid in rats (Makino *et al*., 1998) and compound C48/80 (Ohta *et al*., 2005). Evidence of plaunotol has anti-inflammatory and anti-oxidant properties in the *H. pylori* infection in stomach (Augusto *et al*., 2007) have been reported. This is in line with our finding that plaunotol could inhibit the NO production.

Murakami *et al*. (1999) reported that plaunotol suppressed the secretions of TNF-α and interleukin (IL)-8 in the endotoxin-induced monocytes. They suggested that plaunotol decreased TNF-α production by inhibition on release of neutrophil elastase, increase levels of intracellular calcium and neutrophil activation (Murakami *et al.*, 1999). Study the effect of plaunotol on IL-8 secretion was performed in the human gastric cancer cell line MKN45, induced with *H. pylori*

infection. Secretion of IL-8 by MKN45 was suppressed after co-culture with plaunotol in a dose-dependent manner (Takagi *et al*., 2000). Treatment of plaunotol to the serum-starved rat gastric mucosal (RGM1) cells indicated that plaunotol increased PGE_2 production by the phosphorylation of the (NF-κB) and activation of cyclic AMP response element (CRE) sites of *COX-2* gene promoters (Fu *et al*., 2005). In overview, plaunotol has been shown to have an effect on the innate immune system.

It can be noted that plaunotol increased the prostaglandins (PGE_2 and PGI_2) productions in cultured cells of 3T6 fibroblasts (Ushiyama *et al*., 1987). They suggested that plaunotol increased the prostaglandins level by stimulating the cellular phospholipase activity, not prostaglandin cyclooxygenase activity (Ushiyama *et al*., 1987). Nevertheless, role of plaunotol on COX-2 expression, not COX-1 was reported from study in the (RGM1) cells (Fu *et al*., 2005). From our results, plaunotol could up-regulate significantly the *COX-1* and *COX-2* expressions in the murine macrophage RAW 264.7 cells. This result is in agreement with the previous results.

Anti-inflammatory potential of two furanoditerpenes, namely plaunolide and plaunol E, were assessed in RAW264.7 cells. The results suggested that plaunolide and plaunol E inhibit the NO production with the IC_{50} of 17.09 μM and 2.79 μM, respectively. Transcription profiles of *iNOS*, *COX-1* and *COX-2* of the treated RAW264.7 cells concluded that plaunolide up-regulated all genes and possess via biosynthesis of NO and prostaglandin. In contrast, plaunol E suppressed only COX-2 expression. Slightly increase COX-1 and no effect on iNOS genes expression by plaunol E were observed. From our results, plaunolide was shown to be an anti-inflammatory agent, but has cytotoxic effect at high concentration (more than 100 μM). The biological activity of plaunolide has not been reported so far. Our results suggested for the first time of its activity. More detail of its pharmacological activity and toxicity should be investigated as such in the animal model. In contrary to plaunolide, plaunol E is a toxic molecule as shown in this report. In the experiment of gene expression, cell death was observed although the tested concentration was reduced to 1 μM. On the other hand, this toxic molecule may have potential to be an anti-cancer

agent. Investigation of plaunol E on the inhibition of cancer cell lines is suggested and its mechanism of inhibition during cell growth is also interesting issue.

Acyclic diterpene plaunotol was reported to have anti-angiogenic effect in human umbilical vein endothelial cell (HUVECs) model (Kawai *et al*., 2005). Plaunotol inhibited growth of all gastric cancer cell lines by apoptosis induction (activation of caspase-3, -8 and -9) (Yamada *et al*., 2007; Yoshikawa *et al*., 2009). Plaunol E, a cyclization product of GGPP, probably possesses the inhibition of growth of cancer cell lines with similar mechanism. Thus, we need more knowledge about plaunol E, which also has anti-shay ulcer (Kitazawa *et al.,* 1979, Kitazawa *et al.,* 1980).

From this study, our results provide an insight of anti-inflammatory constituents from Plaunoi (*C. stellatopilosus*). Not only plaunotol can be used as anti-ulcer drug, but also other furanoditerpenes such as plaunolide and plaunol E should be considered for alternative indication.

CHAPTER 5

CONCLUSIONS

1. Preparations of *C. stellatopilosus* leave extracts were obtained from reflux method and maceration method. The reflux method was combined with partition and afforded the fractions of ethanol extract, hexane fraction and residual fraction. Their IC_{50} on inhibition of NO production were 7.20, 49.31 and >100 μg/ml, respectively. For maceration method, extraction solvents including hexane, dichloromethane and ethanol were chosen, affording the hexane, dichloromethane and ethanol extracts. Testing the inhibition of NO production of extracts showed the IC_{50} of those extracts of 8.37, <3 and 5.94 μg/ml, respectively.

2. The hexane fraction (from reflux method) and dichloromethane fraction (from maceration method) were further purified by column chromatography. **CS-1**, **CS-2** and **CS-3** were obtained. By means of spectroscopy, an acyclic diterpene named plaunotol and two furanoditerpenes, namely plaunolide and plaunol E were identified.

3. The inhibition of NO production was determined by treatment of the murine macrophage RAW264.7 cells with the isolated compounds. The IC_{50} values of plaunotol, plaunolide and plaunol E were 3.41, 17.09 and 2.79 μM, respectively, whereas, the IC_{50} values of caffeic phenetylester (CAPE), indomethacin and L-nitroarginine were 3.68, 24.55 and 30.83 μM, respectively. At concentrations of >100 μM for plaunotol and >10 μM for plaunol E, the cytotoxic effect was observed in the MTT assay.

4. The validated method of qRT-PCR provided the information of gene expressions of *iNOS*, *COX-1* and *COX-2* while *GAPDH* gene was used as an endogenous gene and the LPS-treated cells was used as a calibrator. The melting curves of each gene suggested the unique PCR product at expected size. The amplification plot indicated the C_T value, which was used for calculation of RQ value according to the comparative C_T method.

5. Plaunotol suppressed an *iNOS* gene expression significantly and increased the *COX-1* and *COX-2* expressions. The results concluded that plaunotol possesses an anti-inflammation by down-regulation of the inducible nitric oxide synthase in the innate immune system.

6. Plaunolide down-regulated the *iNOS*, *COX-1* and *COX-2* gene expressions in dose-dependent manner. It can be concluded that plaunolide has potential for anti-inflammation via the mixed mechanism on prostaglandin and nitric oxide biosyntheses.

7. Plaunol E caused the RAW264.7 cells death during treatment. It was postulated to have cytotoxic effect and probably be a candidate for anti-cancer agent. Plaunol E has no effect on *iNOS* expression, suppress *COX-2* and increase *COX-1* expressions. More knowledge about plaunol E on inhibition of cancer cell lines should be investigated.

8. From our study, it can be concluded that diterpenes from *C. stellatopilosus* have anti-inflammation potential with different mechanism of inhibition as suggested by transcription level or mRNA level. On the other hand, detection of proteins such as COX-2, NF-κB and TNF-α by western blot should be investigated in order to understand the role of these compounds, controlling the inflammation process.

REFERENCES

Aktan, F. 2004. iNOS-mediated nitric oxide production and its regulation. *Life Sci*. 75, 639-653.

American Type Culture Collection: Catalog search. 2011. ATCC® Number: TIB-71™ http://www.atcc.org/ATCCAdvancedCatalogSearch/ProductDetails/tabid/452/Default.aspx?ATCCNum=TIB-71&Template=cellBiology. (accessed June 6, 2011).

Augusto, A.C., Miguel, F., Mendonça, S., Pedrazzoli, J. and Gurgueira, S.A. 2007. Oxidative stress expression status associated to *Helicbacter pylori* virulence in gastric diseases. *Clin. Biochem*. 40(9-10), 615-622.

Aung H.T., Schroder K., Himes S.R., Brion K., van Zuylen W., Trieu A., Suzuki H., Hayashizaki Y., Hume D.A., Sweet M.J. and Ravasi T. 2006. LPS regulates proinflammatory gene expression in macrophages by altering histone deacetylase expression. *FASEB J.* 20(9), 1315-1327.

Barton, M., Haudenschild, C.C., d'Uscio, L.V., Shaw, S., Munter, K. and Luscher, T.F. 2001. Endothelial ETA receptor blockade restores No-mediated endothelial function and inhibits atherosclerosis in apolipoprotein E-deficient mice. *Proc. Natl. Acad. Sci. USA*. 95, 14367-14372.

Bunyapraphatsara, N. 1989. Plau-noi. *Med Plant Inform Cent Mahidol Univ*. 6, 1-6.

Chien, T.Y., Chen, L.G., Lee, C.J., Lee, F.Y. and Wang, C.C. 2008. Anti-inflammatory constituents of *Zingiber zerumbet*. *Food Chem*. 110(3), 584-589.

Cho, Y.C., Kim, H.J., Kim, Y.J., Lee, K.Y., Choi, H.J., Lee, I.S. and Kang, B.Y. 2008. Differential anti-inflammatory pathway by xanthohumol in IFN-gamma and LPS-activated macrophages. *Int Immunopharmacol.* 8(4), 567-573.

Cobb, J.P., Buchman, T.G., Karl, I.E. and Hotchkiss, R.S. 2000. Molecular biology of multiple organ dysfunction syndrome: injury, adaptation, and apoptosis. *Surg Infect*. 1(3), 207-213.

Coleman, J.W. 2001. Nitric oxide in immunity and inflammation. *Int. Immunopharmacol*. 1(8), 1397-1406.

Cruz-Vega, D.E., Aguilar, A., Vargas-Villarreal, J., Verde-Star, M.J. and González-Garza, M.T. 2002. Leaf extracts of *Carlowrightia cordifolia* induce macrophage nitric oxide production. *Life Sci.* 70(11), 1279-1284.

Dewick, P.M. 2002. Diterpens. Dewick, P.M(eds). *Medicinal natural product: a biosynthetic approach*. (2nd), New York, USA. John Wiley & Son. 203-212.

Esser, H. J., and Chayamarit, K. 2001. Two new species and a new name in Thai *Croton* (Euphorbiaceae). *Thai For. Bull*. 29, 51-57.

Fang, F.C. 1997. Mechanisms of nitric oxide-related antimicrobial activity. *J. Clin. Invest.* 99(12), 2818-2825.

Feghali, C.A. and Wright, T.M. 1997. Cytokine in acute and chronic inflammation. *Front. Biosci*. 2, 12-26.

Foegh, M.L., Hecker, M. and Ramwell, P.W. 1998. The eicosanoids: prostaglandins, thromboxanes, leukotrienes, and related compounds. Katazung, B.G. (ed) *Basic and clinical pharmacology* (7th ed), Stamford, USA. Appleton and lange. 304-318.

Fu, H., Yabe, Y., Asahi, K., Hayashi, Y., Murata, H., Eguchi, H., Tsujii, M., Tsuji, S. and Kawano,.S..2005..(2*E,*6*Z,*10*E*)-7-hydroxymethyl-3,11,15-trimethyl-2,6,10,14-hexadecatetraen-1-ol (Plaunotol) increases cyclooxygenase-2 expression via nuclear factor *kappaB* and cyclic AMP response element in rat gastric epithelial cells. *Eur. J. Pharmacol*. 7, 524(1-3), 38-43.

Hemmrich, K., Kröncke, K.-D., Suschek, C.V. and Kolb-Bachofen, V. 2005. What sense lies antisense inhibition of inducible nitric oxide synthase expression?. *Nitric Oxide*. 12(4), 183-199.

Hevel, J.M., White, K.A. and Marletta, M.A. 1991. Purification of the inducible murine macrophage nitric oxide synthase. Identification as flavoprotein. *J. Biol. Chem.* 266(34), 22789-22791.

Hidaka, O., Mromoto, T., Masuda, Y., Kato, T., Matsuo, R., Inoue, T., Kobayashi, M. and Tadaka, K. 1997, Regulation of masticatory force during cortically. *J. Neurophysiol*. 77(6), 3168-3179.

Huang, M-T., Ghai, G. and Ho, C.-T. 2004. Inflammatory process and molecular targets for anti-inflamatory nutraceuticals. *Compr. Rev. Food Sci. F.* 3(4), 127-139.

Inflammation, 2011. Wikipedia, the free encyclopedia. http://en.wikipedia.org/wiki/Inflammation. (accessed July 7,2008).

Inoue, Y., Shiraishi, A., Hada, T., Hirose, K., Hamashima, H. and Shimada, J. 2004. The antibacterial effects of terpene alcohols on *Staphylococcus aureus* and their mode of action. *FEMS Microbiol. Lett.* 237(2), 325-331.

Kaneko H., Mitsuma T., Nagai H., Harada M., Kotera H., Furusawa A. and Mirase K. 1995. Effect of plaunotol on hypergastrinemia induced by long-term omeprazole administration in humans. *Dig. Dis. Sci.* 40(1), 160-165.

Kang Y.J., Wingerd, B.A., Arakawa T. and Smith W.L. 2006. Cyclooxygenase-2 gene transcription in amacrophage model of inflammation. *J. Immunol.* 177(11), 8111-8122.

Kawai, K., Tsuno, N.H., Kitayama, J., Yazawa, K., AsakageM., Yamashita, H., Watanabe, T., Takahashi, K. and Nagawa, H. 2005. Anti-angigenic properties of plaunotol. *Anticancer Drugs* 16(4), 401-407.

Kim, Y.A., Choi, B.T., Lee, Y.T., Park, D.I. and Rhee, S.H. 2004. Reveratrol inhibites cell proliferation and induces apoptosis of human breast carcinoma MCF-7 cells. *Oncol. Repvol.* 11(2), 441-446.

Kitazawa, E. and Ogiso, A. 1981. Two diterpene alcohols from *Croton sublyratus*. *Phytochemistry*. 20(2), 287-289.

Kitazawa, E., Kurabayashi, M., Kasuga, S., Oda, O. and Ogiso, A. 1982. New esters of a diterpene alcohol from *Croton sublyratus*. *Ann. Rep. Sankyo Res*. *Lab*. 34, 39-41.

Kitazawa, E., Ogiso, A., Takahashi, S., Sato, A., Kurabayashi, M., Kuwano, H., Hata, T. and Tamura, C., 1979. Plaunol A and B, new anti-ulcer diterpene lactones from *Croton sublyratus*. *Tetrahedron Letts.* 20(13), 1117–1120.

Kitazawa, E., Sato, A. Takahashi, S. Kuwano, H. and Ogiso, A. 1980. Novel diterpenelactones with anti-peptic ulcer activity from *Croton sublyratus*. *Chem. Pharm. Bull.* 28(1), 227-234.

Koga ,T., Watanabe, H., Kawada, H., Takahashi, K., Utsui, Y., Domon, H., Ishii, C., Narita, T. and Yasuda, H. 1998. Interactions of plaunotol with bacterial membranes. *J Antimicrob Chemother*. 42(2), 133-140.

Koga, T., Inoue, H., Toshii, C., Okazaki, Y., Domon, H. and Utsui, Y. 2002. Effect of plaunotol in combination with clarithromycin or amoxicillin on *Helicobacter pylori in vitro* and *in vivo*. *J. Antimicrob. Chemother*. 50(1), 133-136.

Koga, T., Kawada, H., Utsui, Y., Domon, H., Ishii, C. and Yasuda, H. 1996. Bactericidal effect of plaunotol, a cytoprotective antiulcer agent, against *Helicobacter pylori*. *J. Antimicrob. Chemother*. 38(3), 387-397.

Kumar, V., Abbas, A.S., Fausto, N. and Mitchell, R.N. 2007. Acute and chronic inflammation. Kurmar, V., Abbas, A.S., Fausto, N. and Mitchell, R.N. (eds). *Robbins basic pathology* (8th ed), Philadelphia, USA. Elsevier Saunders, 31-58.

Lantz, R.C., Chen, G.J., Sarihan, M., Sólyom, A.M., Jolad, S.D. and Timmewmann, B.N. 2007. The effect of extracts from ginger rhizome on inflammatory mediator production. *Phytomedicine* 14(2-3), 123-128.

Lantz, R.C., Chen, G.J., Sólyom, A.M., Jolad, S.D. and Timmewmann, B.N. 2005. The effect of turmeric extracts on inflammatory mediator production. *Phytomedicine* 12(6-7), 445-452.

Macfalane, P.S., Reid, R., Callander, R. 2000. Inflammation. Mcfalane P.S., Reid R., Callander R. (eds.). *Pathology Illustrated* (15th ed). Edinburgh, Scotland. Churchill Livingstone, 32-42.

MacMillan, J. and Beale, M.H. 1999. *Diterpene Biosynthesis*. In Comprehensive Natural Products Chemistry. Vol. 2. (ed. D.E. Cane). Pergamon Press, 217-243.

Makino, M., Inomata, Y., Ito, K. and Tabata, K. 1998. Effect of plaunotol on trinitrobenzene sulfonic acid and acetic acid induced colonic lesions in rats. *Nihon_Yakurigaku_Zasshi.* 112(2), 97-106.

Matsumoto, Y., Hamashima, H., Masuda, K., Shiojima, K., Sasatsu, M. and Arai, T. 1998. The antibacterial activity of plaunotol against *Staphylococcus aureus* isolated from the skin of patients *Microbios.* 96(385), 149-155.

Moncada, S. and Erusalimsky, J.D. 2002. Does nitric oxide modulate mitochondrial energy generation and apoptosis?. *Nat. Rev. Mol. Cell Biol.* 3(3), 214-220.

Moncada, S., Palmer, R.M.J. and Higgs, E.A. 1991. Nitric oxide: physiology, pathophysiology, and pharmacology. *Pharmacol. Rev.* 43(2), 109-142.

Murakami, K., Okajima, K., Harada, N., Isobe, H., Liu, W., Johno, M. and Okabe, H. 1999. Plaunotol prevents indomethacin-induced gastric mucosal injury in rats by inhibiting neutrophill activation. *Aliment Pharmacol. Ther.* 13(4), 521-530.

Murphy, H.S. 2008. Inflammation. Rubin, R., Stayer, D.S., Rubin, E., Michalopoulos, G.K., Trojanowski, J.Q., McDonald, J.M. and Ward, P.A. (eds). *Rubin' s pathology: clinicopathologic foundations of medicine* (5th ed), Philadelphia, USA. Lippincott Williams and Wilkins. 37-70.

Naik, S.R. and Sheth, U.K. 1976. Inflammatory process and screening methods for anti-inflammatory agent-a review. *J. Postgrad. Med*. 22, 5-21.

Nakao, S., Ogtata, Y., Shimizu, E., Yamazaki, M., Furuyama, S. and Sugiya, H. 2002. Tumor necrosis factor α (TNF-α)-induced prostaglandin E_2 release is mediated by the activation

of cyclooxygenase-2 (COX-2) transcription via NF-κB in human gingival fibroblasts. *Mol. Cell. Biochem.* 238(1-2), 11-18.

Nilubol, N. 1992. Process for extraction and purification of plaunotol. United States patent. No. 826702

Nomura H., Kawasaki A., Mizuno Y., Kouyama T. Nakamura M. and Iwao T. 1997. The effect of plaunotol on stomatitis induced by interferon. *Curr. Ther. Res.*, 58(7), 428-433.

Nualkaew, N., De-Eknamkul, W., Kutchan, T.M. and Zenk, M.H. 2006. Membrane-bound geranylgeranyl diphosphate phosphatases: purification and characterization from *Croton stellatopilosus* leaves. *Phytochemistry*. 67(15), 1613-1620.

Oda, T., Ushiyama, S., Matsuda, K. and Iijima, Y. 1988. Effect of an anti-ulcer drug, plaunotol, and its metabolites on NAD^+ dependent 15-hydroxyprostaglandin dehydrogenase from gastric mucosa. *Life Sci.* 43(20), 1647-1652.

Ogiso A, Kitazawa E, Kobayashi S, Komai T, Matsunuma N, Kataumi S. 1985. Plaunotol (CS-684), a new anti-ulcer agent. *Sankyo Kenyusho Nempo*. 37, 1-39.

Ogiso, A., Kitazawa, E., Kurabayashi,M., Sato, A., Takahashi,M., Noguchi, H., Kuwano, H., Kobayashi, S., Mishima, H. 1978. Isolation and structure of antipeptic ulcer diterpene from Thai medicinal plant. *Chem. Pharm. Bull*. 26(10), 3117-3123.

Ohta, Y., Kamiya, Y., Arisawa, T. and Nakano, H. 2005. Plaunotol prevents the progression of acute gastric mucosal induced by compound 48/80, a mast cell degranulator, in rats. *Pharmacology.* 74(4), 182-192.

Ponglux, D., Wongseripipatana, S., Phadungcharoen, T., Ruangrungsi, N. and Likhitwitayawuid, K. 1987. *Medicinal Plants*. The First Princess Chulabhon Science Congress Bangkok, Thailand.

Porth, C.M. 2003. Inflammation, Tissue Repair, and Fever. Porth, C.M. (eds). *Essentials of Pathophysiology: Concepts of Altered Health States*, Philadelphia, USA. Lippincott Williams & Wilkins. 150-167.

Rang, H.P., Dale, M.M. and Ritter, J.M. 1999. Nitric Oxide. Rang, H.P., Dale, M.M. and Ritter, J.M (eds). *Pharmacology* (4th ed), Edinburgh, Scotland. Churchill Livingstone. 188-189.

Raschke, W.C., Baird, S., Ralph, P. and Nakoinz, I. 1978. Functional macrophage cell lines transformed by Abelson leukemia virus. *Cell* 15(1), 261-267.

Rosenberg, H.F. and Gallin, J.I. 1984. Inflammation. Paul, W.E. (eds). *Fundamental immunology* (5th ed), Vasailles, USA. Quebacor. 1151-1169.

Rote, N.S. 2002. Inflammation. McCance, K.L. and Huether, S.E. (eds). *The biologic basis for disease in adults and children* (4th ed), Missouri, USA. Mosby. 197-226.

Salatino, A., Salatino, ML.F. and Negri, G. 2007 Traditional uses, chemistry and pharmacology of Croton species (Euphorbiaceae). *J. Braz. Chem. Soc.* 18(1), 11-33.

Salvemini, D., Currie, M.G. and Mollace, V. 1996. Nitric oxide-mediated cyclooxygenase activation, A key event in the antiplatelet effects of nitrovasodilators. *J. Clin. Invest.* 97(11), 2562-2568.

Salvemini, D., Misko, T.P., Masferrer, J.L., Seibert, K., Currie, M.G. and Needleman, P. 1993. Nitric oxide activates cyclooxygenase enzymes. *Proc. Natl. Acad. Sci. USA*. 90(15), 7240-7244.

Sasaki M., Mizoshita T., Mizushima T., Inoue H., Kamiya T., Kataoka H., Ogaswara N., Wada T., Kubota E., Mori Y., Shimura T., Hirata H., Ando K., Okamoto Y., Ohara H., Nakao H. and Joh T. 2007. Effect of plaunotol in combination with clarithromycin against clarithromycin-resistant *Helicobacter pylori in vitro* and *in vivo*. *J Antimicrob Chemother*. 60(5), 1060-1063.

Schroder, K., Sweet, M.J. and Hume, D.A. 2006. Signal integration between IFNgamma and TLR signalling pathways in macrophages. *Immunobiology*. 211(6-8):511-524.

Shiratori, K., Watanabe, S. and Takeuchi, T. 1993. Role of endogenous prostaglandins in secretin- and plaunotol-induced inhibition of gastric acid secretion in rat. *Am. J. Gastroentrol*. 88(1), 84-89.

Shishodia, S., Majumadar, S., Banerjee, S. and Aggarwal, B.B. 2003. Ursolic acid inhibits neuclear factor-κB activation induced by carcinogenic agents through suppression of IκBα kinase and p65 phosphorylation: correlation with down-regulation of cyclooxygenase 2, matrix metalloproteinase 9, and cyclin D1. *Cancer Res*. 63(15), 4375-4383.

Sitthithaworn, W., Kojima, N., Viroonchatapan, E., Suh, D.Y., Iwanami, N., Hayashi, T., Noji, M., Saito, K., Niwa,Y. and Sankawa, U. 2001. Geranylgeranyl diphosphate synthase from Scoparia dulcis and Croton sublyratus. Plastid localization and conversion to a farnesyl diphosphate synthase by mutagenesis. *Chem. Pharm. Bull.* 49(2), 197-202.

Spurgeon, S.L. and Porter, J.W. 1981. Biosynthesis of carotenoids. Porter, J.W. and Spurgeon, S.L. (eds). *Biosynthesis of isoprenoid compounds* (vol 2), New York. John Wiley & Sons. 1-122.

Steven, S.A. and Lowe, J. 2000. Tissue responses to damage. Steven S.A., Lowe J. (eds). *Pathology* (2nd ed). Edinburgt, Scotland. Butterworth Heine mann. 30-38.

Sugiatno, E., Samsudin, A.R., Ibrahim, M.F. and Sosroseno, W. 2006. The effect of Nitric oxide on the production of prostaglandin E_2 by hydroxyapatite-stimulated a human osteoblast (HOS) cell line. *Biomed. Pharmacother.* 60(4), 147-151.

Takagi, A., Koga, Y., Aiba, Y., Kabir, A.M., Watanabe, S., Ohta-Tada, U., Osaki, T. Kamiya, S. and Miwa, T. 2000. Plaunotol suppresses interleukin-8 secretion induced by *Helicobacter pylori:* therapeutic effect of plaunotol on *H. pylori* infection. *J. Gastroenterol. Hepatol*. 15(4), 374-380.

Takahashi, S., Kurabayashi, M., Kitazawa, E, Haruyama, H., and Ogiso, A. 1983. Plaunolide, a furanoid diterpene from *Croton sublyratus. Phytochemistry.* 22(1), 302-303.

Tansakul, P. and De-Eknamkul, W. 1998. Geranylgeraniol-18-hydroxylase : The last enzyme on the plaunotol biosynthesis in *Croton sublyratus*. *Phytochemistry*. 47, 1241-1246.

Tewtrakul, S. and Itharat, A. 2007. Nitric oxide inhibitory substances from the rhizomes of *Dioscorea membranacea*. *J. Ethnopharmacol*. 109 (3), 412-416.

Thiemermann, C., Szabio, C., Mitcell, J.A. and Vane, J.R. 1997. Vascular hyporeactivity to vasoconstrictor agents and hemodynamic decompensation in hemorrhagic shock is mediated by nitric oxide. *Proc. Natl. Acad. Sci. USA*. 90(1), 267-271.

Ushiyama, S., Matsuda, K., Asai, F. and Yamazaki, M. 1987. Stimulation of prostaglandin production by (2*E*, 6*Z*, 10*E*)-7-hydroxymethyl-3, 11, 15-trimethyl-2, 6, 10, 14-hexadecatetraen-1-ol (plaunotol), a new anti ulcer drug, *in vitro* and *in vivo*. *Biochem. Pharmacol*. 36(3), 369-375.

Vallochi, A.L., Goldberg, A.C., Falcai, A., Ramasawmy, R., Kalil, J., Silveira, C., Belfort Jr, R. and Rizzo, L.V. 2008. Molecular markers of susceptibility to ocular toxoplasmosis, host and guest behaving badly. *Clin. Ophthalmol*. 2(4), 837–848.

Vane, J.R., Mitchell, J.A., Appleton, I., Tomlinson, A., Bishop-Bailey, D., Croxtall, J. and Willoughby, D.A. 1994. Inducible isoforms of cyclooxygenase and nitric oxide synthase in inflammation. *Proc. Natl. Acad. Sci. USA*. 91, 2046-2050.

Wallace, J.L. and Ma, L. 2001. Inflammatory mediators in gastrointestinal defence and injury. *Exp. Biol. Med.* 226(11), 1003-1015.

Welzen, PC.V. (editor), 2010. Flora of Thailand Euphorbiaceae. Nationaal Herbarium Nederland. http://www.nationaalherbarium.nl/thaieuph/ThCspecies/ThCrotonT.htm.(accessed August 7, 2011).

Yamada, J., Kawai K., Tsuno, N.H., Kitayama, J., Tsuchiya, T., Yoneyama, S., Asakage, M., Okaji, Y., Takahashi, K. and Nagawa, H. 2007. Plaunotol induces apoptosis of gastric cancer cells. *Planta Med*. 73(10), 1068-1073.

Yoshikawa, N., Yamada, J., Tsuno, N.H., Okaji, Y., Kawai, K., Tsuchiya, T., Yoneyama, S., Tanaka, J., Shuno, Y., Nishikawa, T., Nakawa, H., Oshima, N. and Takahashi, K. 2009. Plaunotol and geranylgeraniol induce caspase-mediated apoptosis in colon cancer. *J. Surg . Res.* 153(2), 246-253.

APPENDIX

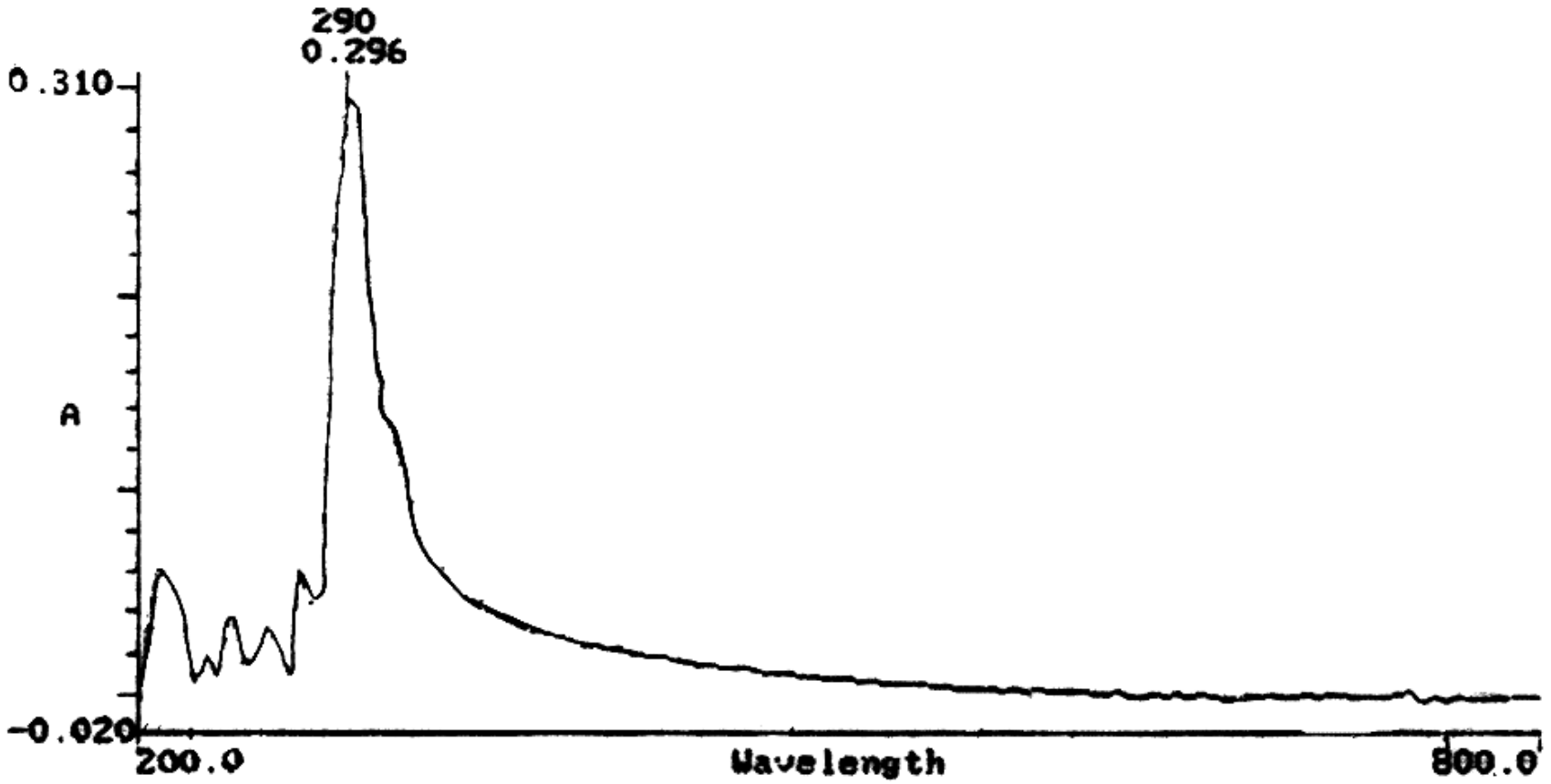

Figure A1 UV spectrum of compound **CS-1** (MeOH)

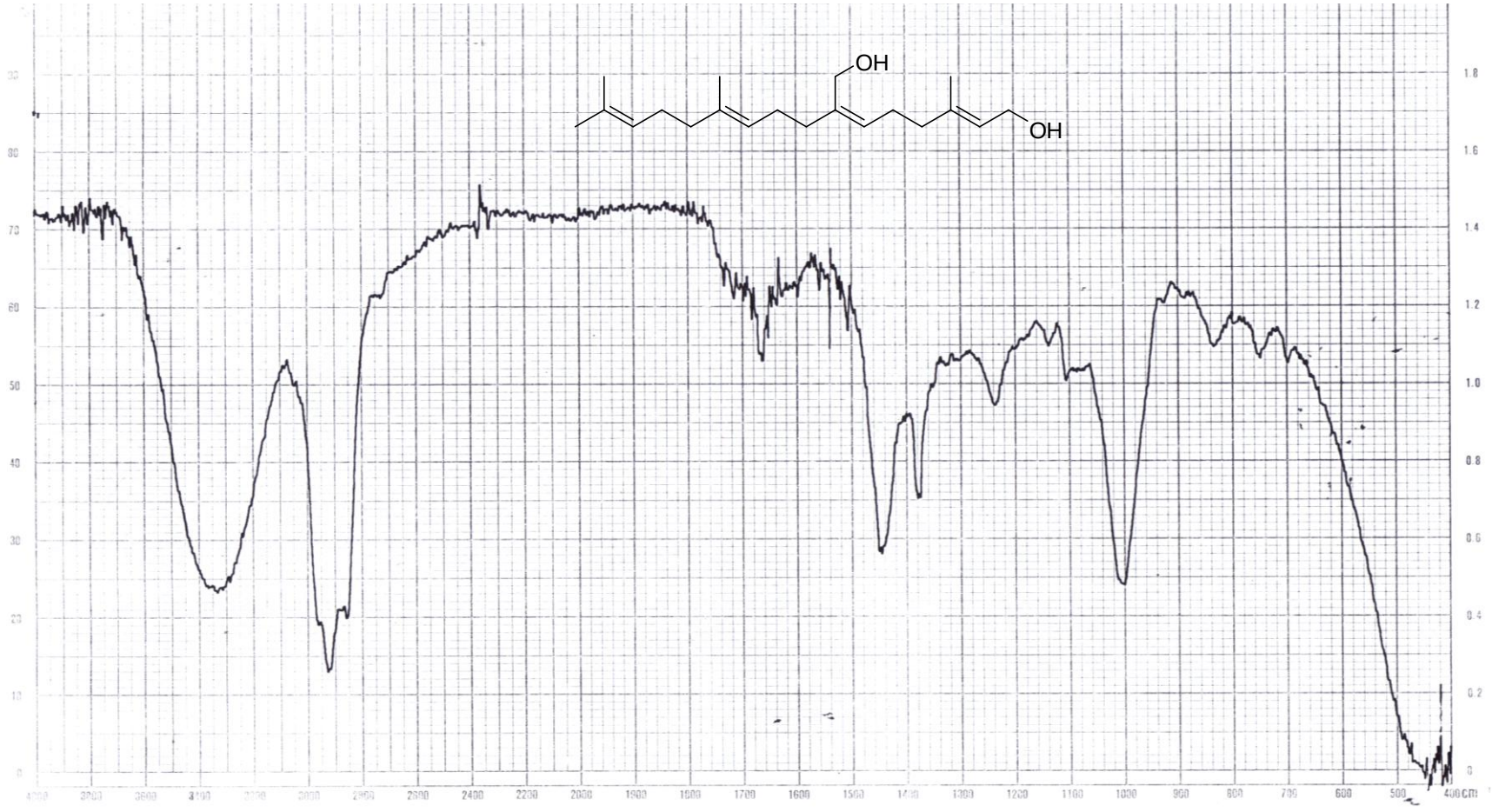

Figure A2 IR spectrum of compound **CS-1** (neat in CH_2Cl_2)

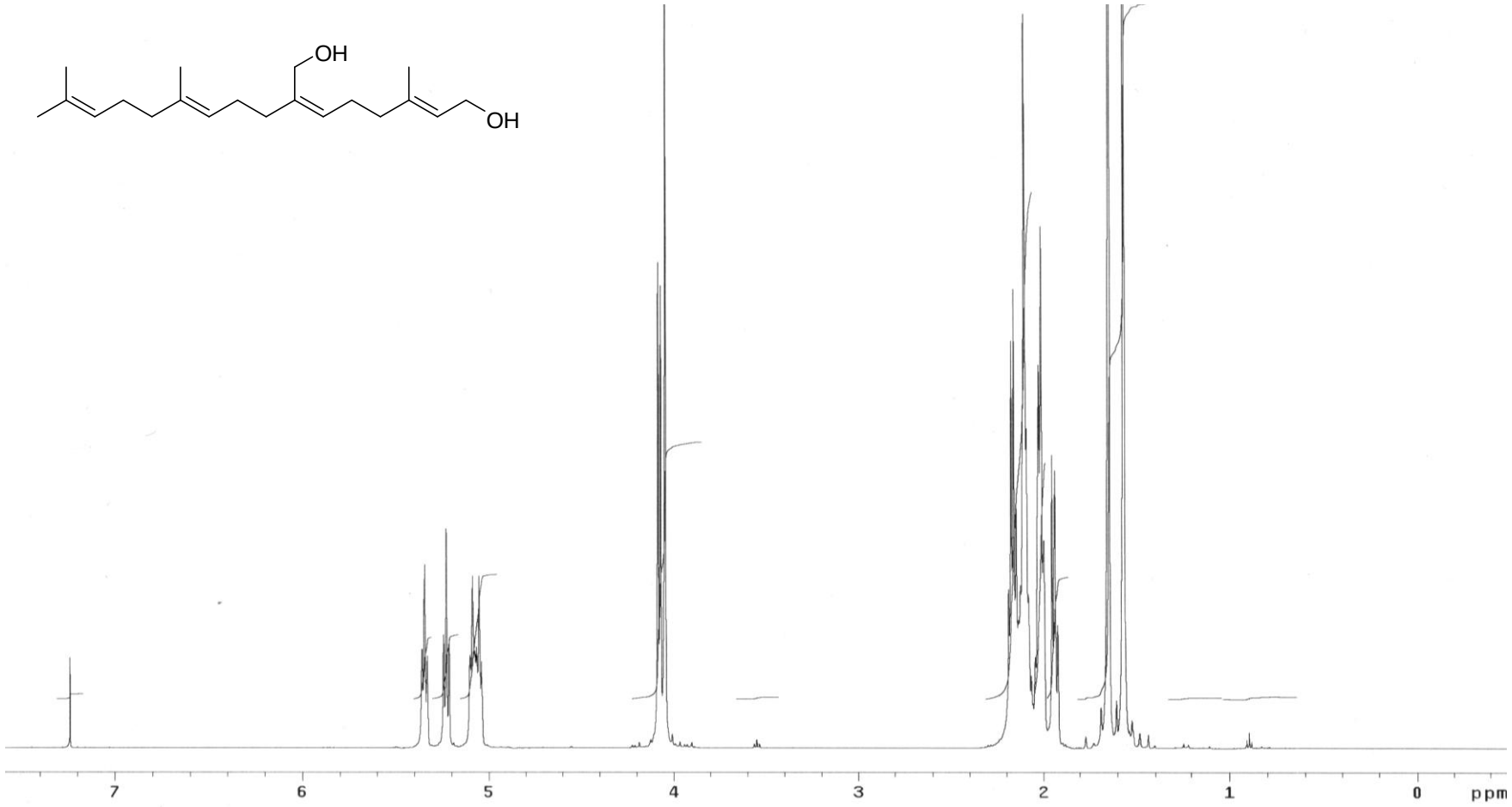

Figure A3 ^{1}H-MMR spectrum of compound **CS-1** (500 MHz, $CDCl_3$)

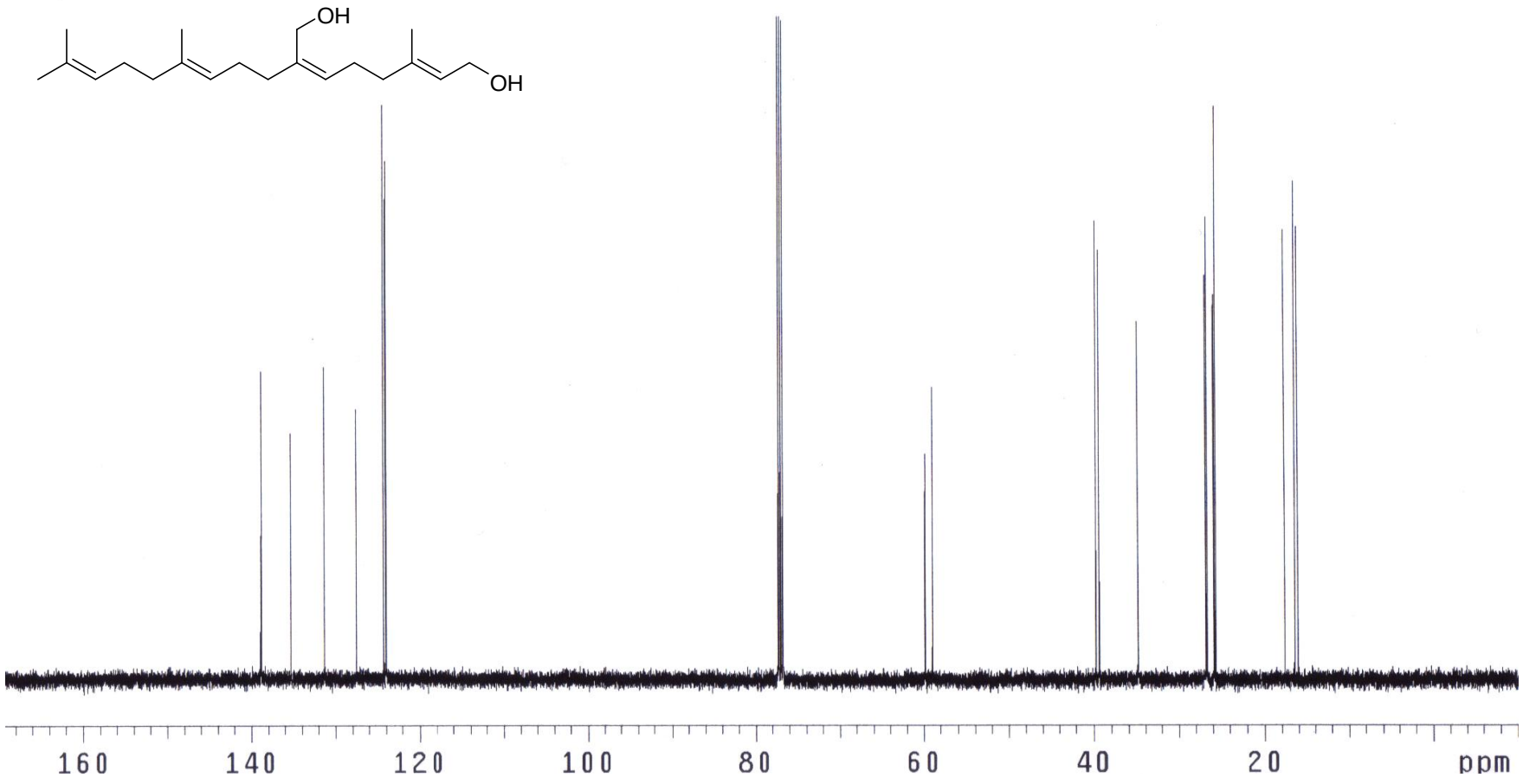

Figure A4 ^{13}C-MMR spectrum of compound **CS-1** (125 MHz, $CDCl_3$)

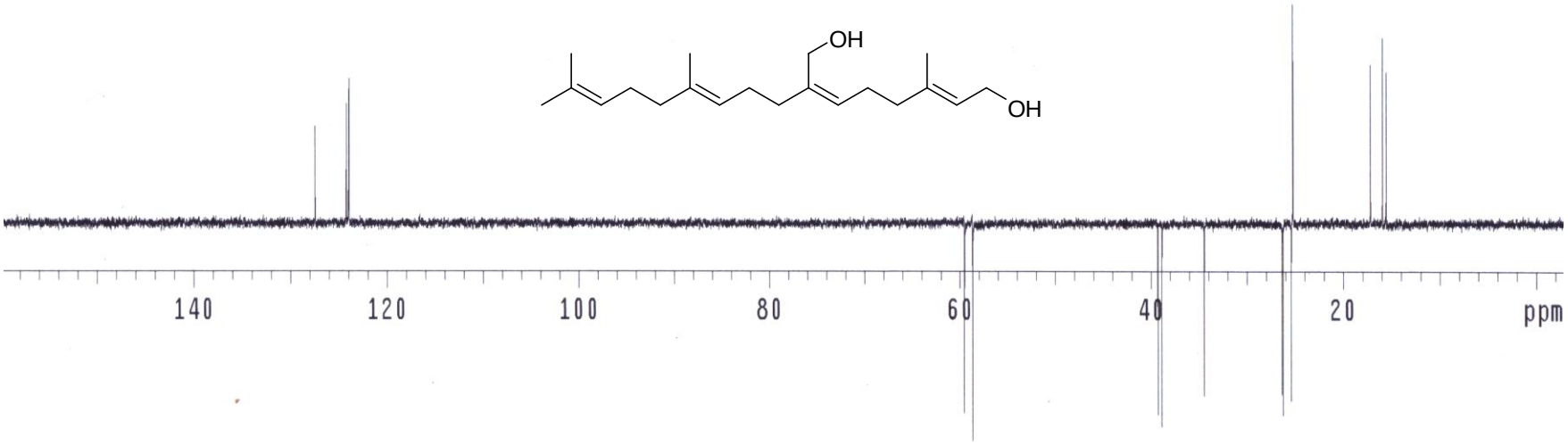

Figure A5 DEPT 135 spectrum of compound **CS-1** ($CDCl_3$)

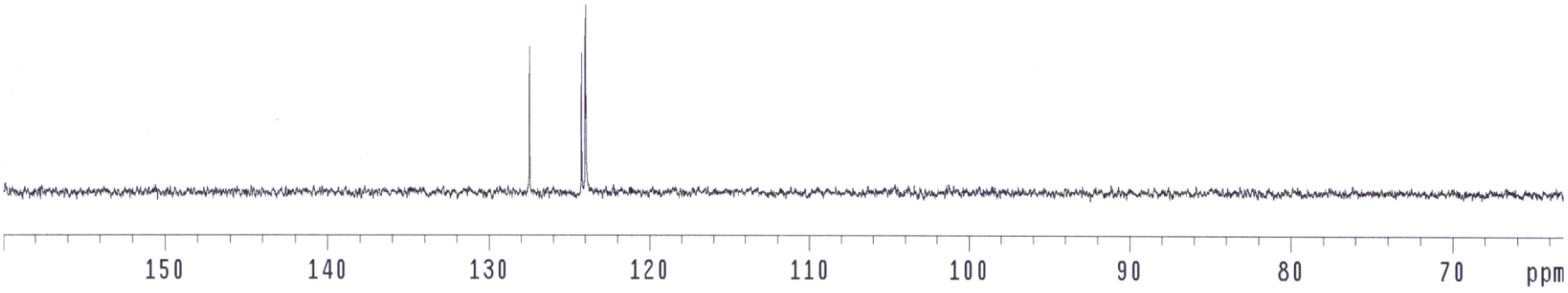

Figure A6 DEPT 90 spectrum of compound **CS-1** ($CDCl_3$)

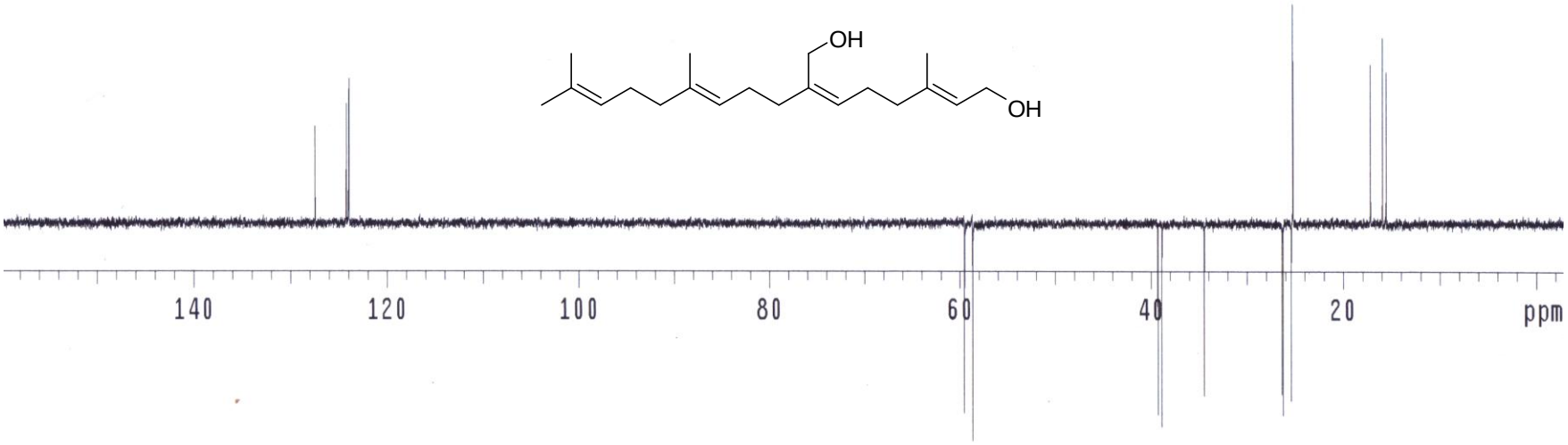

Figure A5 DEPT 135 spectrum of compound **CS-1** ($CDCl_3$)

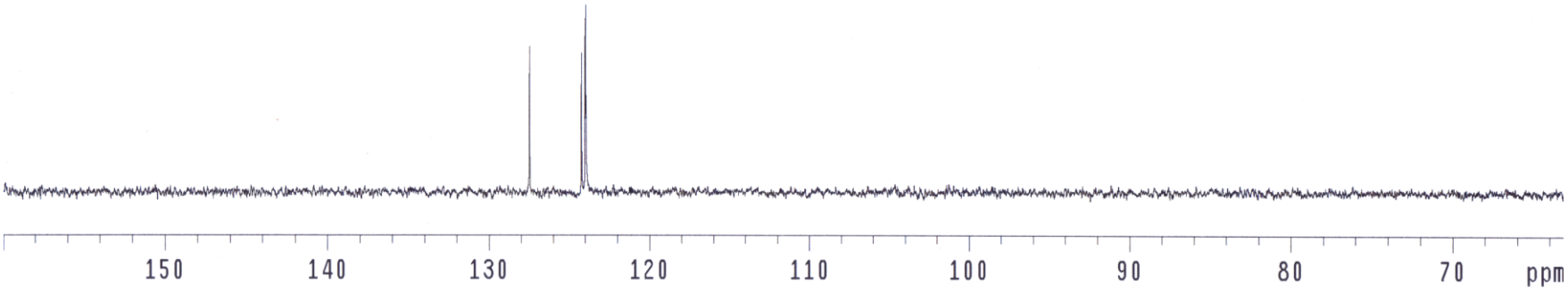

Figure A6 DEPT 90 spectrum of compound **CS-1** ($CDCl_3$)

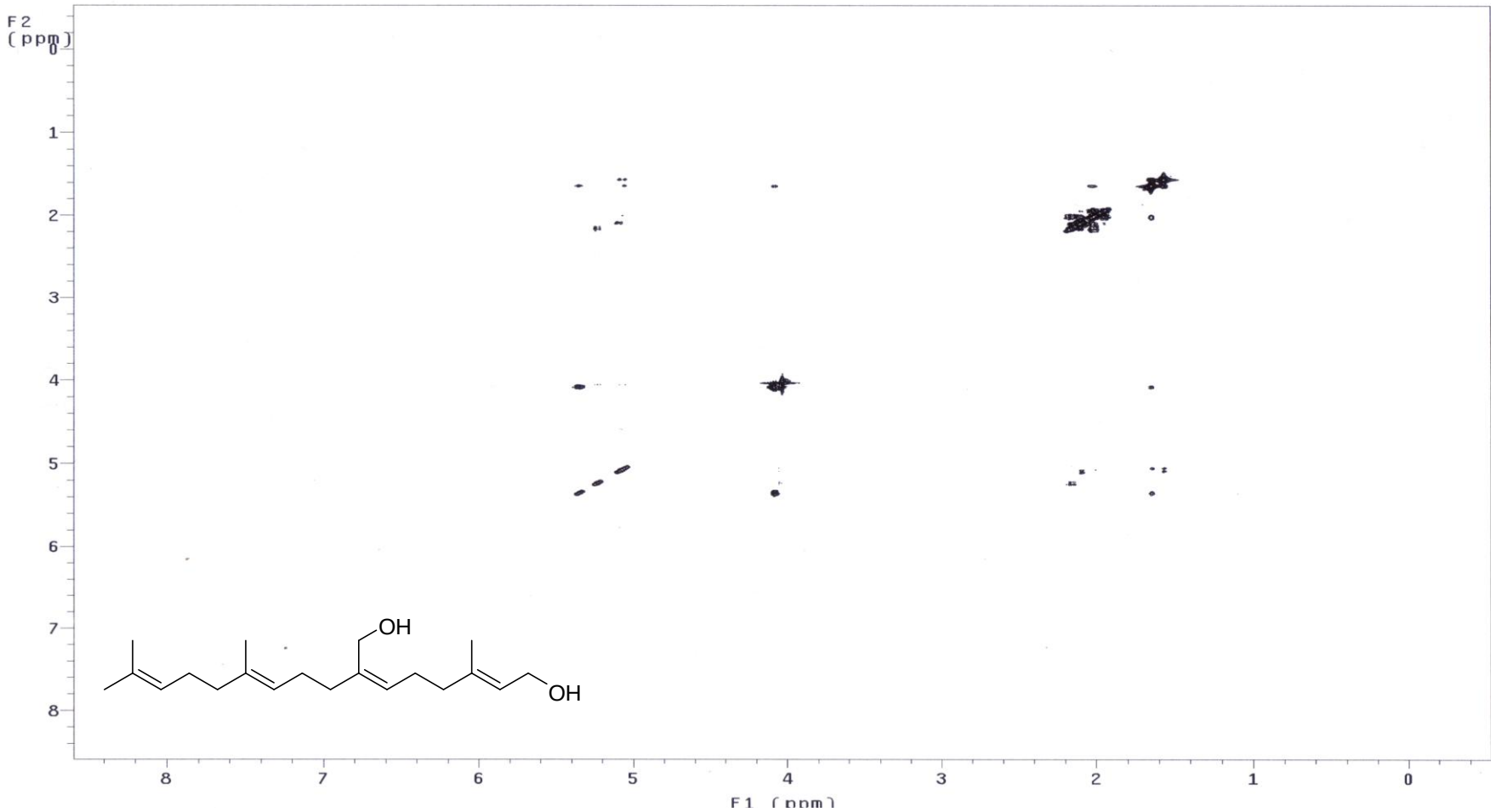

Figure A7 ^{1}H-^{1}H COSY spectrum of compound **CS-1** ($CDCl_3$)

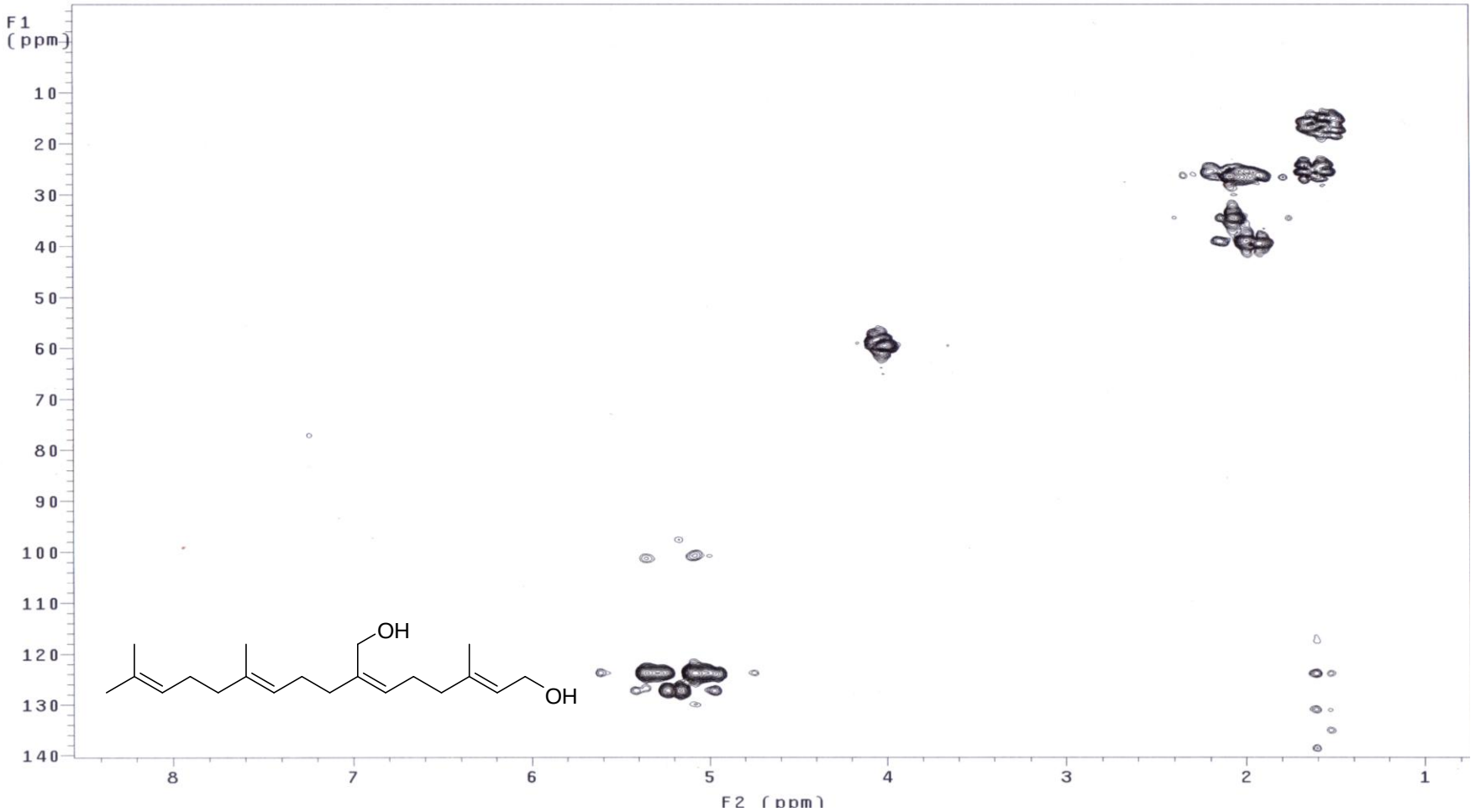

Figure A8 HMQC spectrum of compound **CS-1** ($CDCl_3$)

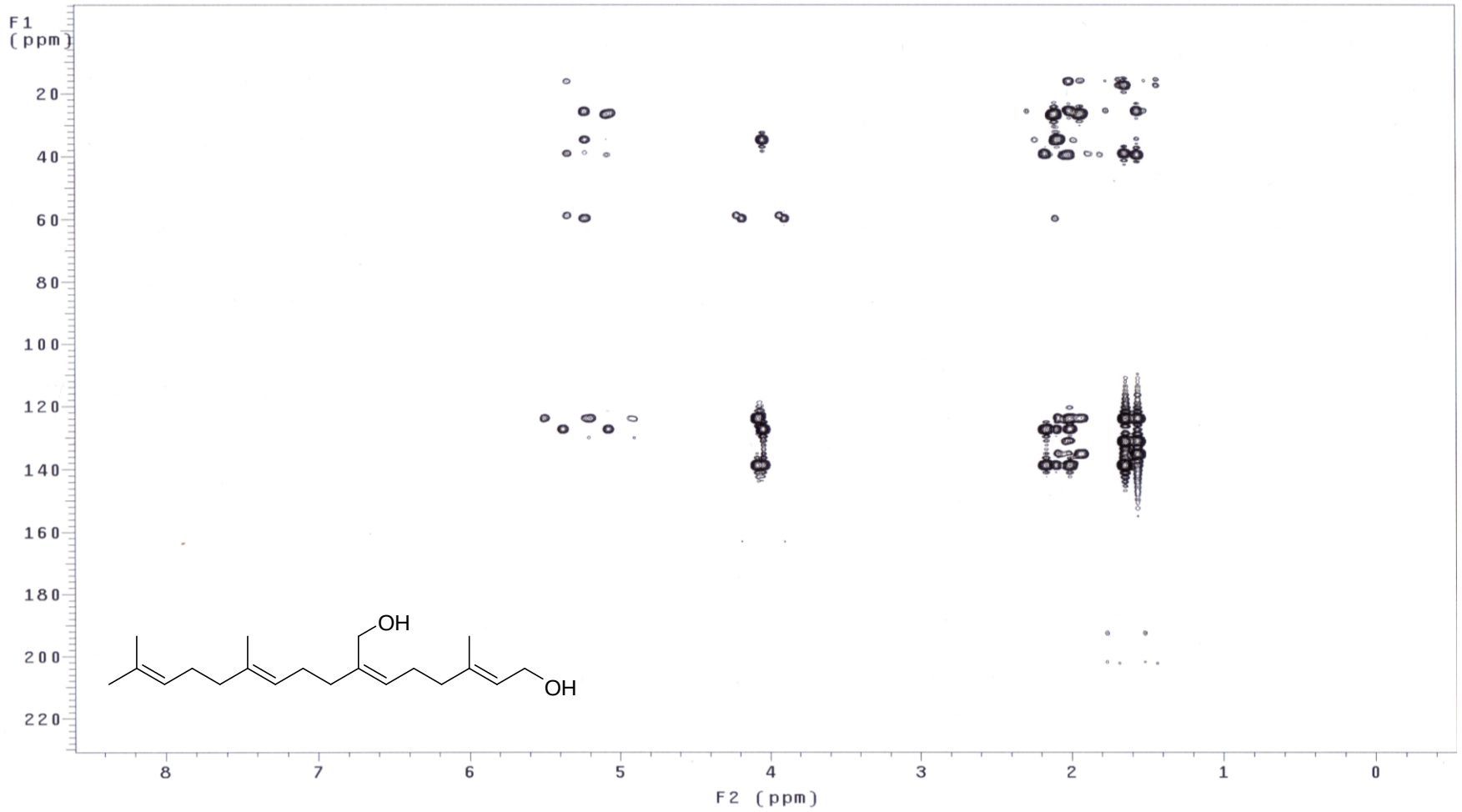

Figure A9 HMBC spectrum of compound **CS-1** ($CDCl_3$)

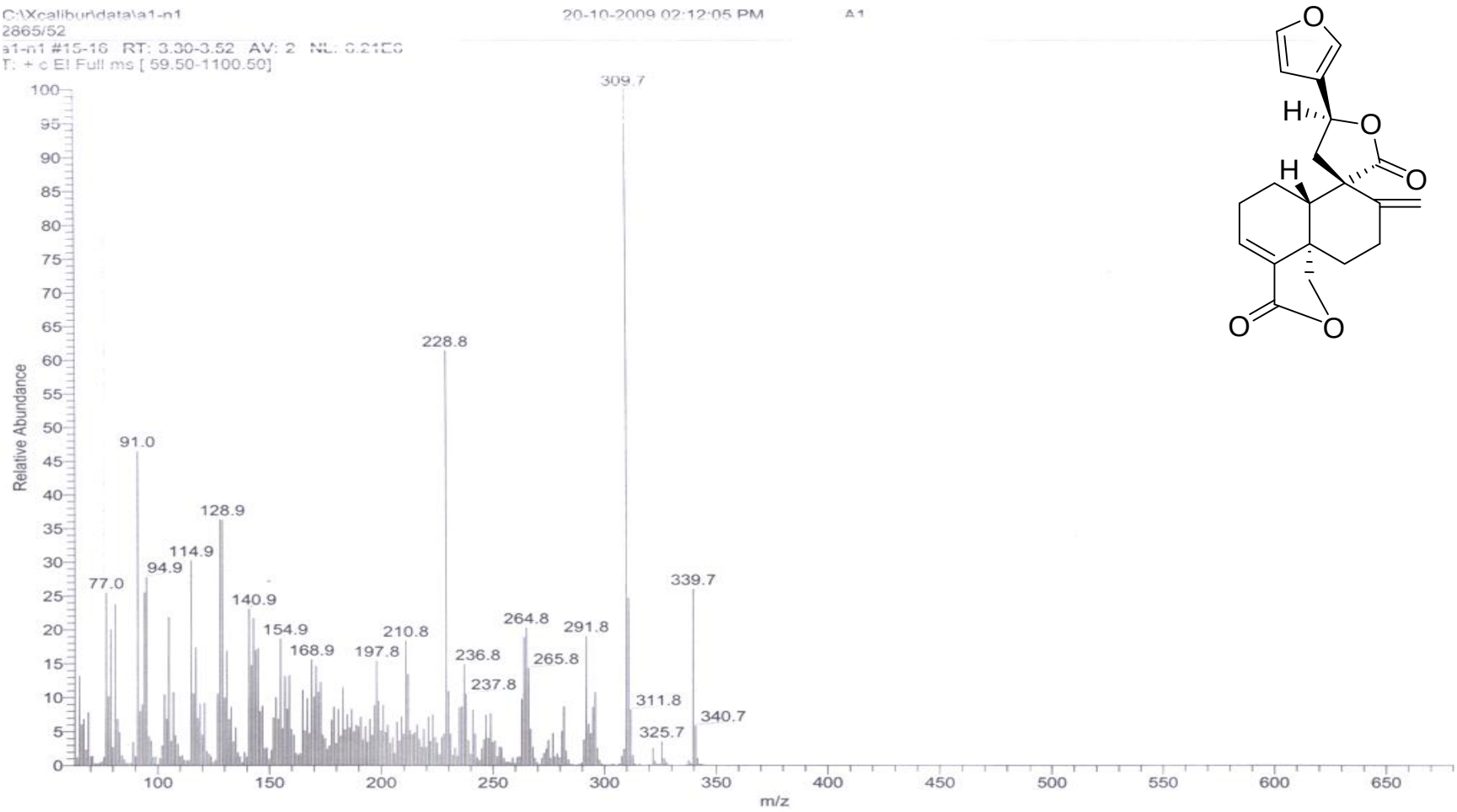

Figure A10 EI-MS spectrum of compound **CS-2**

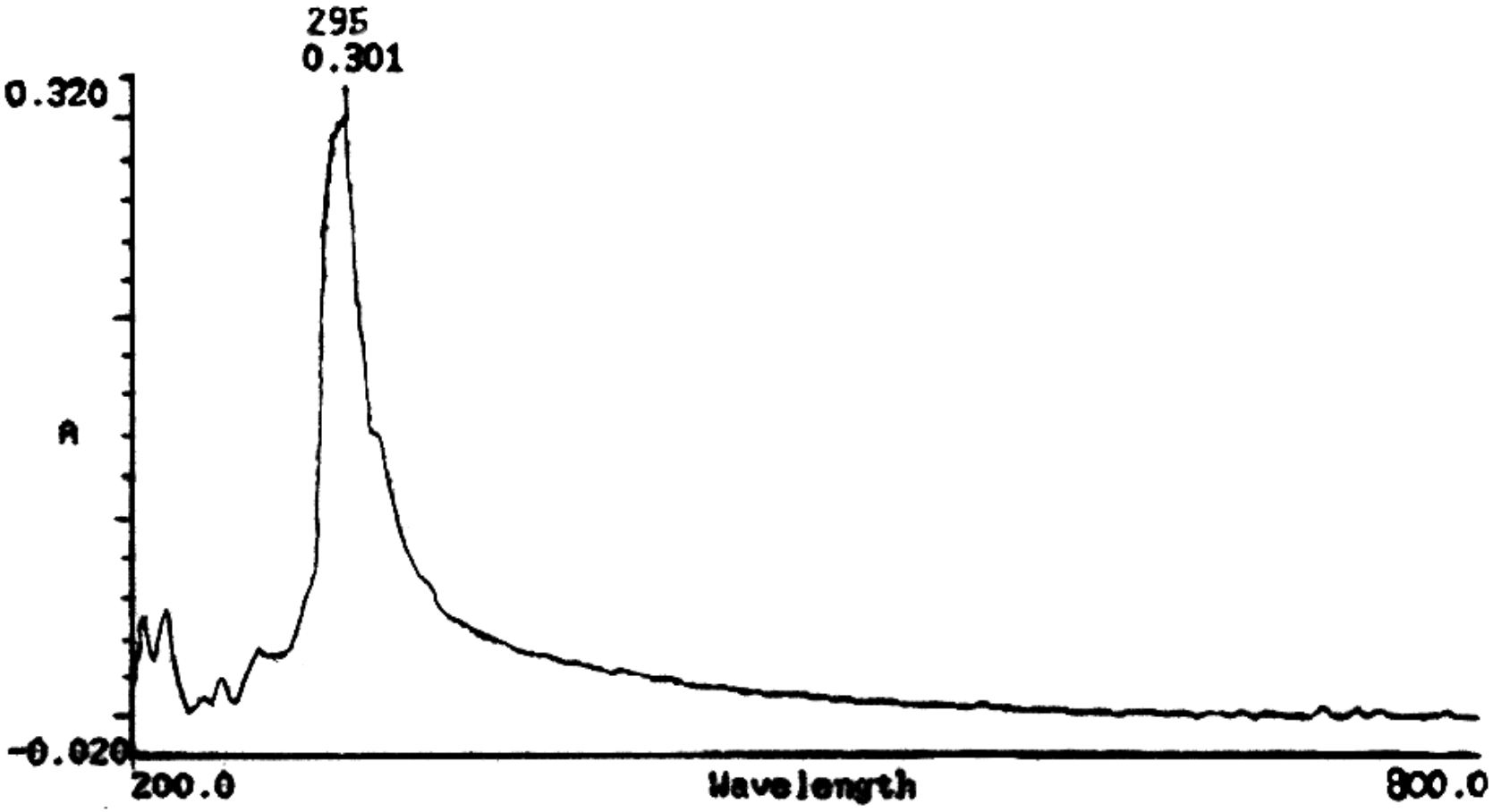

Figure A11 UV spectrum of compound **CS-2** (MeOH)

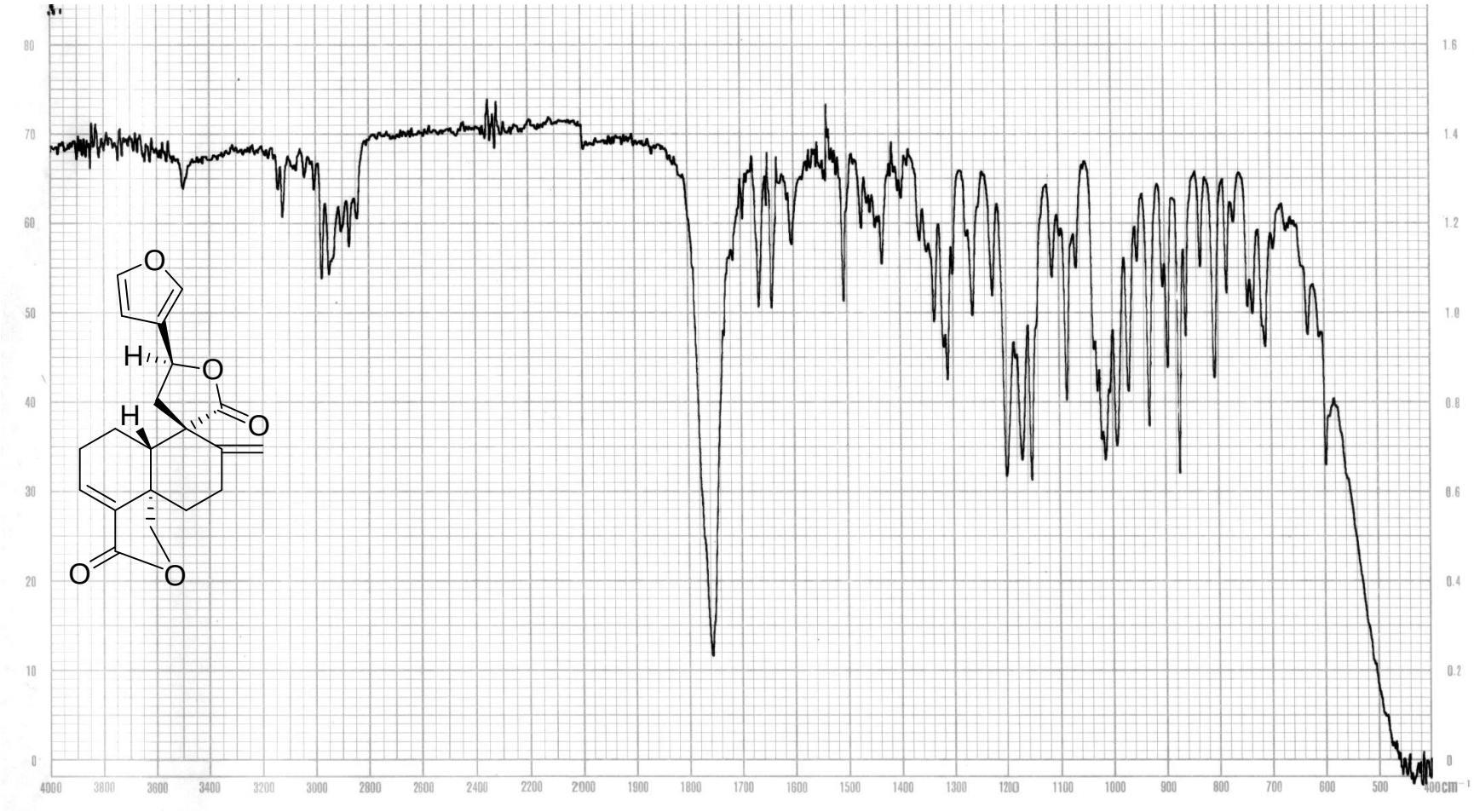

Figure A12 IR spectrum of compound **CS-2** (neat in CH_2Cl_2)

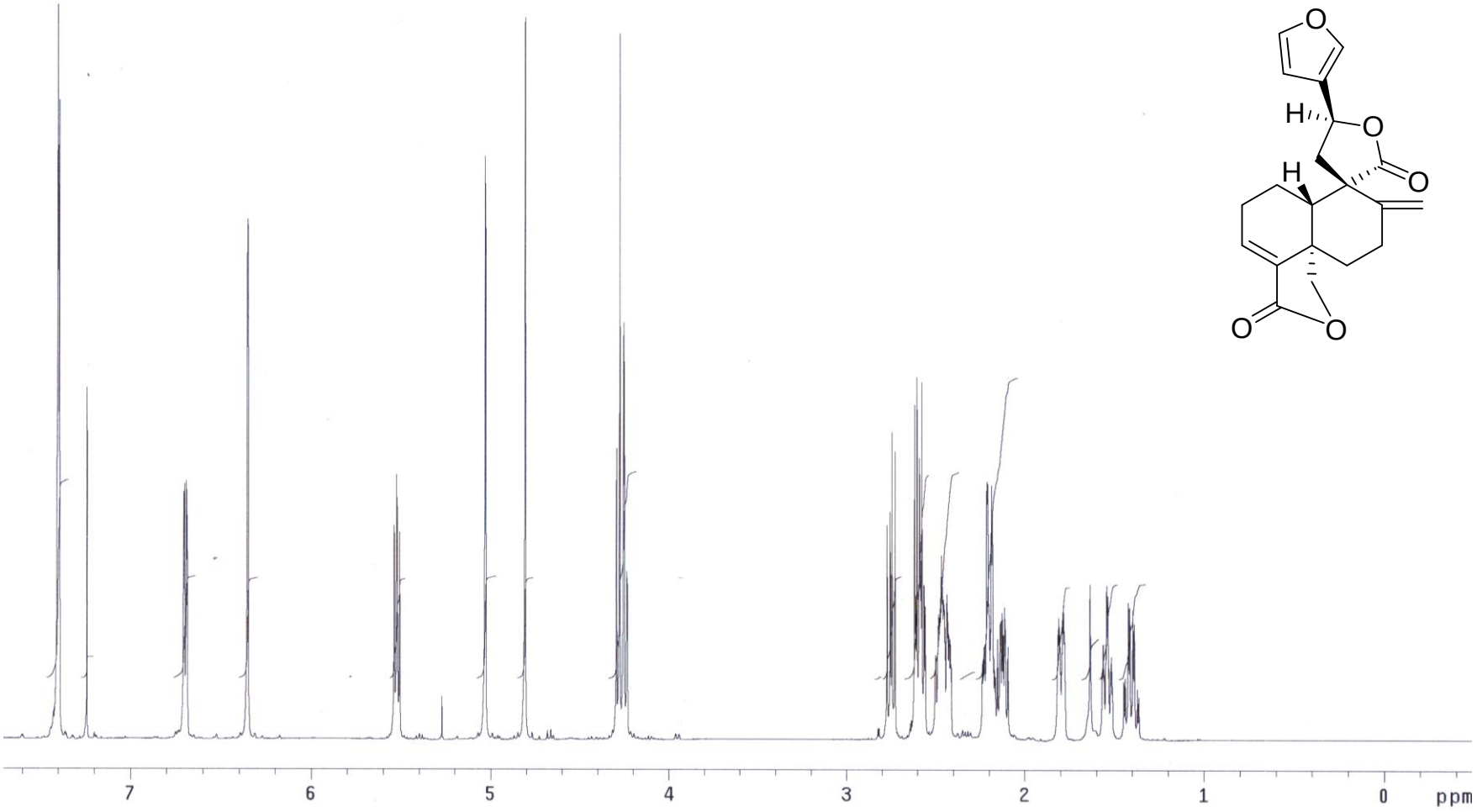

Figure A13 ^{1}H-MMR spectrum of compound **CS-2** (500 MHz, $CDCl_3$)

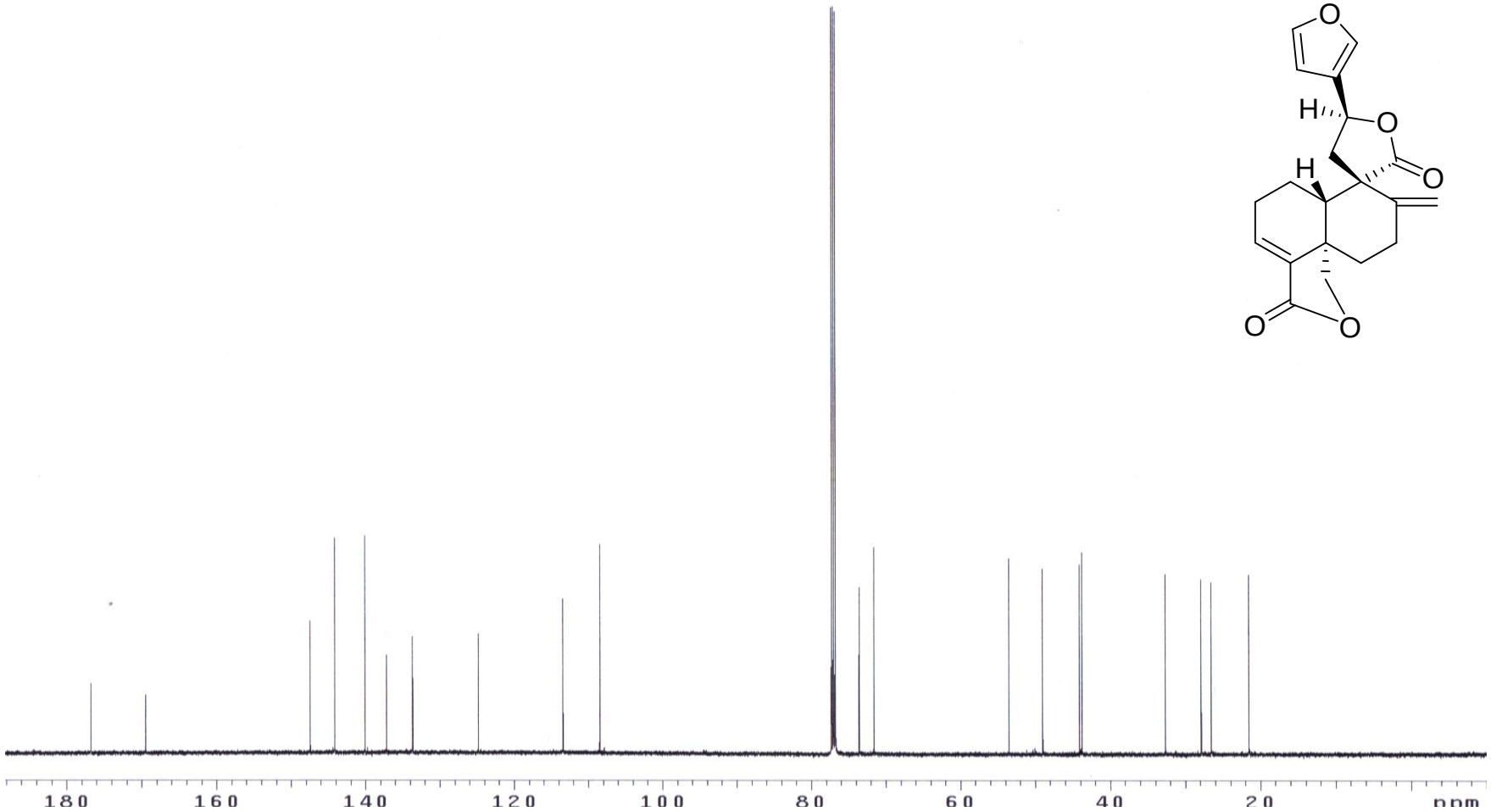

Figure A14 ^{13}C-MMR spectrum of compound **CS-2** (125 MHz, $CDCl_3$)

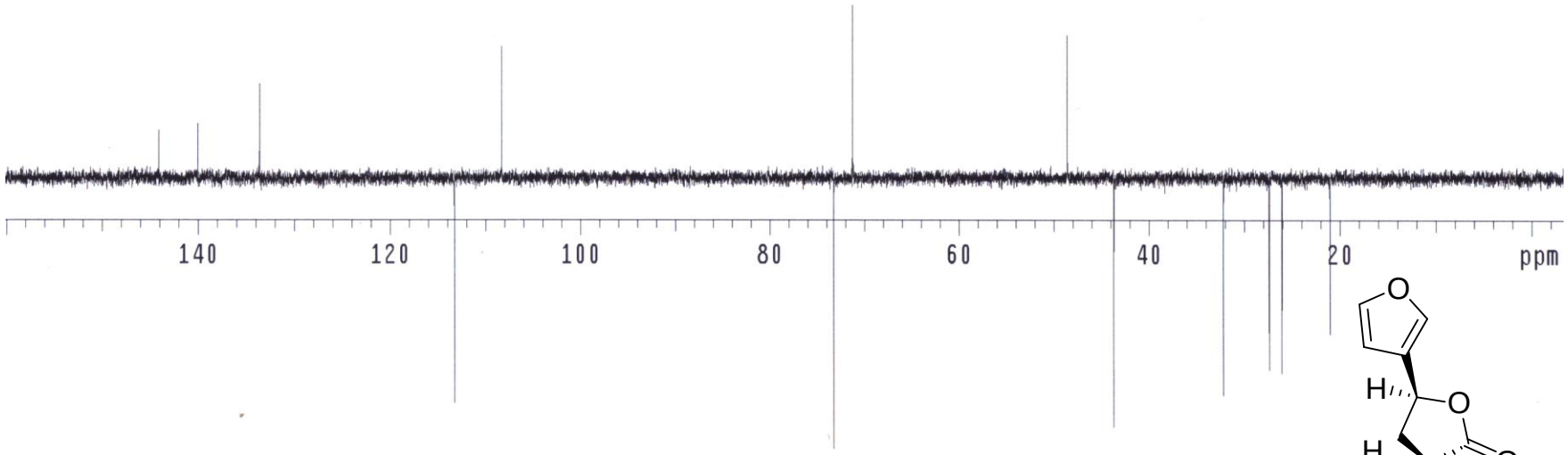

Figure A15 DEPT 135 spectrum of compound **CS-2** ($CDCl_3$)

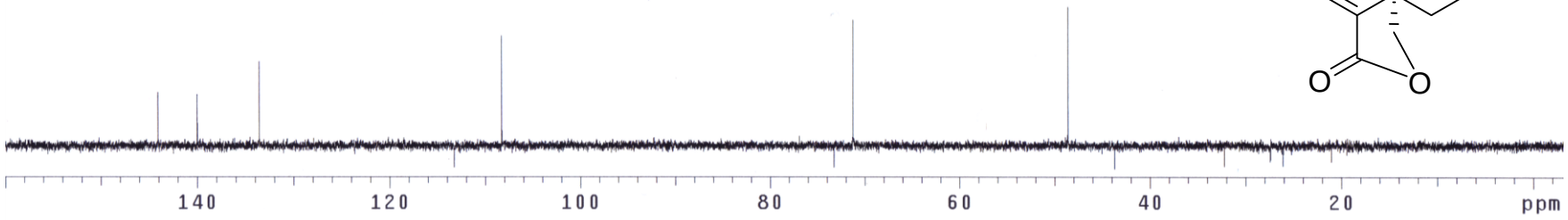

Figure A16 DEPT 90 spectrum of compound **CS-2** ($CDCl_3$)

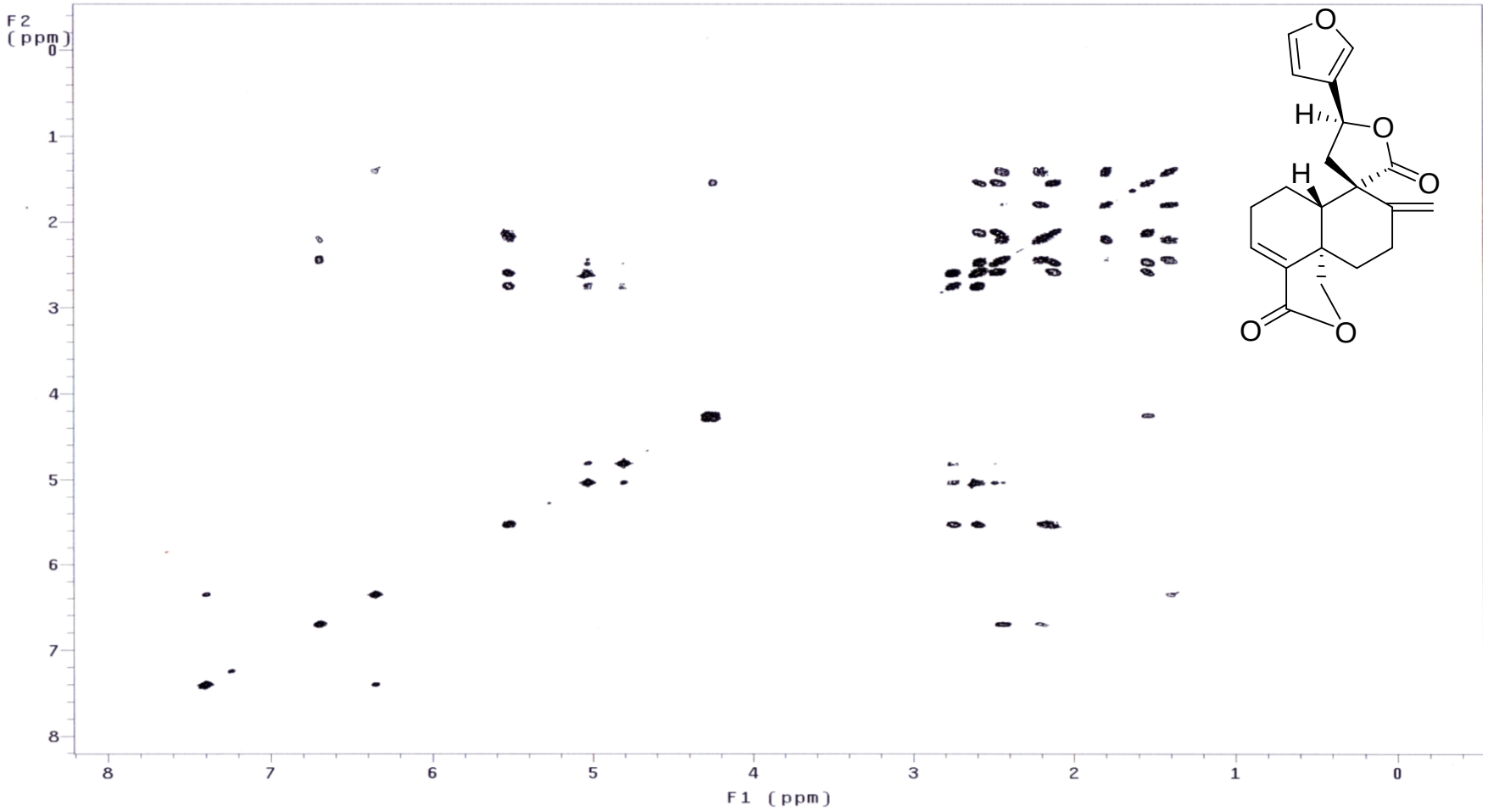

Figure A17 ^{1}H-^{1}H COSY spectrum of compound **CS-2** ($CDCl_3$)

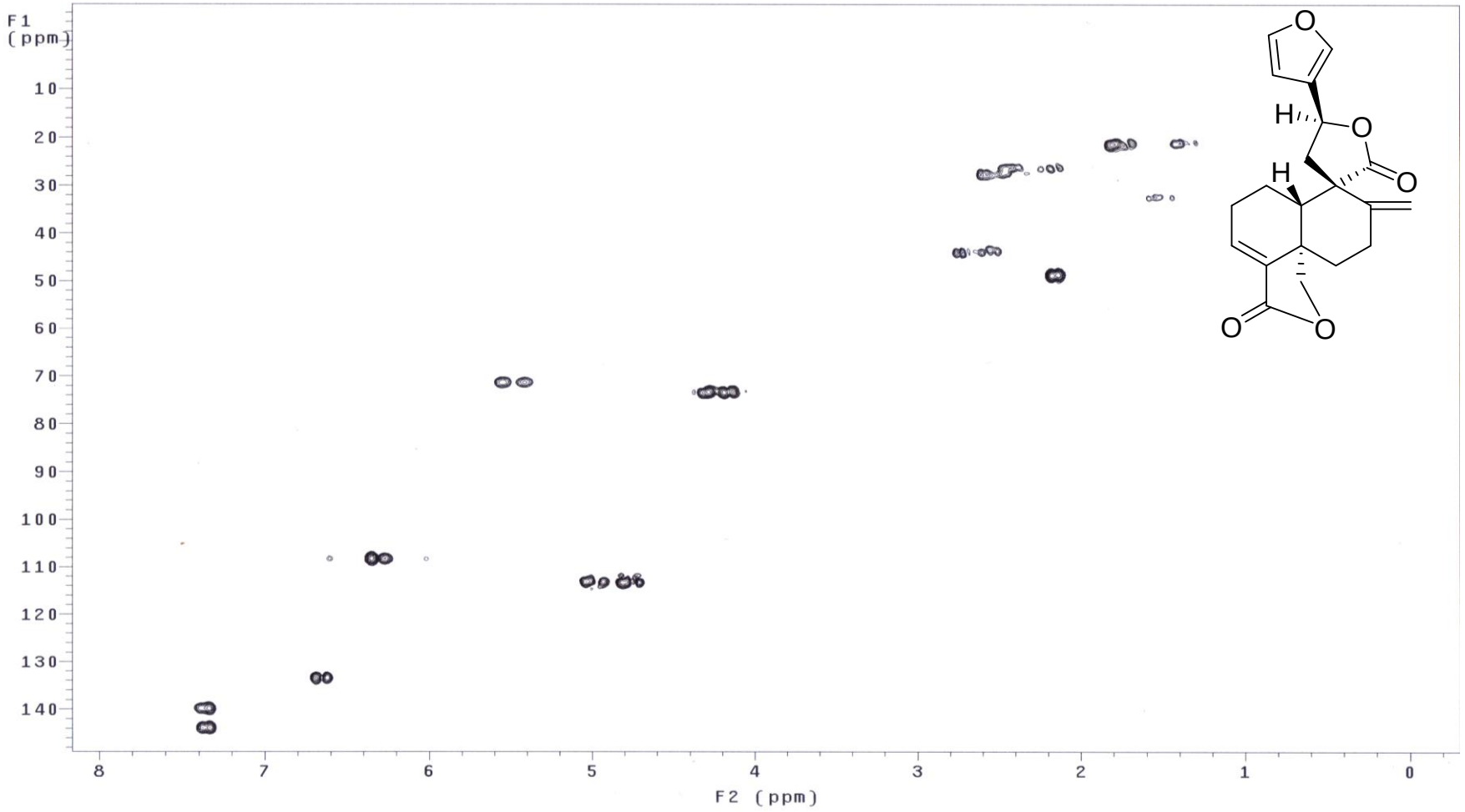

Figure A18 HMQC spectrum of compound **CS-2** ($CDCl_3$)

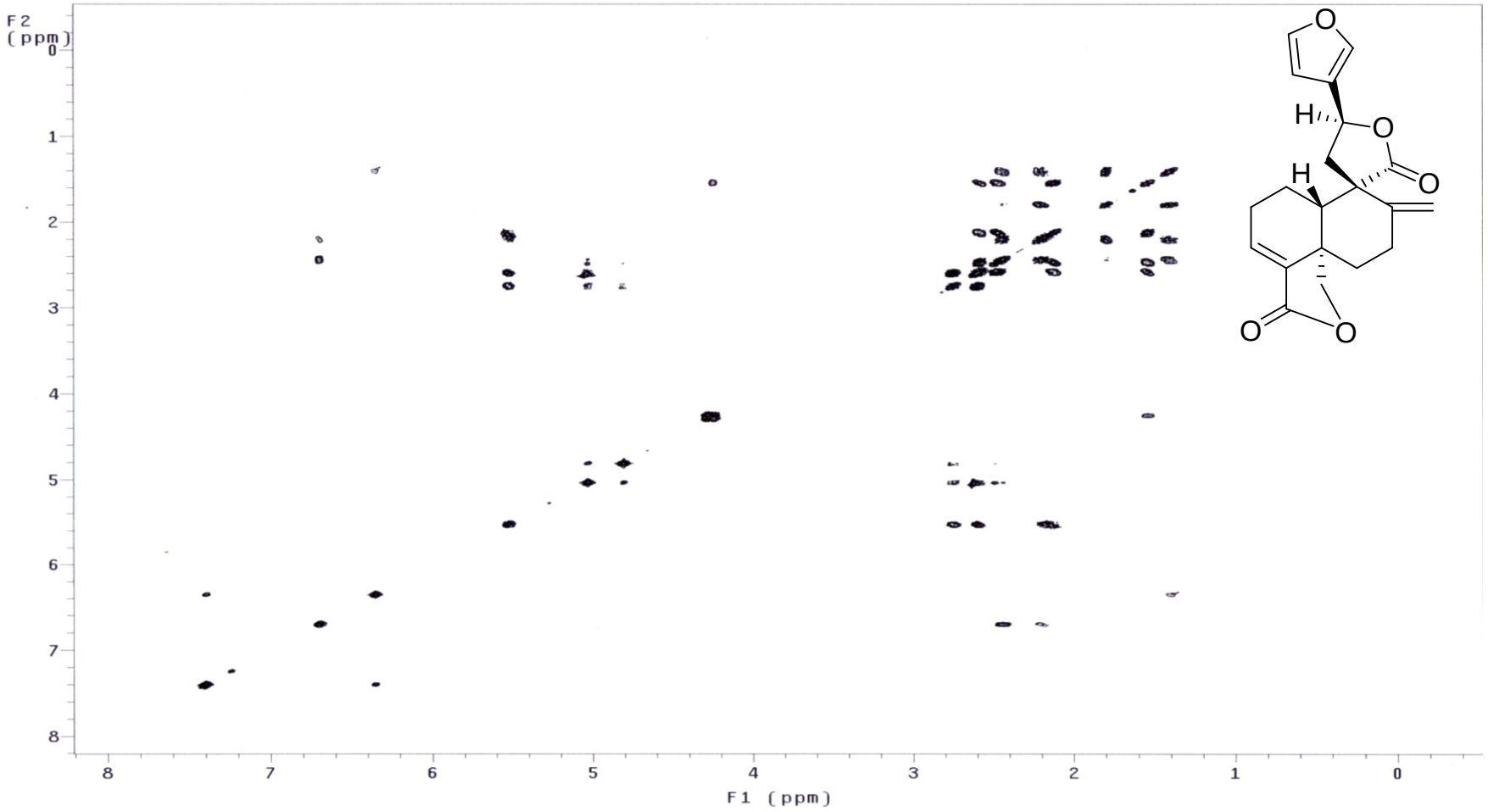

Figure A17 ^{1}H-^{1}H COSY spectrum of compound **CS-2** ($CDCl_3$)

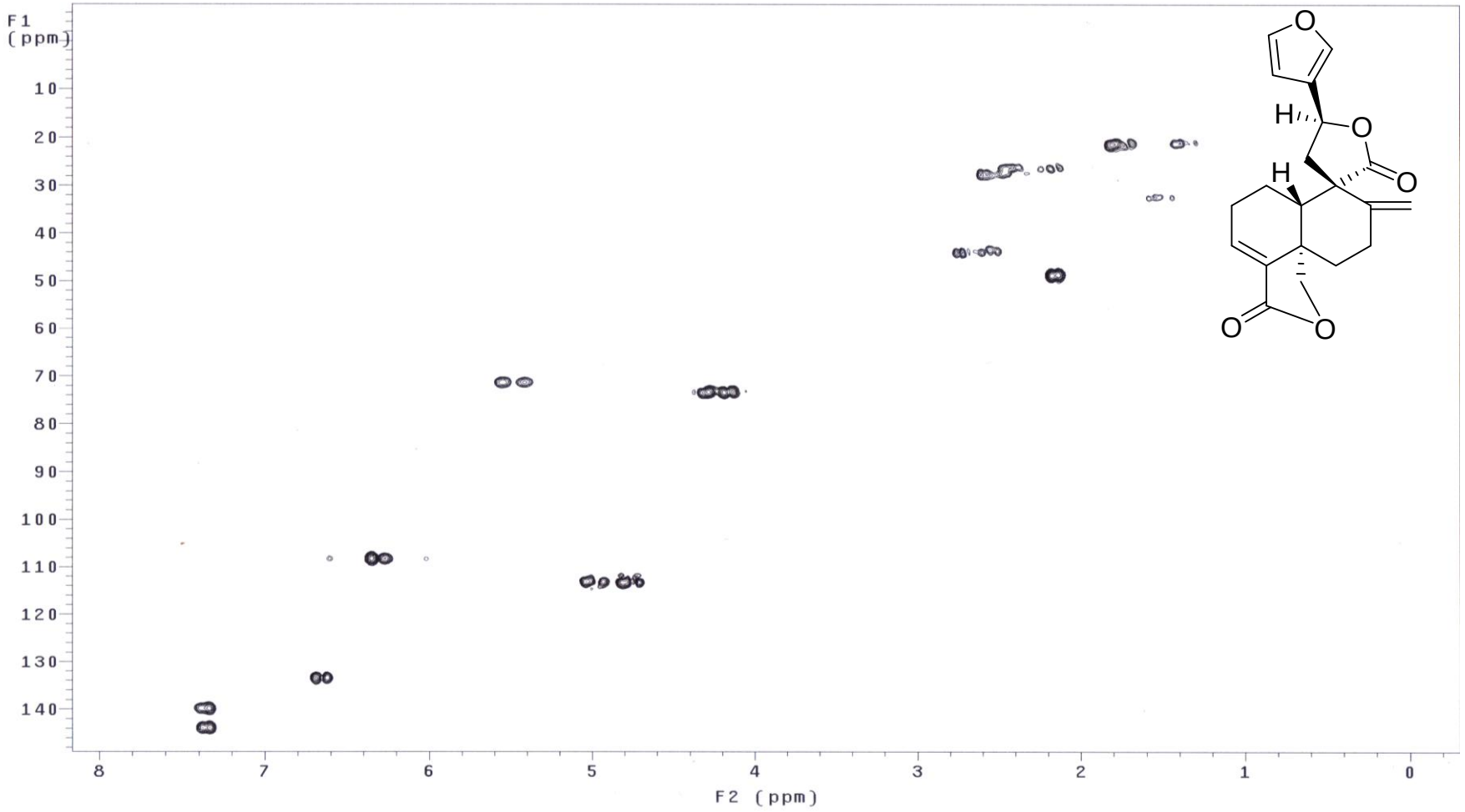

Figure A18 HMQC spectrum of compound **CS-2** ($CDCl_3$)

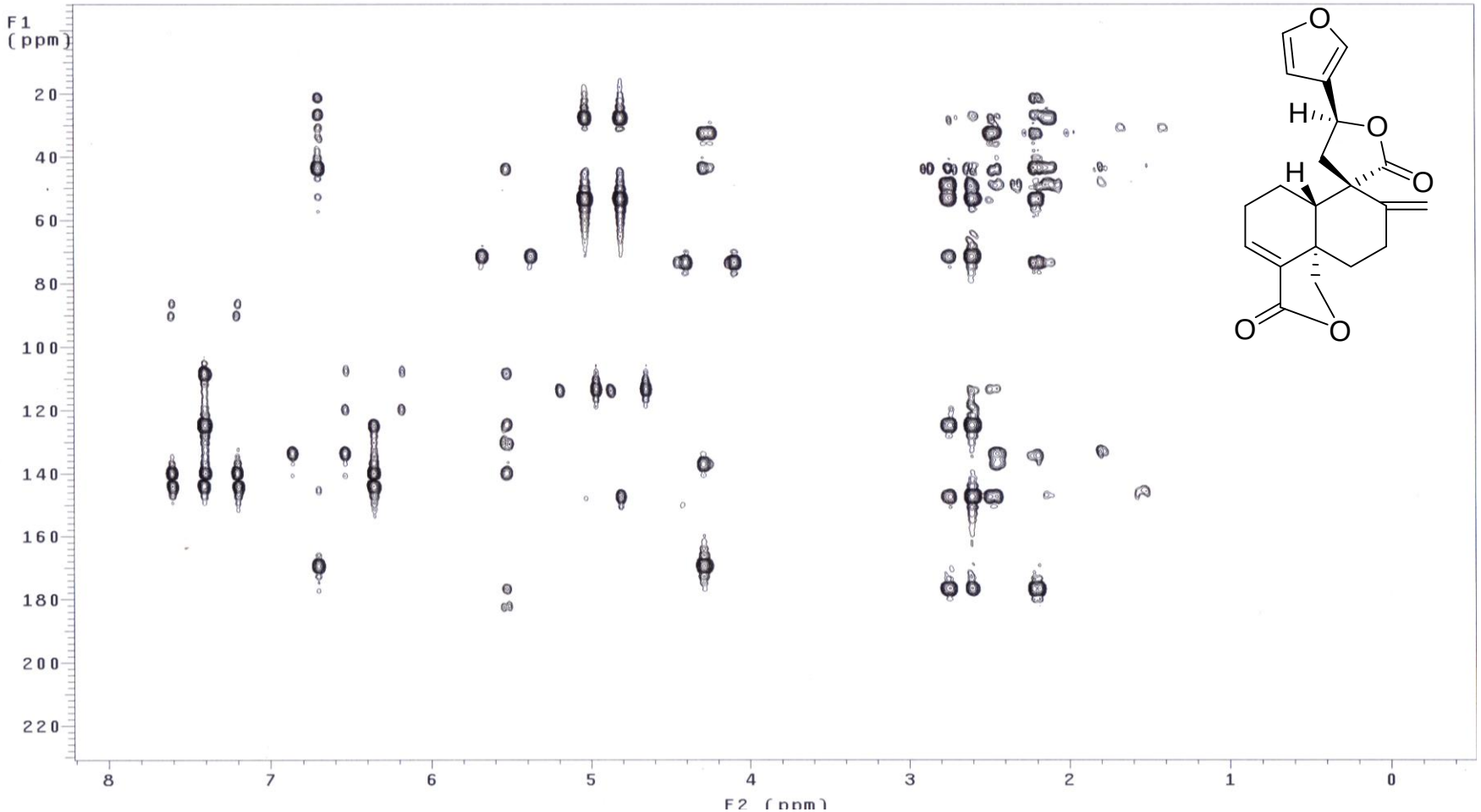

Figure A19 HMBC spectrum of compound **CS-2** ($CDCl_3$)

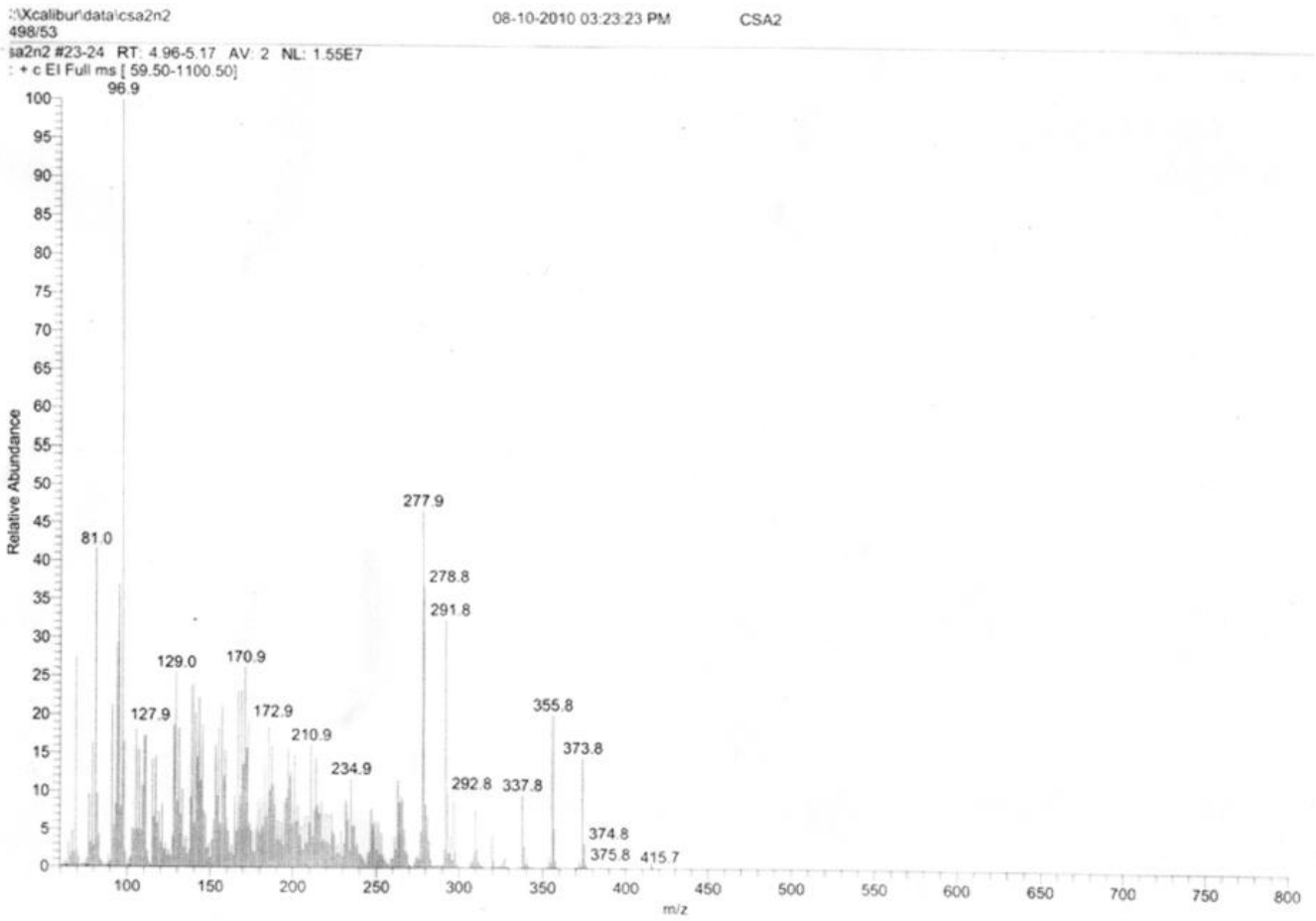

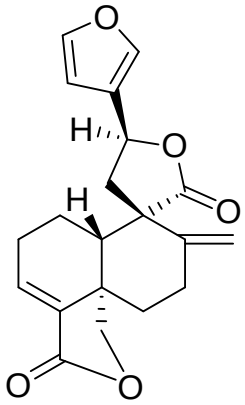

Figure A20 EI-MS spectrum of compound **CS-3**

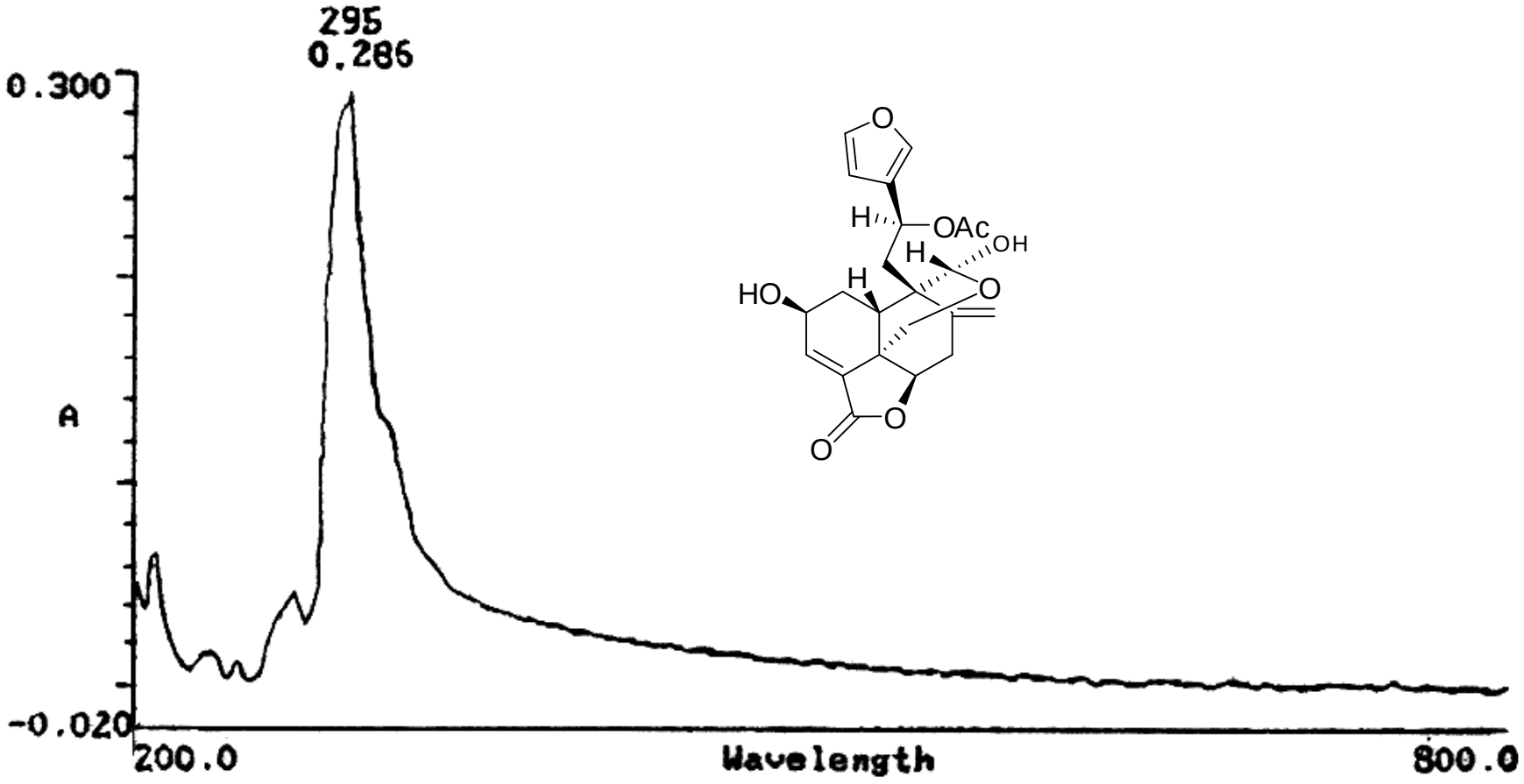

Figure A21 UV spectrum of compound **CS-3** (MeOH)

Figure A22 IR spectrum of compound **CS-3** (neat $CHCl_3$)

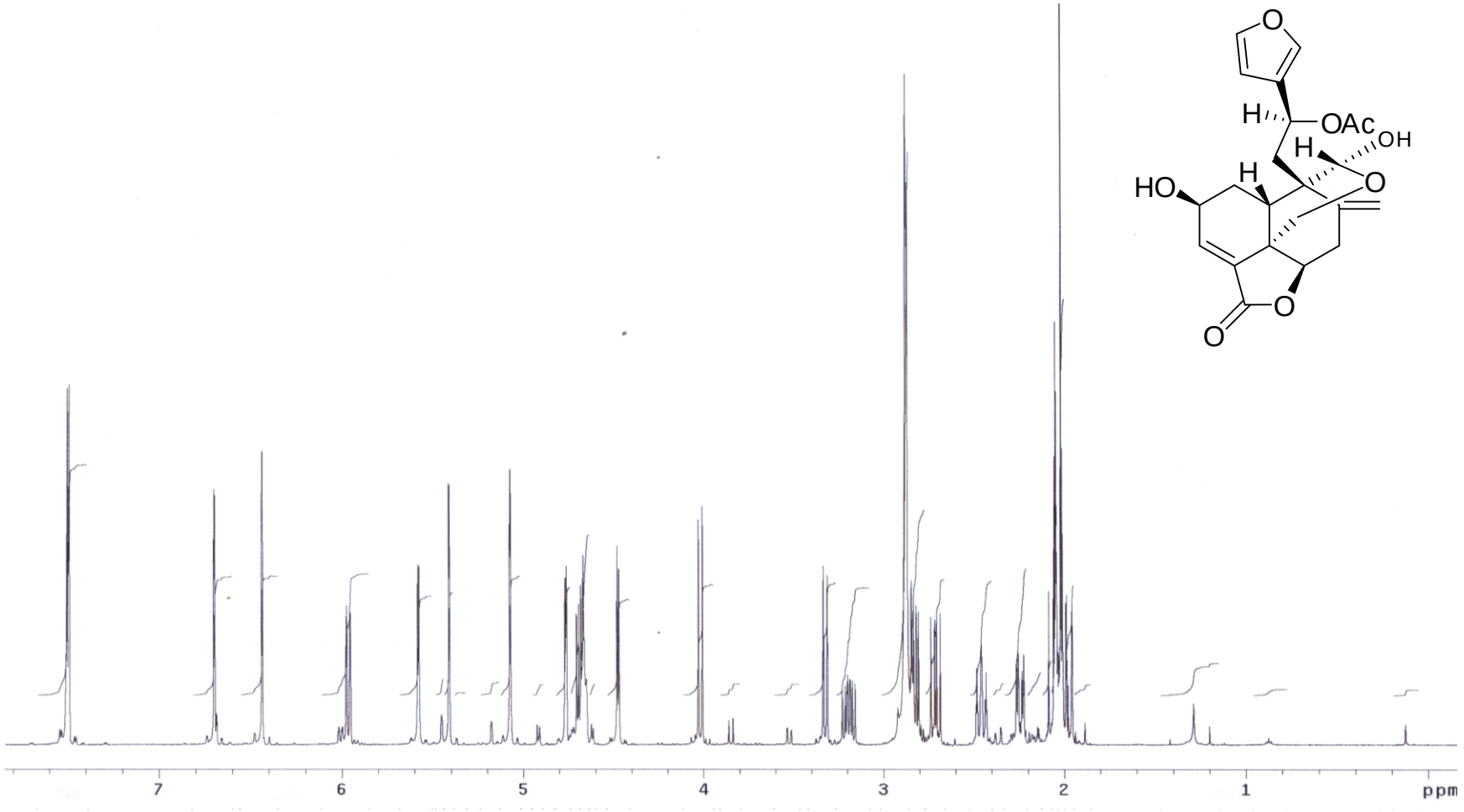

Figure A23 [1]H-MMR spectrum of compound **CS-3** (500 MHz, acetone-*d*6)

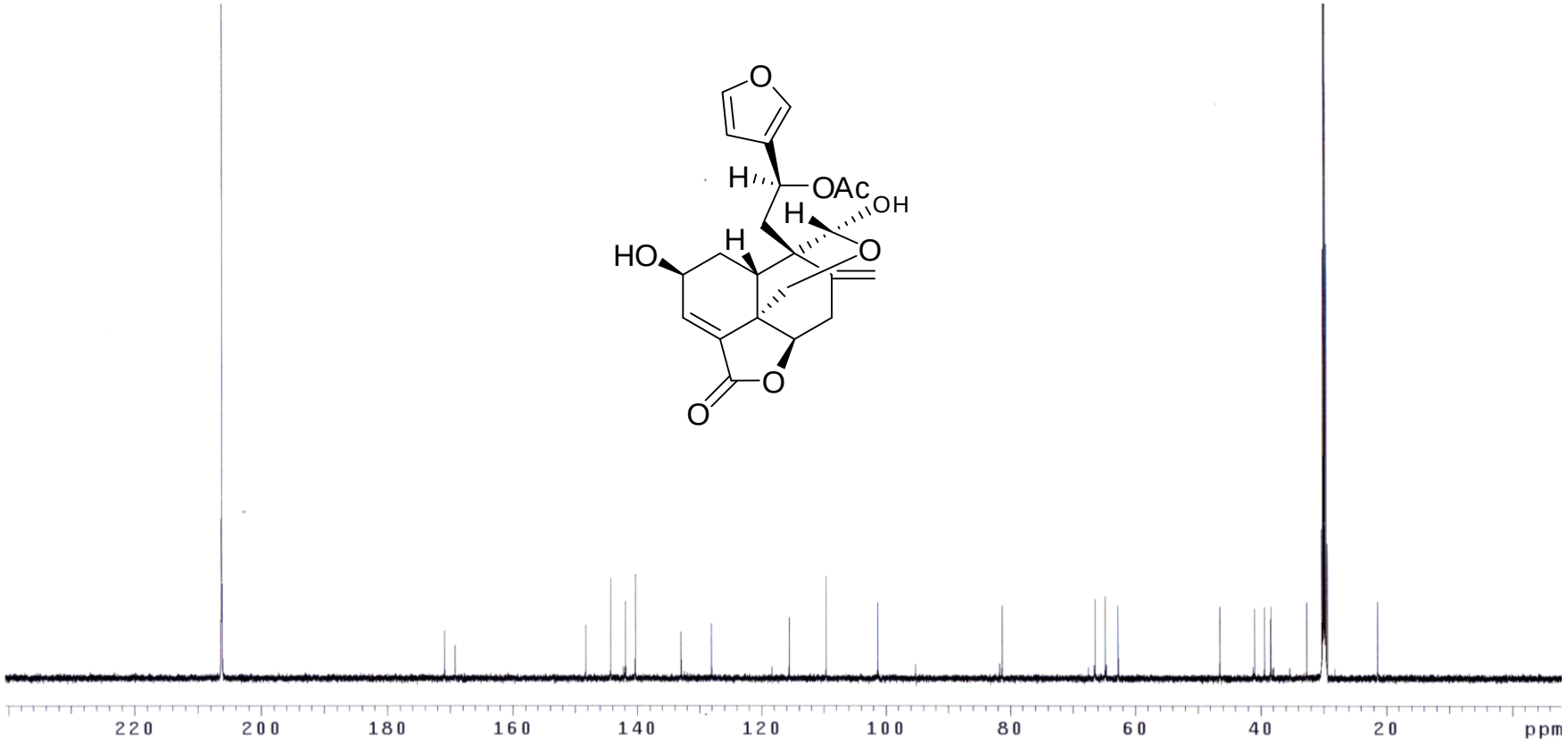

Figure A24 ^{13}C-MMR spectrum of compound **CS-3** (125 MHz, acetone-*d*6)

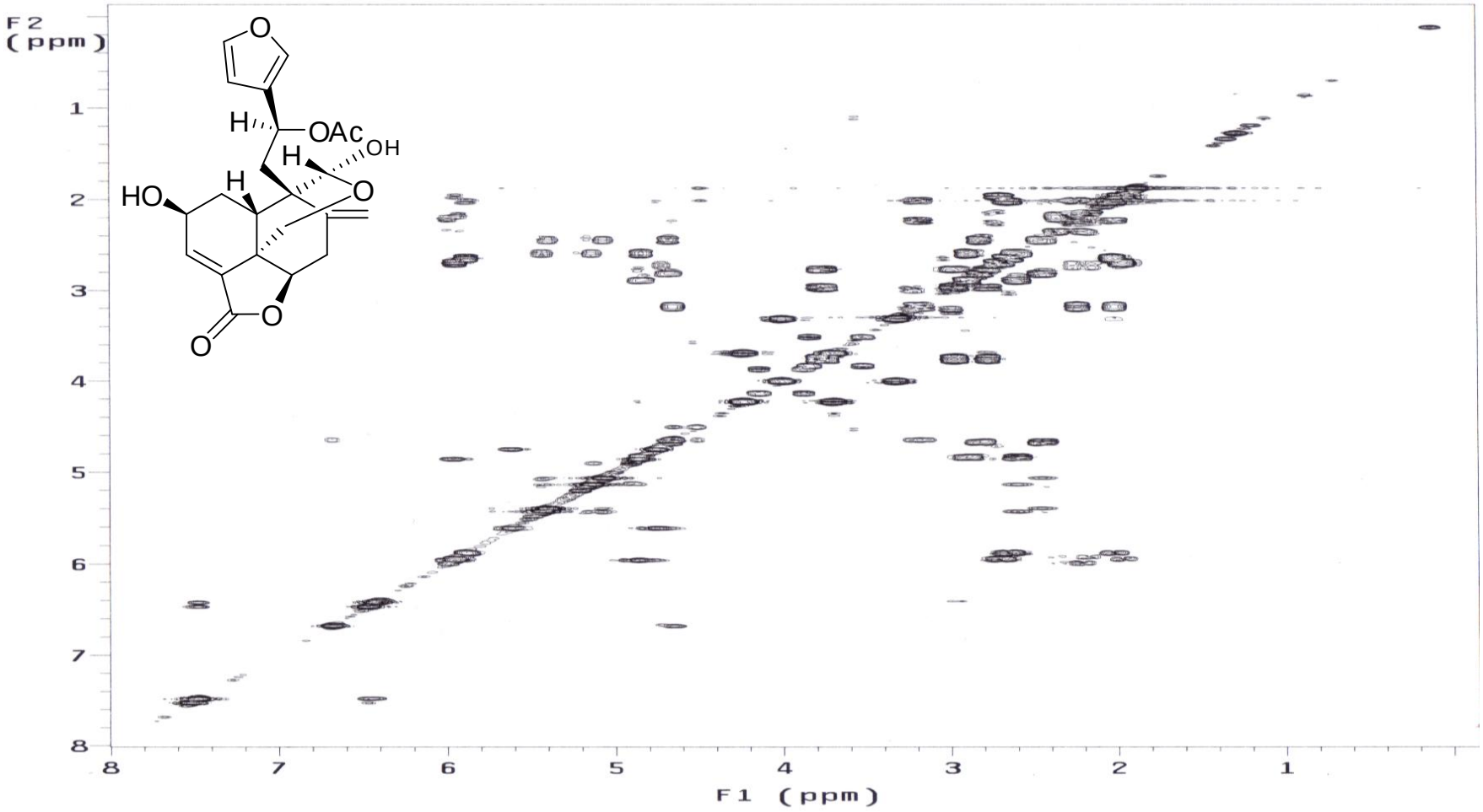

Figure A27 ^{1}H-^{1}H COSY spectrum of compound **CS-3** (acetone-*d*6)

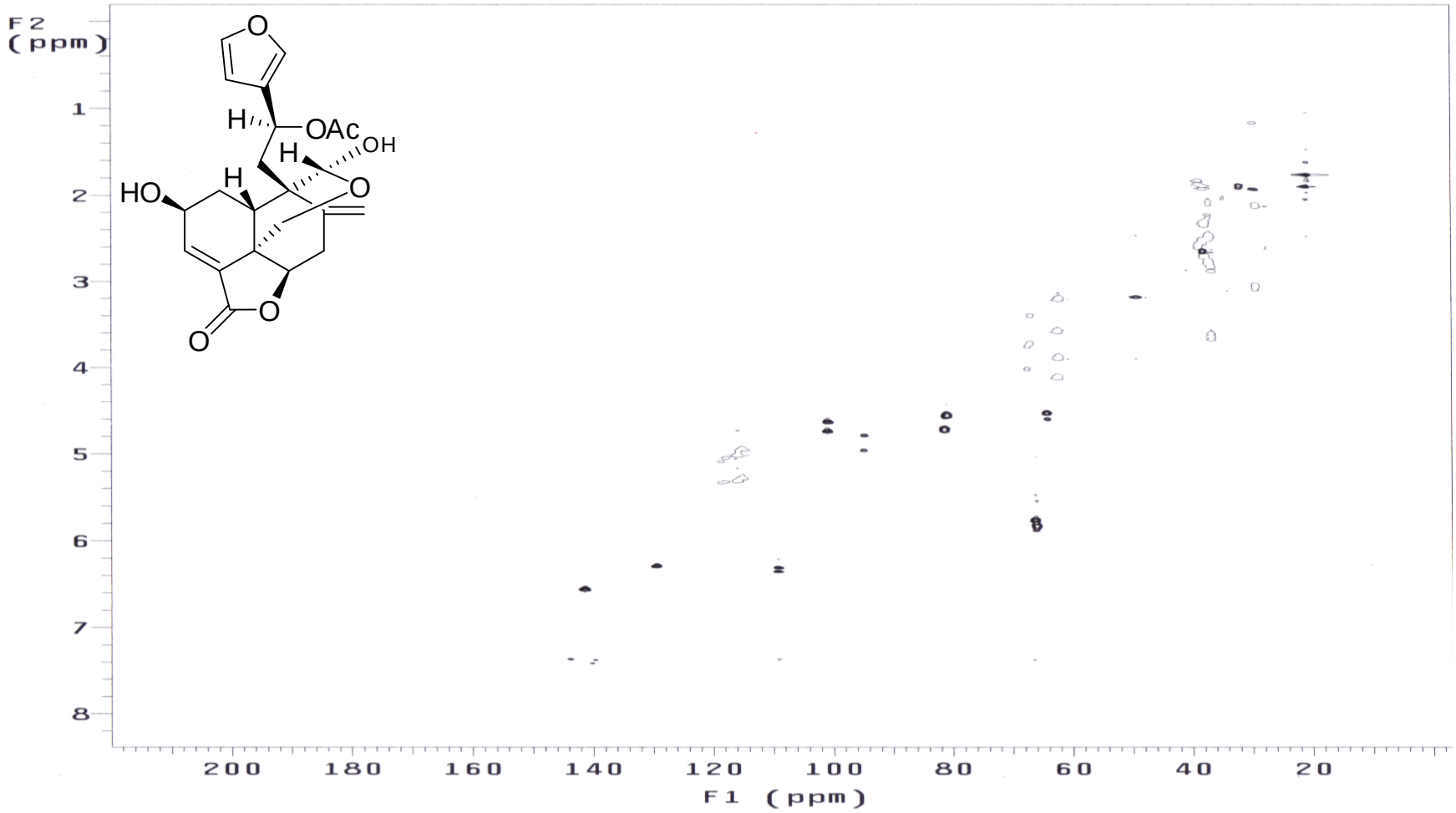

Figure A28 HMQC spectrum of compound **CS-3** (acetone-*d*6)

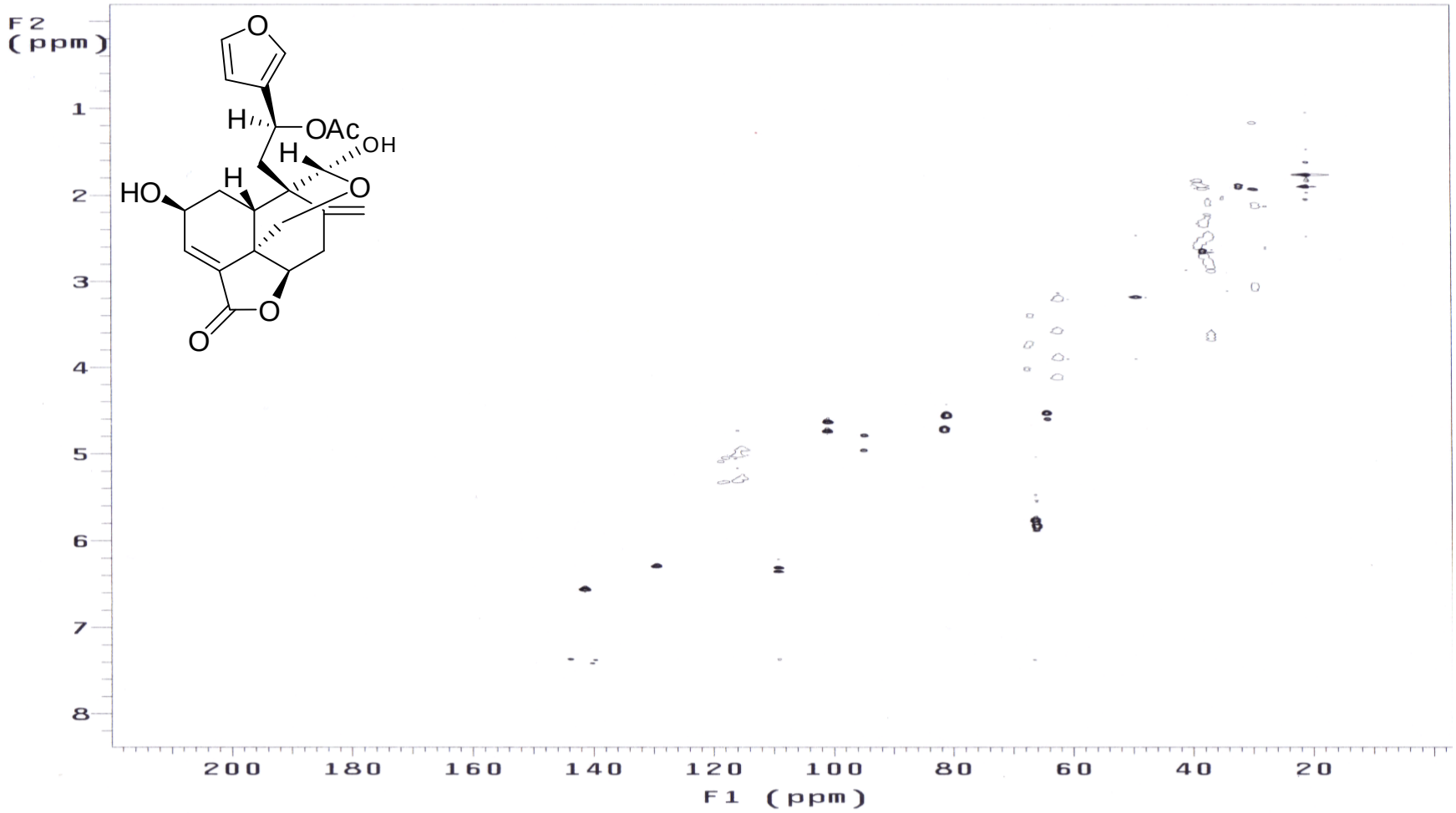

Figure A28 HMQC spectrum of compound **CS-3** (acetone-*d*6)

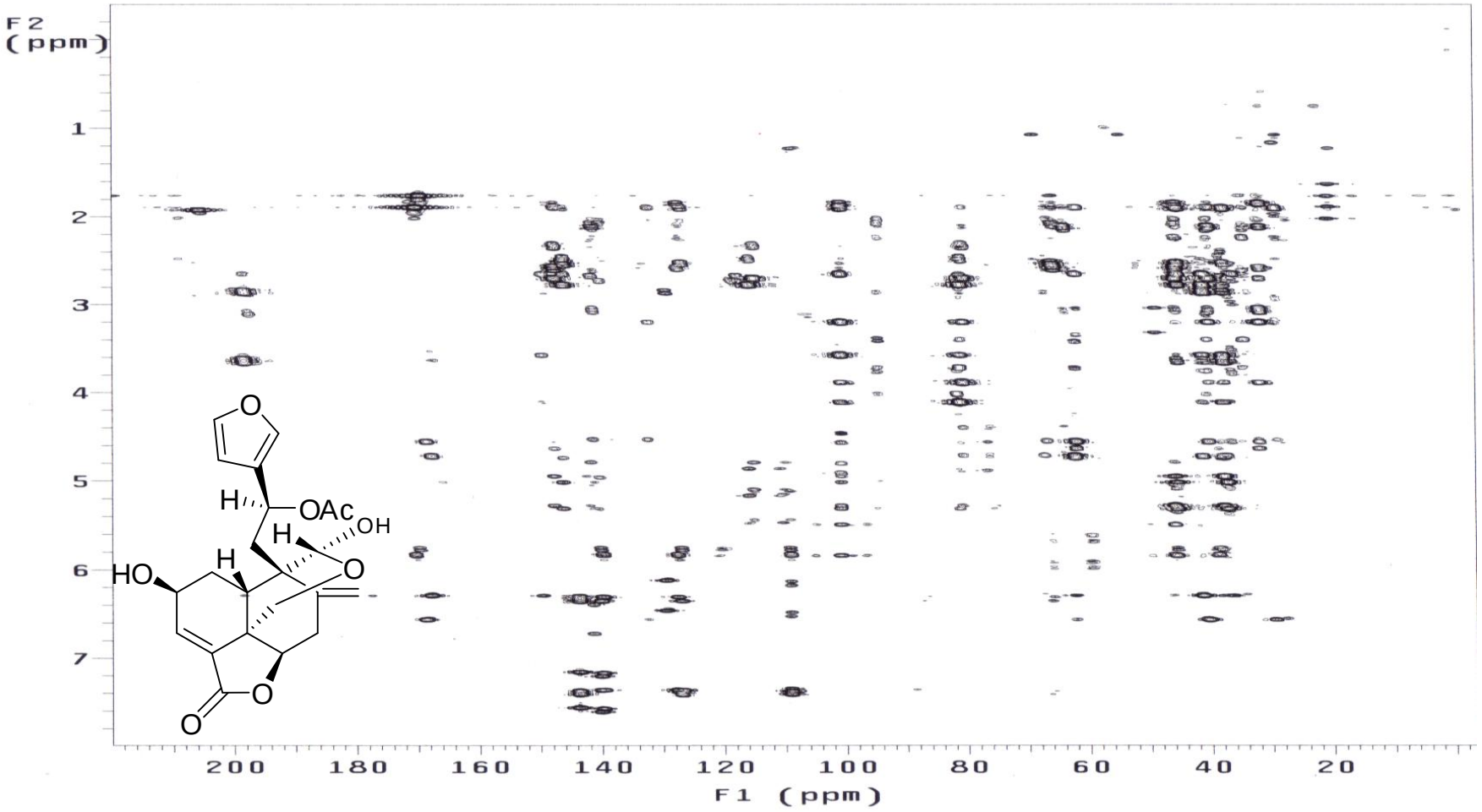

Figure A29 HMBC spectrum of compound **CS-3** (acetone-*d*6)

VITAE

Name Mr. Charoenwong Premprasert

Student ID 5010720006

Education Attainment

Degree	Name of Institution	Year of Graduation
Bachelor of Science (Chemistry - Biology) (2^{nd} Class Honors)	Prince of Songkla University	2007

List of Publication and Proceeding

Pramprasert, J., Tewtakul, S. and Wungsintaweekul, J. 2008. The efficiency of *Croton stellatopilosus* leaves extracts on anti-inflammation and anti-bacterial activity. Proceeding of the 8^{th} joint seminar NRCT-JSPS "innovative research in natural products for sustainable development". Faculty of Pharmaceutical Sciences, Chulalongkorn University, Bankok, Thailand. 189-190.

Pramprasert, C., Tewtrakul, S. and Wungsintaweekul, J. 2010. Anti-inflammatory activity of plaunotol isolated from *Croton stellatopilosus* in murine macrophage RAW264.7 cells. Abstracts of CDD 2010 The 1^{st} Current Drug Development International Conference. Woraburi Phuket Resort & Spa, Phuket, Thailand. 73.